Modelling and assessment of acidifying and eutrophying atmospheric deposition to terrestrial ecosystems (PINETI²)

Part I: Atmospheric deposition to German natural and semi-natural ecosystems during 2009, 2010 and 2011

Umwelt Bundesamt

For our Environment

Modelling and assessment of acidifying and eutrophying atmospheric deposition to terrestrial ecosystems (PINETI[2])

Part I: Atmospheric deposition to German natural and semi-natural ecosystems during 2009, 2010 and 2011

by

Martijn Schaap, Roy Wichink Kruit, Carlijn Hendriks, Richard Kranenburg, Arjo Segers, Peter Builtjes
Netherlands Organisation for Applied Scientific Research (TNO), TA Utrecht

Sabine Banzhaf
Freie Universität Berlin, FB Geowissenschaften, Institut für Meteorologie, Berlin

On behalf of the German Environment Agency

Imprint

Kurzbeschreibung

Die Biodiversität in Europa ist durch den Eintrag von Schad- und Nährstoffen in die Ökosysteme gefährdet. Innerhalb des PINETI-2 Projektes wurden daher die atmosphärischen Einträge dieser Schad- und Nährstoffe für Deutschland für die Jahre 2009, 2010 und 2011 ermittelt. Die trockenen, nassen und feuchten Einträge von NHx, NOy, SOx und die Einträge der basischen Kationen wurden berechnet und zur Gesamtdeposition aufsummiert. Die ermittelten mittleren Depositionsflüsse über Deutschland für Stickstoff und Schwefel betragen im Jahr 2009 1057 und 288 eq ha^{-1} a^{-1}. In 2010 und 2011 liegen die mittleren Einträge für Stickstoff bei 1052 und 962 eq ha^{-1} a^{-1}. Das Jahr 2009 war in Bezug auf das nationale Mittel meteorologisch gesehen ein durchschnittliches Jahr, so dass davon ausgegangen werden kann, dass auch die berechneten Einträge für das Jahr 2009 im nationalen Mittel eher bei einem langjährigen Mittel liegen als die Ergebnisse der Jahre 2010 oder vor allem 2011. Es wurden flächendeckende Karten für die unterschiedlichen Landnutzungsklassen erstellt. Die Karten zeigen, dass die Variabilität der Deposition über Deutschland signifikant ist. Die höchsten Einträge sind in Waldbeständen in oder in der Nähe von Regionen mit intensiver Landwirtschaft und Industrie zu finden. Im Vergleich zu den Ergebnissen des MAPESI-Vorhabens (Builtjes et al., 2011) sind die Ergebnisse der neuen Erhebung etwa 27% niedriger. Dies lässt sich durch eine Verbesserung der Methodik zur Bestimmung der nassen Deposition und der Konsolidierung neuer Prozessbeschreibungen im LOTOS-EUROS Modell erklären. Letztere Modellentwicklungen haben zu einem besseren Vergleich der Modellergebnisse zu Beobachtungen geführt. Die PINETI-2 Einträge stimmen besser mit Daten aus dem „Integrated Monitoring" Programm und mit der Depositionskartierung von EMEP überein als die MAPESI Ergebnisse. Der Vergleich mit Resultaten der Kronenraumbilanzmodellierung zeigt, dass sich die Unterschätzung dieser Daten im Vergleich zu MAPESI vergrößert hat. Die Unterschätzung ist an Standorten in Höhenlagen, an welchen ein erhöhter Eintrag durch feuchte Deposition anzunehmen ist, am größten. Die Bewertung des Eintrages in Bezug auf Risiken für terrestrische Ökosysteme wird im Teil 2 des Berichts beschrieben.

Abstract

Biodiversity in Europe is strongly affected by the deposition of nitrogen and sulfur on terrestrial ecosystems. In this study we present new quantitative estimates of the deposition of atmospheric nitrogen and sulfur compounds as well as base cat-ions to ecosystems across Germany. On average, the nitrogen and acid deposition in Germany in 2009 were 1057 and 1345 eq ha^{-1} yr^{-1}, respectively. For 2010 und 2011 average nitrogen depositions of 1052 and 962 eq ha^{-1} a^{-1} were obtained. In terms of annual deposition the year 2009 was a very representative year. As such we expect the result for 2009 are more likely to represent a 5 year mean average than the surrounding years. Separate maps are available for the major land use classes. These maps show considerable variability across the German territory with highest deposition on forest ecosystems in or near the main agricultural and industrial areas. The results of this study are systematically lower (27 %) than provided in earlier studies, i.e. MAPESI (Builtjes et al., 2011). The main reasons are an improved wet deposition estimation and the consolidation of improved process descriptions in the LOTOS-EUROS model, which has led to a better agreement with observations. The methodologies applied in this study reflect the current state-of-the-art. The PINETI-2 deposition estimates show a better agreement with results obtained by integrated monitoring and deposition mapping by EMEP than MAPESI results. A challenge that remains is that the underestimation of canopy budget model estimates is more pronounced in PINETI-2 than in MAPESI. It appears that the underestimation is especially present at elevations locations with potentially high impacts of occult deposition. The critical load exceedances in Germany are reported in part 2 of the report.

Inhaltsverzeichnis

Abbildungsverzeichnis

Tabellenverzeichnis

Abkürzungsverzeichnis

a	Year, Jahr
ara	Arable – Ackerland Landnutzungsklasse
BC	Basische Kationen
Ca^{2+}	Kalzium
Cl^-	Chlorid
CLC	Corine Land Cover
CLRTAP	Convention on long-range transboundary air pollution
cnf	Coniferous – Nadelwald Landnutzungsklasse
COR	temporal correlation coefficient
crp	Crops – Dauerkulturen Landnutzungsklasse
CTM	Chemical Transport Model
dec	Deciduous – Laubwald Landnutzungsklasse
DEPAC	Deposition of Acidifying Compounds,
DWD	Deutscher Wetterdienst
ECMWF	European Centre for Medium-Range Weather Forecasts
EMEP	European Monitoring and Evaluation Programme
eq	Versauerungsequivalent
grs	Grasland Landnutzungsklasse
ha	Hektar
HNO_3	Salpetersäure
IB	ion balance
K^+	Kalium
MAPESI	Modelling Air Pollutants and Ecosystem Impact (Forschungsprojekt)
Mg^{2+}	Magnesium
mix	Mixed forest – Mischwald Landnutzungsklasse
N	Stickstoff
Na^+	Natrium
NH_3	Ammoniak
NH_4	Ammonium
NH_x	Reduzierte Stickstoffkomponenten
NO_2	Stickstoffdioxid
NO_3	Nitrat
NO_y	Oxidierte Stickstoffkomponenten
nss	Non sea-salt, seesalzkorrigiert

oth	other - Andere Landnutzungsklassen
PAREST	Particle Reduction Strategies (Forschungsprojekt)
PINETI	Pollutant Input and Ecosystem Impact (Forschungsprojekt)
QAQC	Quality Assessment and Quality Control
RMSE	root mean squared error
S	Schwefel
sem	Semi-natural – seminatürliche Ökosysteme Landnutzungsklasse
SO₂	Schwefeldioxid
SO₄	Sulfat
SOₓ	Oxidierte Schwefelverbindungen
STD	standard deviation
urb	Urban – bebaute Gebiete Landnutzungsklasse
wat	Water – Gewässer Landnutzungsklasse

Zusammenfassung

Die Biodiversität in Europa ist durch den Eintrag von Schad- und Nährstoffen in die Ökosysteme gefährdet. Das Ziel des PINETI-2 Projektes war daher die atmosphärischen Einträge dieser Schad- und Nährstoffe für Deutschland für das Jahr 2009, 2010 und 2011 zu ermitteln. Dazu werden die trockenen, nassen und feuchten Einträge von NHx, NOy, SOx und die Einträge der basischen Kationen Ca^{2+}, Mg^{2+}, K^+ und Na^+ berechnet und zur Gesamtdeposition aufsummiert. Anhand der Ergebnisse und den Critical Load werden die Überschreitungen der Critical Load für empfindliche Ökosysteme berechnet. Die Beschreibungen der Kapitel 1 bis Kapitel 8 beziehen sich im Wesentlichen auf das Modelljahr 2009; im Kapitel 10 werden die Ergebnisse für das Jahr 2009 mit den Ergebnissen der Jahre 2010 und 2011 verglichen.

Ermittlung der Einträge

Für die Ermittlung des vollständigen Schad- und Nährstoffeintrags in Ökosysteme müssen alle drei Eintragspfade berücksichtigt werden. In der vorliegenden Studie werden hierfür fünf Berechnungsschritte durchgeführt:

1. **Berechnung der Depositions- und Konzentrationsfelder auf Basis von Emissions- und Meteorologiedaten mit einem Chemie-Transport-Modell** (Ergebnis: trockene Deposition für N und S). Die trockene Deposition wird derzeit nur im Rahmen von Forschungsvorhaben messtechnisch erfasst; ein entsprechendes Messnetz gibt es nicht. Die flächendeckende Ermittlung der trockenen Deposition muss daher mit Chemie-Transport-Modellen erfolgen. Die Güte dieser Modelle kann u.a. durch Vergleiche mit Messungen, z.B. der Luftkonzentration, oder mit den Ergebnissen anderer Modelle untersucht werden.

   In der vorliegenden Studie wurde das Modell LOTOS-EUROS verwendet, welches seit vielen Jahren zur Beantwortung von Fragestellungen u.a. im Hinblick auf den Stickstoff- und Schwefelkreislauf genutzt wird und seine Güte in verschiedenen internationalen Vergleichsstudien unter Beweis stellte (e.g. Schaap et al., 2015; Im et al., 2015; Vautard et al., 2006). In der verwendeten Version beinhaltet LOTOS-EUROS auch die Parametrisierung eines Ammoniak-Kompensationspunktes und berücksichtigt damit den bi-direktionalen Austausch von Ammoniak, für das Ökosysteme sowohl Senke, als auch Quelle sein können. Das Modell wird in Deutschland mit einem Raster von etwa 7*7 km² betrieben. Wesentliche Eingangsgrößen sind die meteorologischen Daten, die Landnutzung und die Emissionen aus der offiziellen Berichterstattung. Die räumliche Verteilung der aktuellen Emissionen erfolgte auf Basis der Ergebnisse des PAREST Vorhabens. Die meteorologischen Daten wurden vom European Centre of Medium Range Weather Forecasting (ECMWF). Details zu der Modellierung finden sich in Abschnitt 3.1.

2. **Berechnung der nassen Depositionsfelder auf Basis von Messdaten.** Die flächendeckende Interpolation der gemessenen Konzentrationen im Niederschlag erfolgt durch geostatistische Verfahren, wobei für N und S zusätzlich die Informationen über die räumliche Verteilung aus dem Chemie-Transport-Modell genutzt werden (Ergebnis: nasse Deposition). Das methodische Vorgehen ist im Detail in Wichink Kruit et al. (2014) dargestellt; eine Kurzfassung findet sich in Kapitel 4.1.

3. **Verwendung eines heuristischen Ansatzes zur Abschätzung der Nebeldeposition.** Hierfür wird die Konzentration im Nebelwasser über empirische Faktoren aus der Konzentration im Niederschlag (vgl. Punkt 2) abgeleitet. Der Nebeleintrag wird anschließend über berechnete Depositionsgeschwindigkeiten ermittelt (Ergebnis: feuchte Deposition). Das genaue methodische Vorgehen ist in Kapitel 5 beschrieben.

4. **Verwendung eines scavenging ratio Ansatzes zur Berechnung der trockenen Deposition für die basischen Kationen**. In diesem Ansatz wird die Luftkonzentration mit empirischen Faktoren

aus der Konzentration im Niederschlag abgeleitet. Die trockene Deposition wird anschließend über berechnete Depositionsgeschwindigkeiten ermittelt (Ergebnis: trockene Deposition für BC). Eine Beschreibung der Methode findet sich in Kapitel 6

5. **Transformation der Ergebnisse der trockenen und feuchten Deposition auf das feiner aufgelöste 1*1km²-Raster und Addition aller Teilflüsse zur Gesamtdeposition mit einer räumlichen Auflösung von 1*1 km²** (Ergebnis: Gesamtdeposition).

Table 1 und Figure 1 zeigen für die einzelnen Komponenten, welche der oben dargestellten Berechnungsschritte ausgeführt werden und welche Grundlagendaten einfließen.

Table 1.   Berechnungsschritte für die Ermittlung der Deposition reduzierter und oxidierter Stickstoffverbindungen, sowie von oxidiertem Schwefel und der basischen Kationen

Methodik	NHx	NOy	SOx	Basische Kationen
Trockene Deposition auf Basis von Chemie Transport Modellierung	√	√	√	
Nasse Deposition auf Basis von Messdaten	√	√	√	√
Feuchte Deposition auf Basis eines heuristischen Ansatzes	√	√	√	√
Trockene Deposition auf Basis eines scavenging ratio Ansatzes				√
Addierung aller Flüsse	√	√	√	√

Figure 1.   Schematische Darstellung der innerhalb des Vorhabens verwendeten Methodik zur Ermittlung der Depositionsflüsse. Das Schema zeigt die wichtigsten Eingangsdaten (dunkelblaue Zellen), wichtige Zwischenergebnisse (hellblaue Zellen), Berechnungsschritte (gestrichelte Zellen) und Endergebnisse (grüne Zellen). Die Pfeile kennzeichnen die Abhängigkeitsverhältnisse. Einige Datenflüsse sind von ermittelten Komponenten, welche in der Grafik angegeben sind, abhängig.
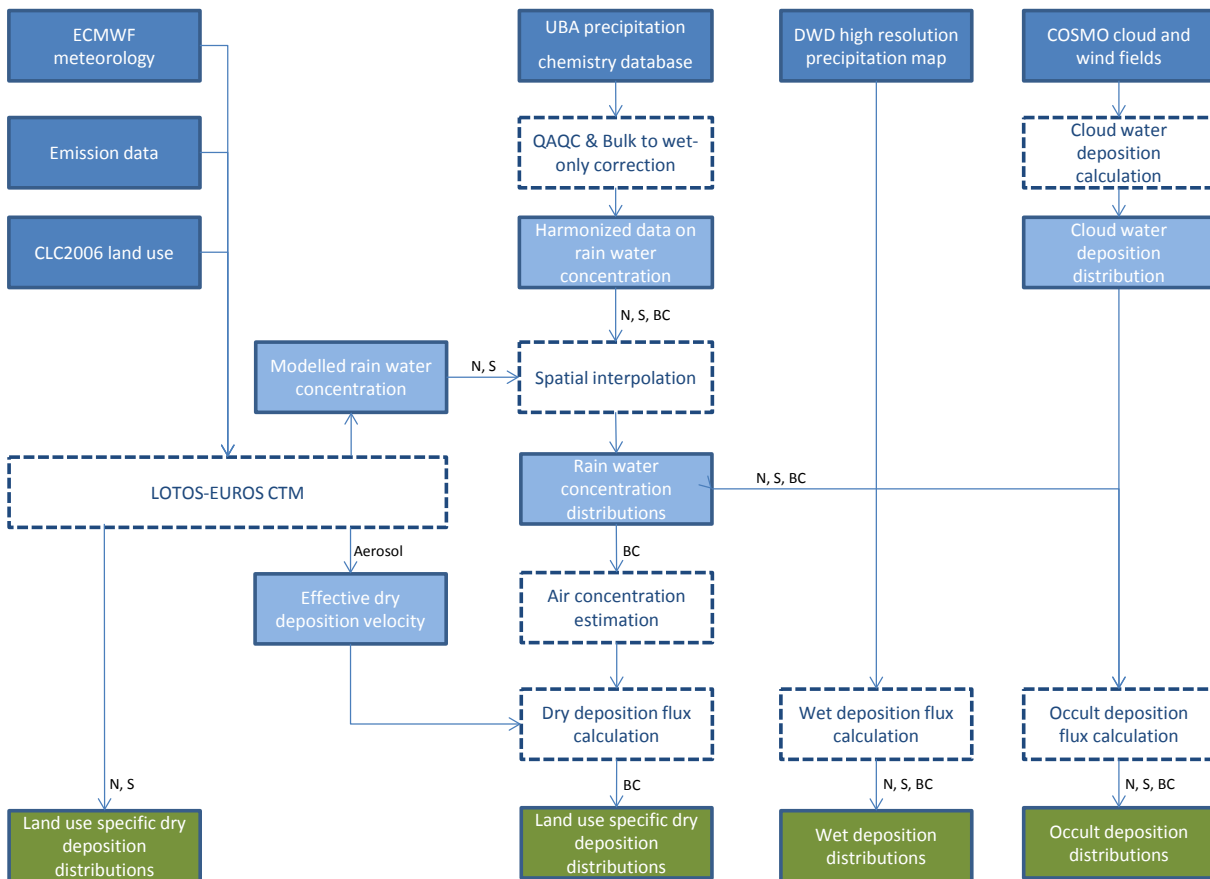
Figure 2. Übersicht der Verteilung der Gesamtdeposition für alle betrachteten Komponenten über Deutschland für das Jahr 2009
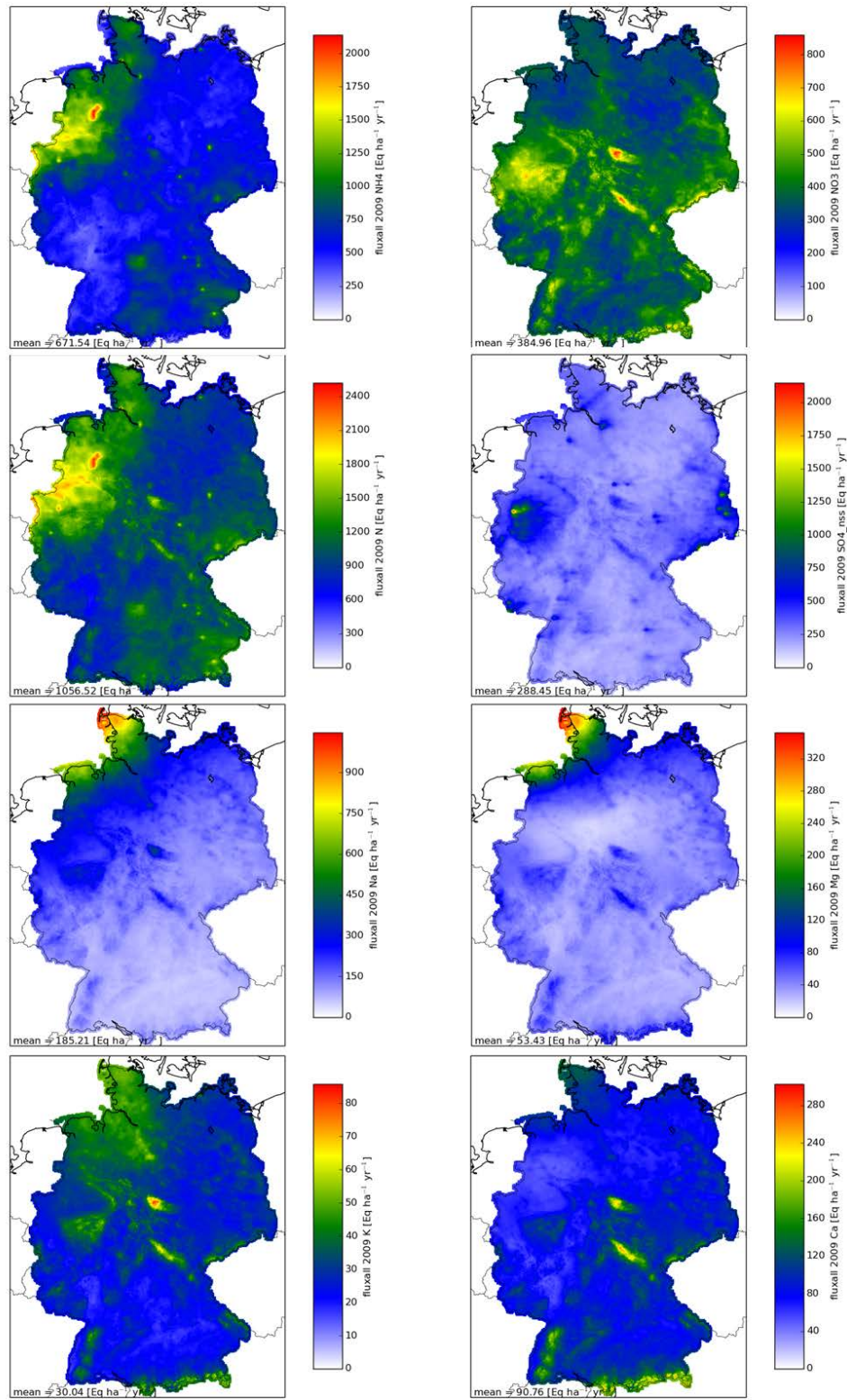
<u>Ergebnisse</u>

Die ermittelte Gesamtdeposition sowie die einzelnen Teilflüsse für die unterschiedlichen betrachteten Komponenten sind gemittelt über Deutschland in Table 2 gegeben. Figure 2 zeigt die räumliche Verteilung der Gesamtdeposition für die unterschiedlichen Komponenten für das Jahr 2009. In Table 3 ist darüber hinaus für Gesamtstickstoff und Schwefel die mittlere Gesamtdeposition für die zehn betrachteten Landnutzungsklassen gezeigt. Die Gesamtdeposition von N beträgt im Mittel über Deutschland 1057 eq ha^{-1} a^{-1} während die Gesamtdeposition von Schwefel (S_nss) im Mittel 288 eq ha^{-1} a^{-1} beträgt. Die Maxima der Stickstoff-Gesamtdeposition liegen im Nordwesten und Südosten des Landes, da diese Regionen landwirtschaftlich am intensivsten bewirtschaftet sind. An dieser Stelle sei darauf hingewiesen, dass die Depositionen von oxidiertem und reduziertem Stickstoff voneinander abweichende Verteilungen über Deutschland aufweisen. Oxidierter Stickstoff trägt in nicht landwirtschaftlich genutzten Regionen einen großen Beitrag zur Stickstoff-Gesamtdeposition bei und bedingt in Regionen wie zum Beispiel dem Schwarzwald über die Hälfte der Stickstoff-Gesamtdeposition. Die Schwefel-Gesamtdeposition weist die höchsten Werte im Ruhrgebiet auf. Sekundäre Maxima zeigen sich in den Mittelgebirgen. Die Einträge in Waldbestände sind etwa 25-50% höher als die in Wasserflächen, was durch die Rauhigkeitslänge bedingt wird.

Die Basischen Kationen Natrium (Na$^+$) und Magnesium (Mg$^+$), deren Hauptquelle Seesalz ist, weisen Depositionsmaxima an der Nordseeküste auf. Die Verteilung der Deposition von Kalium weist ein eher anthropogen geprägtes Muster auf, mit maximalen Werten in Regionen mit den höchsten Niederschlägen. Kalzium stammt sowohl aus anthropogenen Quellen als auch aus Seesalz. Daher weist die Deposition von Kalzium sowohl in den Mittelgebirgen als auch in Küstenregionen Maxima auf.

Nach der Validierung der Berechnungen für 2009 wurden auch die Depositionskarten für 2010 und 2011 ermittelt.

Table 2. Übersicht der resultierenden über Deutschland gemittelten nassen, trockenen, feuchten und Gesamt-Depositionsflüsse für reaktiven Stickstoff, Schwefel und die Basischen Kationen. Die Daten wurden anhand der effektiven Landnutzungsverteilung erhoben.

Komponente	Einheit	Nass	Trocken	Feucht	Gesamt
Ca^{2+}	eq ha^{-1} yr^{-1}	72	17	1	91
Ca^{2+}-nss	eq ha^{-1} yr^{-1}	66	16	1	83
K$^+$	eq ha^{-1} yr^{-1}	25	5	0.3	30
K$^+$-nss	eq ha^{-1} yr^{-1}	22	4	0.3	26
Mg^{2+}	eq ha^{-1} yr^{-1}	41	11	0.5	53
Mg^{2+}-nss	eq ha^{-1} yr^{-1}	11	3	0.1	14
BC-nss	eq ha^{-1} yr^{-1}	99	23	1	123
Na$^+$	eq ha^{-1} yr^{-1}	147	37	2	185
SO$_x$-S	eq ha^{-1} yr^{-1}	187	120	4	311
SO$_x$-S-nss	eq ha^{-1} yr^{-1}	170	115	3	288
NH$_x$-N	eq ha^{-1} yr^{-1}	327	337	8	672
NO$_y$-N	eq ha^{-1} yr^{-1}	248	131	6	385
N	eq ha^{-1} yr^{-1}	575	467	14	1057

Table 3. Übersicht der resultierenden über Deutschland gemittelten Gesamtdepositionsflüsse für reaktiven Stickstoff und Schwefel pro Landnutzungskategorie.

Landnutzung	Code	Gesamt N [eq ha⁻¹ yr⁻¹]	Gesamt SOx [eq ha⁻¹ yr⁻¹]
Grassland	grs	901	291
Semi-natural	sem	948	301
Arable	ara	982	247
Permanent crops	crp	1043	315
Coniferous forest	cnf	1287	358
Deciduous forest	dec	1183	356
Mixed forest	mix	1235	357
Water	wat	861	291
Urban	urb	1248	283
Other	oth	894	221

Figure 3. Vergleich der N-Gesamtdeposition für 2009 aus dieser Studie (PINETI2) mit dem Endergebnis des MAPESI Projektes für das Jahr 2005 und dem Endergebnis des PINETI Projektes für das Jahr 2009.
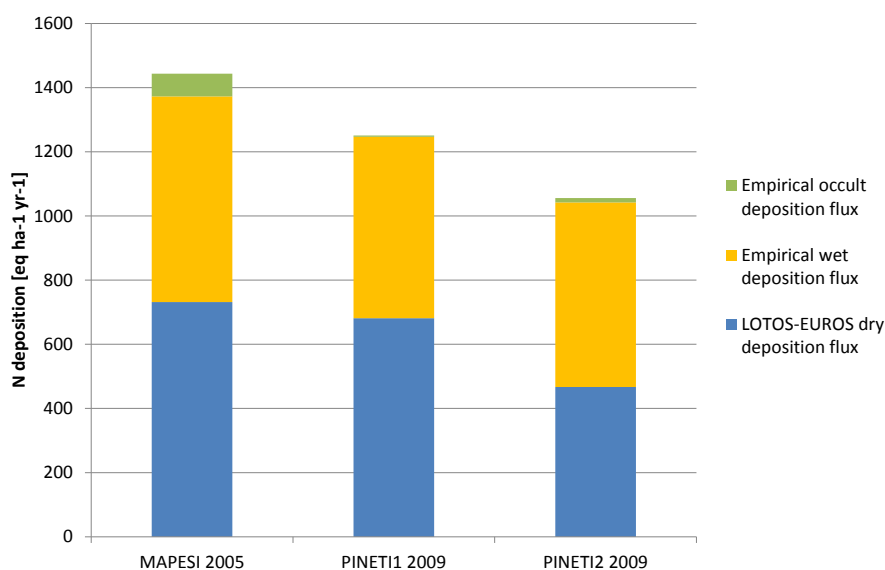
Qualitätssicherung

Zur Qualitätssicherung und zum besseren Verständnis der Ergebnisse wurden die Ergebnisse mit Beobachtungen und anderen Studien verglichen.

1. Vergleich mit den Ergebnissen früherer nationaler Berechnungen

Für die vorliegende Studie wurden Ergebnisse aus drei Vorhaben miteinander verglichen:

- MAPESI-Vorhaben (letztes Jahr der Zeitreihe: 2007; vgl. Builtjes et al, 2011)

- PINETI-Vorhaben (letztes Jahr der Zeitreihe: 2009; vgl. Wichink Kruit et al. (2014))

- Sowie das Jahr 2009 aus dem aktuell vorliegenden Vorhaben (PINETI-2).

Zwischen MAPESI und PINETI2 kommt es zu einer systematischen Abnahme der Stickstoffdeposition um 27% (Figure 3). Diese Abnahme beruht v.a. auf einer Verbesserung der Verfahren zur räumlichen

Interpolation der nassen Deposition und dem Rückgang der Emissionen (zwischen MAPESI und PI-NETI) sowie der überarbeiteten Parametrisierungen in LOTOS-EUROS, die zu einer Abnahme der trockenen Deposition führt (zwischen PINETI und PINET-2)[1].

2. Vergleich mit Depositionsschätzungen aus Intensivmesskampagnen

Innerhalb Deutschlands gibt es für drei Stationen Depositionsschätzungen aus Intensivmesskampagnen: Forellenbach (Bayerischer Wald), Neuglobsow (Brandenburg) und Bourtanger Moor (Niedersachsen). Zwar werden die Stickstoffeinträge auf Basis unterschiedlicher Beobachtungs- oder Messmethoden abgeschätzt und jede dieser Methoden birgt Unsicherheiten, der Vergleich zeigt jedoch deutlich, dass die PINETI-2 Daten die jetzt vorliegen näher an diesen Schätzungen liegen als die Ergebnisse des MAPESI Projektes. Während die PINETI-2 Daten innerhalb 25% der Schätzungen liegen, sind die MAPESI Daten an allen drei Standorten 50-100% höher (Table 4).

3. Vergleich mit Depositionsschätzungen von EMEP

Der Vergleich der PINETI-2 Daten mit den modellierten Depositionsflüssen des EMEP Modells zeigt, dass die neuen Schätzungen innerhalb 4 % der EMEP Modellierung liegen (Table 5). Die beiden unterschiedlichen EMEP Datensätze zeigen, dass sich auch die EMEP Resultate aufgrund neuer Entwicklungen in der Modellierung und in den Emissionsdaten kontinuierlich ändern.

Table 4. Vergleich zwischen der ermittelten Gesamtdeposition von MAPESI für 2007 und PINETI--2 für 2009 und Abschätzungen der Gesamtdeposition aus Intensivmesskampagnen (kg N ha^{-1} yr^{-1}) für drei Stationen in Deutschland: Forellenbach (Beudert and Breit, 2014), Neuglobsow (Schulte-Bisping and Beese, 2016) und Bourtanger Moor (Mohr et al., 2013)

	Empirische Daten	MAPESI	PINETI-2
Forellenbach (Nadelwald)	13-15	37	19
Neuglobsow (Nadelwald)	11	18	12
Bourtanger Moor (semi-natürlich)	25 (16-35)	38	20

Table 5. Vergleich der Gesamtdeposition von NOy, NHx und N zwischen PINETI-2, EMEP und EMEP_rec2013 (= Neuberechnung aus dem Jahr 2013) für das Jahr 2009

Variable	Einheit	PINETI-2	EMEP	EMEP_rec2013
NOy	eq ha^{-1}	385	351	428
NHx	eq ha^{-1}	672	711	670
total N	eq ha^{-1}	1057	1062	1098

---

[1] Für die Ermittlung der Gesamtdeposition wird – wie oben beschrieben – nicht die modellierte nasse Deposition, sondern die interpolierte gemessene nasse Deposition verwendet. Zur weitgehenden Erhaltung der Massenbilanz sollte allerdings die modellierte und die gemessene nasse Deposition im Mittel etwa gleich groß sein. Dies war in der Vergangenheit nicht der Fall. Durch die Abnahme der trockenen Deposition kommt es modellintern zu einer Verschiebung zur nassen Deposition, die nun im Mittel besser mit der gemessenen nassen Deposition übereinstimmt.

4. Vergleich mit Luftkonzentrationsmessungen

Die modellierte trockene Deposition lässt sich nur indirekt validieren. Figure 4 zeigt den Vergleich der modellierten Konzentrationen der Vorläufergase mit Beobachtungen aus den Ländermessnetzen. Für Ammoniak ist es der erste Vergleich der LOTOS-EUROS Modellierung mit Messungen an mehreren Stationen über Deutschland. Die Validierung zeigt, dass das LOTOS-EUROS Modell die räumliche Variabilität der Konzentrationen über Deutschland größtenteils gut wiedergeben kann. Innerhalb der einzelnen Bundesländer ist die Streuung jedoch größer. Letzteres gilt besonders für Ammoniak, das stark von der Emissionsverteilung beeinflusst wird, welche jedoch in den Emissionsdaten nicht ausreichend detailliert vorliegt. Lediglich für NO_2 weist der Vergleich darauf hin, dass LOTOS-EUROS die gemessenen Werte unterschätzt. Dies wird auch durch den Vergleich der modellierten zu gemessenen nassen Depositionsdaten bestätigt.

Ein Vergleich der Variabilität der berechneten trockenen Depositionsgeschwindigkeiten für Ammoniak mit einer Bandbreite messbasierter Depositionsgeschwindigkeiten aus der Literatur zeigt, dass die modellierten Werte die Spanne der empirischen Daten abbilden. Zusammenfassend gesagt, die LOTOS-EUROS Modellierung repräsentiert den aktuellen Stand der Wissenschaft.

Figure 4.   Vergleich der modellierten (y-Achse) und gemessen (x- Achse) Konzentrationen von Schwefeldioxid, Stickstoffdioxide und Ammoniak. Gezeigt werden die Jahresmittelwerte.
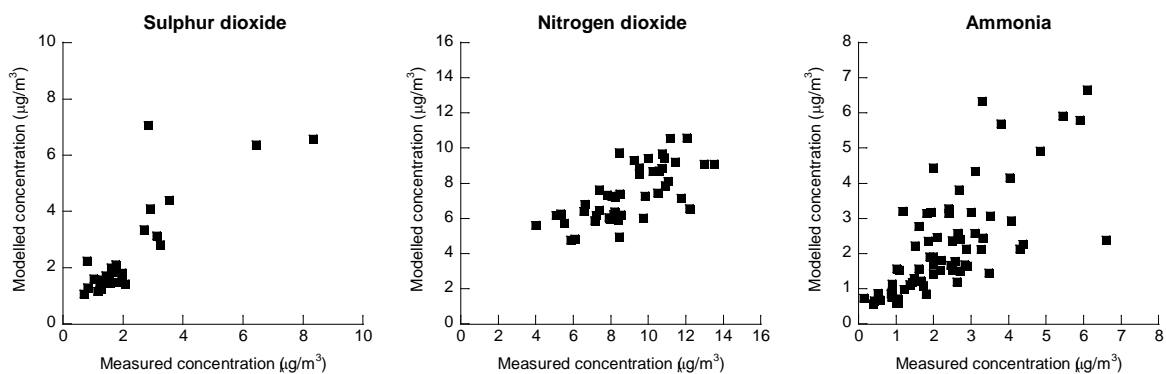
5. Vergleich mit Depositionsschätzungen auf Basis von Messungen des Bestandniederschlags

Eine weitere Möglichkeit die N-Gesamtdeposition abzuschätzen bietet die Kronenraumbilanzmodellierung (KRB), welche auf Messungen und Analyse des Bestandsniederschlags basiert. Bei erster Betrachtung des Vergleiches der Ergebnisse der KRB Modellierung mit PINETI-2 an allen verfügbaren KRB-Standorten scheint kein positiver Zusammenhang zwischen den Datensätzen zu bestehen (siehe Kapitel 8.2.5). An manche Stellen ist die Unterschätzung durch die PINETI-2 Modellierung sogar noch größer als erwartet und der Vergleich zeigt signifikante Unterschiede von Bundesland zu Bundesland. Eine detailliertere Analyse hat jedoch ergeben, dass der Vergleich für relativ flache Regionen deutlich besser ausfällt als für höher gelegene Stationen, d.h. in Gebirgsregionen. Table 6 zeigt die mittlere N-Gesamtdeposition an den KRB Standorten aufgeteilt in vier Höhenklassen. Die Werte der KRB Daten zeigen mit steigender Höhe des KRB Standortes eine steigende Tendenz der modellierten N-Gesamtdeposition. Die PINETI-2 Modellierung hingegen zeigt eine geringe Variabilität über die verschiedenen Höhenbereiche. Eine Analyse am Standort Schauinsland hat ergeben, dass unter Verwendung der gemessenen Schadstoffkonzentrationen in der Luft, die anhand der KRB Methode bestimmten Flüsse nur durch den Einsatz außergewöhnlich hoher Depositionsgeschwindigkeiten reproduziert werden konnten. Außerdem werden die Ergebnisse des Vergleichs der PINETI-2 Daten mit den KRB Daten nicht durch die zuvor gezeigte Validierung gestützt. Folglich ist es möglich, dass die PINETI-2 Ergebnisse den (lokalen) Einfluss der feuchten Deposition unterschätzen.

Die hier begonnene Analyse zeigt die Notwendigkeit auf, die beobachteten Unterschiede zwischen KRB Modellierung und den PINETI-2 Resultaten in Zusammenarbeit mit den Messnetzbetreibern im Detail zu untersuchen und zu analysieren. Hierbei sollte besonderes Augenmerk auf die Repräsentativität der Station in Hinblick auf Höhenlage und Landnutzung, den Einfluss feuchter Deposition, die Rolle von organischem Stickstoff und die Annahmen hinsichtlich der Deposition von Natrium unter kontinentalen Bedingungen gelegt werden. Diese Untersuchung sollte unsere Annahme bestätigen oder falsifizieren, dass die PINETI-2 Ergebnisse nicht im Widerspruch zu den KRB Modellierungen stehen, da die in PINETI-2 ermittelten Hintergrundbelastungen für Standorte, die hohen Einträgen durch feuchte Deposition ausgesetzt sind, nicht repräsentativ sind.

Table 6.   Anzahl der KRB Standorte, über Standorte gemittelte KRB Modellierung, über Standorte gemittelte PINETI-2 Modellierung und Verhältnis KRB/PINETI-2 für Gesamt-N eingeteilt in verschiedene Höhenbereiche der KRB Standorte.

Höhenbereich	N Stationen	KRB ($eq\ ha^{-1}\ yr^{-1}$)	PINETI-2 ($eq\ ha^{-1}\ yr^{-1}$)	Verhältnis KRB/PINETI-2
0-250	14	1250	1217	1.03
250-500	15	1667	1267	1.32
500-750	20	1709	1205	1.42
> 750	10	1861	1158	1.61

Fazit

Die Biodiversität in Deutschland ist noch immer durch den Eintrag von Schad- und Nährstoffen in die Ökosysteme gefährdet. Innerhalb des PINETI-2 Projektes wurden daher die atmosphärischen Einträge dieser Schad- und Nährstoffe für Deutschland für das Jahr 2009, 2010 und 2011 ermittelt. Die trockenen, nassen und feuchten Einträge von NHx, NOy, SOx und die Einträge der basischen Kationen wurden berechnet und zur Gesamtdeposition aufsummiert. Die ermittelten mittleren Depositionsflüsse über Deutschland für Stickstoff und Schwefel in 2009 betragen 1057 und 288 $eq\ ha^{-1}\ a^{-1}$. Die Ergebnisse für 2010 sind im Durchschnitt über Deutschland ähnlich wie 2009. Die ermittelten Flüsse für 2011 sind systematisch niedriger, weil es ein sehr trockenes Jahr war, und wurden nicht als repräsentativ klassifiziert. Es wurden flächendeckende Karten für die unterschiedlichen Landnutzungsklassen erstellt. Die Karten zeigen, dass die Variabilität der Deposition über Deutschland signifikant ist. Die höchsten Einträge sind in Waldbeständen in oder in der Nähe von Regionen mit intensiver Landwirtschaft und Industrie zu finden. Im Vergleich zu den Ergebnissen des MAPESI-Vorhabens (Builtjes et al., 2011) sind die Ergebnisse der neue Erhebung etwa 27% niedriger. Dies lässt sich durch eine Verbesserung der Methodik zur Bestimmung der nassen Deposition und der Konsolidierung neuer Prozessbeschreibungen im LOTOS-EUROS Modell erklären. Letztere Modellentwicklungen haben zu einem besseren Vergleich der Modellergebnisse zu Beobachtungen geführt. Die PINETI-2 Einträge stimmen besser mit Daten aus dem „Integrated Monitoring" Programm und mit der Depositionskartierung von EMEP überein als die MAPESI Ergebnisse. Der Vergleich mit Resultaten der Kronenraumbilanzmodellierung zeigt, dass sich die Unterschätzung dieser Daten im Vergleich zu MAPESI vergrößert hat. Die Unterschätzung ist an Standorten in Höhenlagen, an welchen ein erhöhter Eintrag durch feuchte Deposition anzunehmen ist, am größten.

Summary

Biodiversity in Europe is strongly affected by the deposition of pollutants and nutrients on terrestrial ecosystems. The goal of the PINETI-2 project was to quantify the atmospheric deposition of these pollutants and nutrients for Germany in the years 2009, 2010 and 2011. To this end the dry, wet and occult deposition of NH_x, NO_y, SO_x and base cations Ca^{2+}, Mg^{2+}, K^+ und Na^+ were calculated, that together form the total deposition. Critical load exceedances for sensitive ecosystems were derived from the calculated deposition and information on the critical loads for specific ecosystems. Chapters 1 and 2 contain an introduction to the topic and a description of the methodology. Chapters 3 to 8 further describe the methodology of each separate step in the process and presents the results for 2009. In Chapter 9 the results for 2010 and 2011 are presented and compared to 2009.

Determination of deposition

For the quantification of the total influx of pollutants and nutrients into ecosystems via deposition, the three deposition pathways all need to be considered. In this study, five calculation steps are carried out to this end:

1. **Calculation of deposition and concentration fields based on meteorological data and an emission database using a chemistry transport model** (Result: dry deposition for N and S). Dry deposition measurements are currently only performed during research projects; there is no observation network for dry deposition. This means that the dry deposition for the whole of Germany can only be determined through use of a chemistry transport model. These models can be validated using observations of e.g. concentrations of substances in air or precipitation or by comparing the results to those of other models.

   In this study the LOTOS-EUROS model is used, that has been applied among others to answer questions in the field of the nitrogen and sulphur cycle and that has proved its quality in several international comparison studies (e.g. Schaap et al., 2015; Im et al., 2015; Vautard et al., 2006). In the version used in this work LOTOS-EUROS includes a parameterization of the compensation point for ammonia, thus accounting for the bi-directional exchange of ammonia for which ecosystems can be sinks as well as sources. The model is run over Germany with a resolution of about 7*7 km². Crucial input data are meteorological data, land use data and the officially reported emission database. The spatial distribution of emissions was done following the method developed in PAREST. Meteorological data from the European Centre of Medium Range Weather Forecasting (ECMWF). Details of the model setup are described in Section 3.1.

2. **Calculation of wet deposition fields based on observations.** The interpolation of observations of measured concentrations in rain to produce a deposition field covering the entire surface of Germany is performed using geostatistical methods, whereby the information about the spatial distribution from the chemistry transport model is also used for N and S (result: wet deposition). The methodology is described in detail in Wichink Kruit et al. (2014); a summary can be found in section 4.1.

3. **Use of a heuristic approach to estimate occult deposition.** The concentration in fog water is derived from the concentration in rainwater (see point 2) using empirical factors. Using calculated deposition rates, the contribution of fog water to deposition is calculated (result: occult deposition). Details on the methodology can be found in chapter 5.

4. **Use of a scavenging ratio approach for the calculation of the dry deposition for the base cations.** In this approach, the air concentration is derived from the concentration in rain using empirical factors. The dry deposition is then determined using calculated deposition rates (result: dry deposition for base cations). The method is described in chapter 6.

5. **Transformation of the results of dry and occult deposition on the finely resolved 1*1 km² raster and addition of all partial flows to the total deposition with a spatial resolution of 1*1 km² (result: total deposition).**

Table 7 and Figure 5 show for each component which of the calculation steps listed above are carried oud and what data are underlying the calculations.

Table 7.   Overview of the calculation schemes used to assess the deposition for reduced and oxi-dized nitrogen, sulfur and base cat-ions

Approach	NHx	NOy	SOx	Base cations
Chemistry transport modelling	√	√	√	
Empirical wet deposition	√	√	√	√
Empirical occult deposition	√	√	√	√
Empirical dry deposition				√
Addition of all fluxes	√	√	√	√

Figure 5.   Schematic of the assessment methodology used in this study. The scheme introduces important input data (dark blue boxes), key intermediate results (light blue boxes), calculation steps (dashed boxes) and final results (Green boxes). The arrows indicate dependencies. Some data flows are dependent on the assessed components, which are indicated.
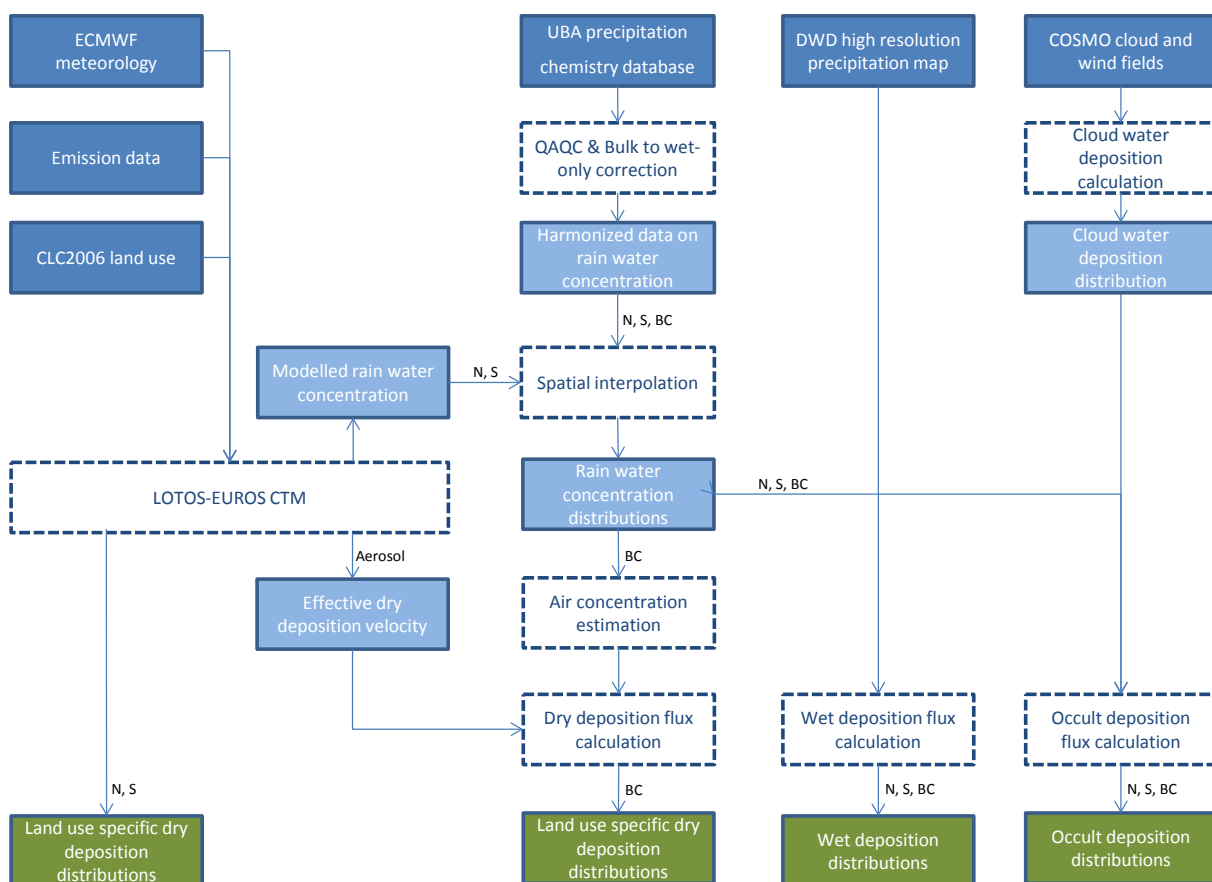
Figure 6.   Overview of the spatially resolved total deposition for all components considered for Germany, 2009
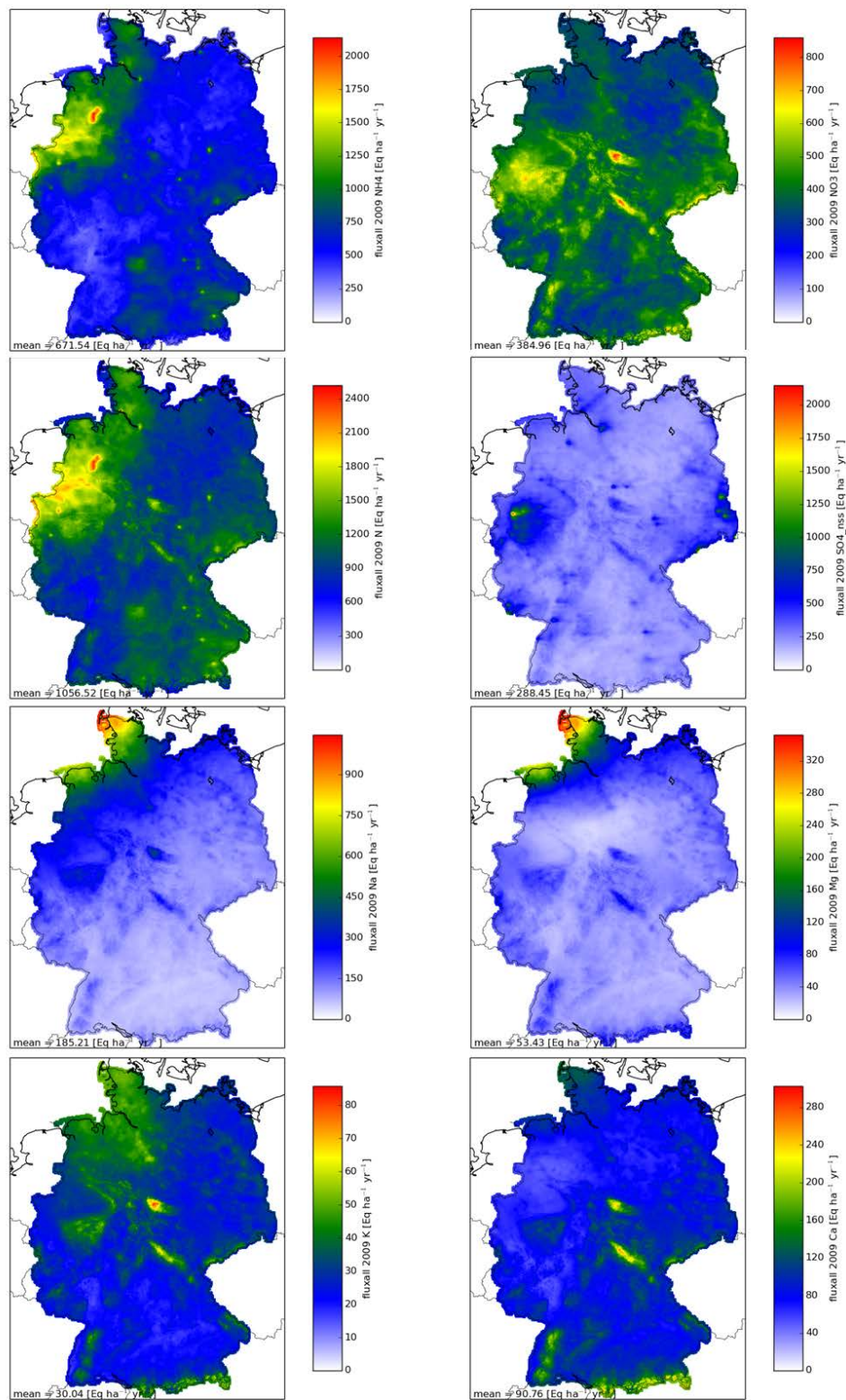
Results

The calculated total deposition as well as the separate wet, dry and occult deposition for all components, averaged over Germany for the year 2009 are listed in Table 1. Figure 6 shows the spatial distribution of the total deposition for all components for 2009. Table 9 lists the average total deposition for the ten land use classes taken into account for total nitrogen and sulfur. On average over Germany the total deposition of N is 1057 eq ha^{-1} yr $^{-1}$, for non sea salt sulfur this is 288 eq ha^{-1} yr $^{-1}$. The maximum of total N deposition is in the North-West and South-East of Germany, because these are the areas with the highest intensity of agriculture. Note that the spatial distribution of oxidized nitrogen differs from that of reduced nitrogen. In regions without intensive agriculture, the relative contribution of oxidized nitrogen to the total nitrogen deposition is larger. In regions like the Black Forest, over half of total nitrogen deposition is oxidised. Sulfur deposition is highest in the Ruhr area with secondary maxima occuring in the Central Uplands. The deposition on forests is about 25-50% higher than on water bodies, which is caused by the roughness of the terrain and vegetation.

For the base cations sodium (Na$^+$) and magnesium (Mg$^+$) the most important source is sea salt and the deposition maxima occur along the North Sea coast. The distribution of the deposition of potassium reflects anthropogenic influence, with maximum values in regions with the highest precipitation. Calcium comes from anthropogenic sources as well as from sea salt, resulting in deposition maxima in the Central Uplands and coastal regions.

After validation of the simulation results for 2009 the deposition maps for 2010 and 2011 were also produced.

Table 8. Overview of averaged estimates of total deposition fluxes across the German territory for reactive nitrogen, sulphur and base cat-ions in 2009. Data are obtained using the CORINE-2006 land use distribution.

Component	Unit	Wet	Dry	Occult	Total
Ca^{2+}	eq ha^{-1} yr^{-1}	72	17	1	91
Ca^{2+}-nss	eq ha^{-1} yr^{-1}	66	16	1	83
K^+	eq ha^{-1} yr^{-1}	25	5	0.3	30
K^+-nss	eq ha^{-1} yr^{-1}	22	4	0.3	26
Mg^{2+}	eq ha^{-1} yr^{-1}	41	11	0.5	53
Mg^{2+}-nss	eq ha^{-1} yr^{-1}	11	3	0.1	14
BC-nss	eq ha^{-1} yr^{-1}	99	23	1	123
Na^+	eq ha^{-1} yr^{-1}	147	37	2	185
SO_x-S	eq ha^{-1} yr^{-1}	187	120	4	311
SO_x-S-nss	eq ha^{-1} yr^{-1}	170	115	3	288
NH_x-N	eq ha^{-1} yr^{-1}	327	337	8	672
NO_y-N	eq ha^{-1} yr^{-1}	248	131	6	385
N	eq ha^{-1} yr^{-1}	575	467	14	1057

Table 9.   Overview of averaged estimates of deposition fluxes per land use category across the German territory for reactive nitrogen and sulphur in 2009.

Land use	Code	total N [eq ha^{-1} yr^{-1}]	total S_nss [eq ha^{-1} yr^{-1}]
Grassland	grs	901	291
Semi-natural	sem	948	301
Arable	ara	982	247
Permanent crops	crp	1043	315
Coniferous forest	cnf	1287	358
Deciduous forest	dec	1183	356
Mixed forest	mix	1235	357
Water	wat	861	291
Urban	urb	1248	283
Other	oth	894	221

Figure 7.   Comparison of the 2009 total N deposition from this study (PINETI-2) and the final assessment in the MAPESI project for 2005 and in the PINETI project for 2009.
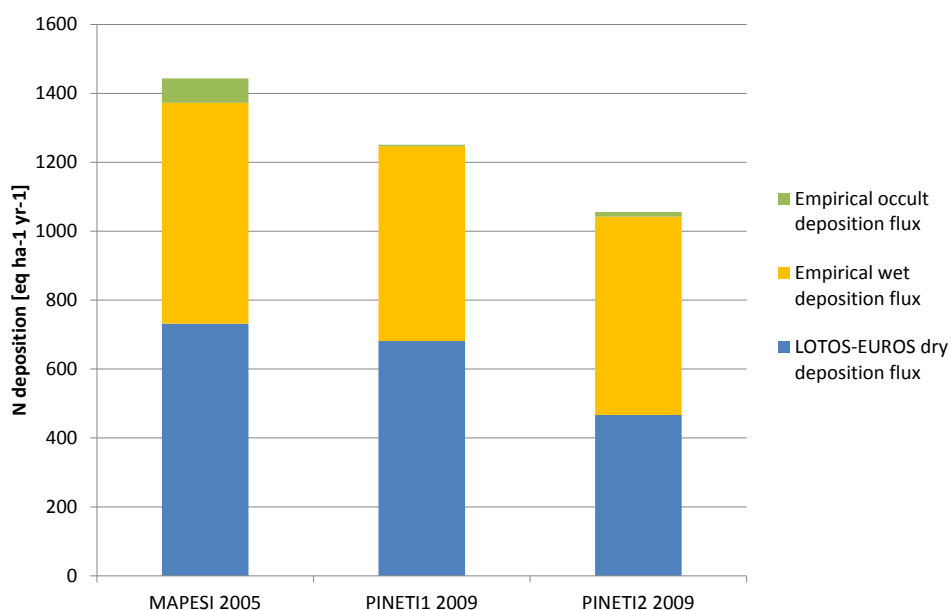
Validation

To validate and better understand the outcomes of PINETI2, the results are compared to observations and other studies.

1. Comparison with previous national deposition calculations

Results of two earlier deposition calculations for Germany were compared to the current results:

- MAPESI project (last year of time series: 2007; Builtjes et al, 2011)
- PINETI project (last year of time series: 2009; Wichink Kruit et al., 2014)
- The year 2009 of the current study (PINETI-2).

Between MAPESI and PINETI-2 there is a systematic decrease of calculated nitrogen deposition of 27% (Figure 7). This decrease is due to an improvement of the spatial interpolation method for the wet deposition observations and a decrease in emissions (between MAPESI and PINETI) and a revision of the parameterisation of several processes in LOTOS-EUROS, which leads to a lower dry deposition (between PINETI and PINETI-2).

2. Comparison with deposition estimates from measurement campaigns

Within Germany there are three stations for which a deposition estimate from dedicated measurement campaigns are available: Forellenbach (Bayerischer Wald), Neuglobsow (Brandenburg) und Bourtanger Moor (Niedersachsen). Although the nitrogen inputs are estimated on the basis of different observation or measurement methods and each of these methods contains uncertainties, the comparison clearly shows that the PINETI-2 data which are now available are closer to these estimates than the results of the MAPESI project. While the PINETI-2 data is within 25% of the estimates, the MAPESI data are 50-100% higher at all three locations (Table 10).

3. Comparison with deposition estimates from EMEP

The comparison of the PINETI-2 results with modelled deposition fluxes from the EMEP model shows that the PINETI-2 deposition estimates are within 4% of the EMEP results (Table 11). Comparing the two EMEP datasets it is clear that also the EMEP results are not constant because of developments in the model and the emission data.

Table 10. Comparison of best estimate results of MAPESI for 2007 and PINETI-2 for 2009 with monitored total N deposition (kg N ha^{-1} yr^{-1}) at three sites across Germany: Forellenbach (Beudert and Breit, 2014), Neuglobsow (Schulte-Bisping and Beese, 2016) and Bourtanger Moor (Mohr et al., 2013)

	total N monitored at station	total N MAPESI 2007	total N PINETI-2 2009
Forellenbach (coniferous forest)	13-15	37	19
Neuglobsow (coniferous forest)	11	18	12
Bourtanger Moor (semi-natural)	25 (16-35)	38	20

Table 11. Comparison of total NOy, NHx and N deposition for 2009 in PINETI-2, EMEP and the 2013 EMEP recalculation.

Variable	Unit	PINETI-2	EMEP	EMEP_rec2013
NOy	eq ha^{-1}	385	351	428
NHx	eq ha^{-1}	672	711	670
total N	eq ha^{-1}	1057	1062	1098

4. Comparison with ambient air concentrations

Modelled dry deposition can only be validated indirectly due to lack of observations. Figure 8 shows the comparison of modelled precursor gases with observations from the state observation networks. For ammonia, it is the first comparison of the LOTOS-EUROS modelling with observations at multiple stations in Germany. The validation shows that all in all, the LOTOS-EUROS model captures the spatial variability of precursor gas concentrations over Germany well. Within separate states the spread is larger. This is especially true for ammonia concentrations, which are strongly influenced by the spatial variability in emissions. This variability is not detailed enough in the emission database to capture the local ammonia gradients in the modelling. The comparison with measurements shows that for NO₂ LOTOS-EUROS underestimates the measured values. This is confirmed by the comparison of modelled and measured wet deposition.

A comparison of the variability of calculated dry deposition velocities for ammonia with a range of observation-based deposition velocities from literature shows that the modelled values are within the range of empirical data. In short, LOTOS-EUROS modelling represents the scientific state of the art.

Figure 8.   Comparison of modelled (y-axis) and measured (x-axis) concentrations of sulphur dioxide, nitrogen dioxide and ammonia in air. Annual average values are shown.
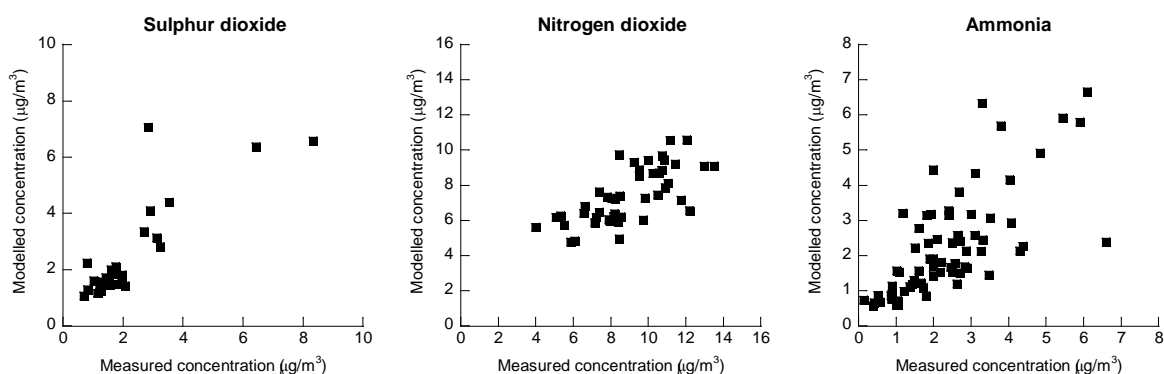
5. Comparison with deposition estimates based on canopy budget measurements and modelling

Another possible method to estimate total N deposition is the use of canopy budget models (Kronenraumbilanz, KRB), which are based on observations and analysis of deposition on vegetation. At first sight, the comparison of KRB modelling results and PINETI-2 results for all available KRB-locations seems to lack correlation (see section 8.2.5). In some places, the underestimation of the KRB results by the PINETI-2 results is even greater than expected. The comparison shows significant differences from state to state. A more detailed analysis, has shown that the comparison is significantly better for relatively flat regions than for stations in mountainous regions. Table 12 shows the mean N total position at the KRB locations divided into four elevation classes. The KRB model results show an increasing tendency of total N deposition with increasing elevation of the KRB station. The PINETI-2 modeling, on the other hand, shows a low variability over the different elevation classes. An analysis at Schauinsland has shown that using the measured concentrations of pollutants in the air, the flows determined using the KRB method could only be reproduced by using exceptionally high deposition velocities. In addition, the results of the comparison of the PINETI-2 data with the KRB data are not supported by the other validation approaches described earlier. The discrepancy between KRB and PINETI-2 could indicate that PINETI-2 results underestimate the (local) influence of occult deposition. The analysis started here shows the need to examine and analyze the observed differences between

KRB modeling and the PINETI-2 results in cooperation with the network operators. Particular attention should be paid to the representativeness of the station in terms of altitude and land use, the influence of occult deposition, the role of organic nitrogen and the assumptions regarding the deposition of sodium under continental conditions. This investigation should confirm or falsify our assumption that the PINETI-2 results are not in contradiction with the KRB modeling since the background loads found in PINETI-2 are not representative for sites exposed to high occult deposition.

Table 12.　　Comparison of PINETI-2 total deposition (eq ha^{-1} yr^{-1}) to deposition estimates derived from canopy budget models after categorizing the stations as function of altitude range. The means over N stations are provided as well as the ratio of the fluxes.

Altitude range	N stations	KRB (eq ha^{-1} yr^{-1})	PINETI-2 (eq ha^{-1} yr^{-1})	Ratio KRB/PINETI-2
0-250	14	1250	1217	1.03
250-500	15	1667	1267	1.32
500-750	20	1709	1205	1.42
> 750	10	1861	1158	1.61

Conclusion

Biodiversity in Germany is still endangered by the deposition of harmful substances and nutrients on ecosystems. Within the PINETI-2 project the atmospheric inputs of these substances for Germany were determined for 2009, 2010 and 2011. The dry, wet and occult deposition of NHx, NOy, SOx as well as basic cations were calculated and summed to the total position. The average deposition fluxes over Germany for nitrogen and sulfur in 2009 are 1057 and 288 eq ha^{-1} a^{-1}. The results for 2010 are, on average for Germany, similar to 2009. The calculated fluxes for 2011 are systematically lower because it was a very dry year and are not viewed as representative. Maps for the various land use classes were developed. The maps show that the variability of deposition over Germany is significant. The highest deposition is in forest stands in or near regions with intensive agriculture and industry. Compared to the results of the MAPESI project (Builtjes et al., 2011), the results of the new survey are about 27% lower. This can be explained by an improved methodology for the determination of wet deposition and the consolidation of new process descriptions in the LOTOS-EUROS model. The latter model developments have led to a better comparison of the model results with observations. The PINETI-2 deposition estimates are more consistent with data from the "Integrated Monitoring" program and the deposition mapping of EMEP than the MAPESI results. The comparison with the results of canopy budget modelling efforts shows that the underestimation of these data has increased compared to MAPESI. The underestimation is greatest at locations at high altitudes, where an increased entry by occult deposition is to be assumed.

1 Introduction

1.1 Background

Biodiversity in Europe is strongly affected by eutrophication and acidification of soils and surface waters. Atmospheric deposition is often the dominating source of reactive nitrogen and sulphur compounds that cause these problems. Current estimates indicate that about 48% of the area of natural and semi-natural ecosystems receive reactive nitrogen at a rate exceeding the critical load. The critical load is the exposure below which significant harmful effects on specified sensitive ecosystems do not occur according to present knowledge. In addition the critical loads for acidification are exceeded on about 8% of the ecosystem area in Germany.

Atmospheric reactive nitrogen compounds can be categorized in oxidized and reduced nitrogen. These two main groups have different sources and fates in the atmosphere as their chemical cycles are different. Nitrogen oxides are emitted during combustion processes. Hence, major sources of oxidized nitrogen are road transport, electricity generation, and shipping. Nitrogen oxides play a key role in atmospheric chemistry. They do not deposit close to their sources as the nitrogen oxides need to be further oxidized before they are effectively deposited. Reduced nitrogen emissions in the form of ammonia are mostly associated with agriculture, though other minor sources play a role. Ammonia is emitted during and after application of fertilizer to the land, from senesces of plants, animal excretion in housing systems, during grazing and after application of manure, in food processing, at industries using NH3 and as a byproduct from car exhaust equipped with a three-way catalyst (Erisman et al., 2007; Galloway et al., 2003). The atmospheric lifetime of ammonia is limited to several hours as it is effectively removed by dry and wet deposition and it readily reacts with sulfuric and nitric acid to form its particulate ammonium salts (Fowler et al., 2009). In contrast to oxidized nitrogen a large proportion of reduced nitrogen is deposited relatively close to its source. Through the formation of ammonium nitrate the atmospheric cycling of reduced and oxidized nitrogen are connected. The particulate salts have a longer atmospheric life time providing a means of long range transport of nitrogen. Assessments of the exposure of sensitive ecosystems and consequent development of mitigation strategies need to take into account the different behaviors among the nitrogen compounds.

The base cat-ions calcium (Ca^{2+}), magnesium (Mg^{2+}) and potassium (K^+) are important nutrients in forest ecosystems. In addition, their concentration – together with sodium – is needed to calculate the deposited acid neutralizing capacity in the assessment of acidification risks. The base cat-ions are associated to alkaline particles, mostly sea salt and combustion particles. Hence, sodium and magnesium are for a large part of natural origin. Calcium is emitted during combustion and may originate from dust suspension. Hence, it is mostly anthropogenic derived. The latter also holds for potassium, which is associated to biomass combustion. Assessments for base cat-ions are challenging as reliable emission information is not available.

To assess the deposition of pollutants to ecosystems one has to take into account the atmospheric budget of these pollutants. Removal from the atmosphere can occur via different deposition pathways: dry deposition, wet deposition and occult deposition:

1. *Dry deposition:* Dry deposition is the direct deposition of gases or aerosols at terrestrial or aquatic surfaces. The dry deposition of gases and particles is a continuous process and governed by their air concentrations, turbulent transport processes in the boundary layer, the chemical and physical nature of the depositing species, and the capability of the surface to capture or absorb the species.

2. *Wet deposition:* Wet deposition or scavenging is defined as the removal of gases and aerosol from the atmosphere by precipitation (rain, hail and snow). The incorporation of pollutants in clouds and precipitation include many different processes. Particles are removed through interception by falling rain or snow, a process known as washout or by incorporation of the particle into cloud

droplets within clouds, a process known as rainout. Other terms often used are in-cloud and below cloud scavenging. Gases are incorporated in and below cloud through solution and oxidation processes. The effectivity of the scavenging processes is highly dependent on particle size and solubility of gases.

3. *Occult deposition:* Occult deposition is associated to orographic clouds and radiation fog. Cloud and fog droplets are large enough to impact efficiently on vegetation. Normally, occult deposition accounts for a small fraction of the total deposition but it is important for hills which are frequently shrouded in clouds. As the air pollutant concentrations in hill clouds are enhanced, this deposition pathway may lead to very high deposition fluxes at exposed locations.

The relative contributions from dry, wet and total deposition may vary largely from location to location. In general, the importance of wet deposition increases with distance to source areas as the concentrations of primary gaseous pollutants with high dry deposition velocities decline through oxidation and gas to particle formation. The latter are most effectively removed by wet deposition.

The development of European mitigation strategies to reduce ecosystem exposure within the UNECE-CLRTP convention is supported by atmospheric modelling using the EMEP model (Simpson et al., 2012). This modelling system is a consensus model applied to the full European domain with a course resolution. In the nineties the EMEP model was used on a 125 km resolution, which was increased to 56 km in the new century. Currently, the assessments are performed at a 28 km resolution. In Germany, and most other countries, it was recognized that this resolution does not provide sufficient detail as it does not give right to the large gradients in reactive nitrogen compounds within these distances. For national and local assessments the resolution provided by EMEP is often not sufficient. Hence national models are needed to provide complementary high-resolution data. A national effort to establish deposition maps through the use of observations and independent modelling is important for several additional reasons. First, it builds knowledge and capacity within the country. Second, national activities provide a means to incorporate the best available information available within Germany. Third, provides valuable feedback and experience needed to improve the international consensus model. Finally, being independent secure that the requirements of national praxis are met.

In short, to underpin the assessment of critical load exceedances as well as supporting environmental impact assessments for new economic activities insight in the deposition distribution to ecosystems is necessary.

1.2   Goals

The main goal of this study it to provide quantitative estimates of the deposition of atmospheric pollutants to ecosystems across Germany and to compare these against available critical load distributions. The requirements for the deposition maps are:

-    The maps should be covering the whole German territory at 1x1 km² resolution

-    Separate maps should be available for the major land use classes; Grass land, arable land, permanent crops, semi-natural vegetation, deciduous forest, coniferous forest, mixed forest, urban areas and water bodies.

-    The maps should be available for nitrogen compounds, sulphur compounds and base cat-ions.

-    The maps should differentiate the three main deposition pathways; wet, dry and occult deposition.

-    The maps should be delivered in Gauss-Krüger coordinate system in an ESRI-compatible format for inclusion in the UBA GIS database.

1.3   Structure of the report

In chapter 2 an overview of the approach for the deposition mapping is provided. The approach can be divided in four different steps related to the assessment of the three deposition pathways and a separate treatment of base cat-ion deposition. The methodologies and results of these steps are presented in chapter 3 to 6. In chapter 7 the total deposition estimates for 2009 are presented, after which the results are discussed in more detail in chapter 8. In chapter 9 the results for 2010 and 2011 are briefly presented. Finally, a short summary is given in chapter 10 and recommendations for improvements are made.

2 Methodology of the deposition mapping

To estimate the deposition of atmospheric pollutants to ecosystems across the German territory one has to make a complete assessment of the different deposition pathways. As the observation basis and modelling capacity for the three pathways and individual components differ largely, it is not possible to make an assessment with one consistent methodology. Hence, we use a tiered approach in which five calculation schemes can be differentiated. These schemes are:

1. Chemistry transport modelling (dry deposition)
2. Empirical wet deposition
3. Empirical occult deposition
4. Empirical dry deposition
5. Addition of all fluxes

As there are a number of interdependencies between these schemes this is also the order in which the calculations take place. Below, we discuss these steps shortly as they are provided in more detail in following chapter. Table 13 and Figure 9 provide an overview of the approach.

Table 13.　　　Overview of the calculation schemes used to assess the deposition for reduced and oxidized nitrogen, sulfur and base cat-ions

Approach	NHx	NOy	SOx	Base cations
Chemistry transport modelling	√	√	√	
Empirical wet deposition	√	√	√	√
Empirical occult deposition	√	√	√	√
Empirical dry deposition				√
Addition of all fluxes	√	√	√	√

2.1 Chemistry transport modelling of wet and dry deposition (step 1)

As there is a lack of dry deposition observations we rely on chemistry transport modelling to assess the land use specific dry deposition distributions across Germany. Here we use the LOTOS-EUROS model. It is a regional 3-D Chemistry Transport Model (CTM) that simulates emission, transport, chemistry and deposition of air pollutants in the lower troposphere (Schaap et al., 2008). The LOTOS-EUROS model has a long history studying the atmospheric nitrogen and sulphur cycles. The LOTOS-EUROS model is state-of-the-art and is one of the few chemistry transport models that uses a description of the bi-directional surface–atmosphere exchange of NH_3 (Wichink Kruit et al., 2010; 2012). The model is used to model the dry deposition distributions for nitrogen and sulphur components at 7x7 km² across Germany. For this purpose we use ECMWF meteorology and emission data for the respective years. Long range transport is incorporated by nesting the German study area into a simulation over Europe as a whole. Besides the deposition fluxes also the modelled dry deposition velocities and wet deposition maps are used in the next steps of the deposition assessment.

2.2 Empirical wet deposition (step 2)

The LOTOS-EUROS model used in this study has a tendency to underestimate the observed wet deposition. Moreover, the variability in wet deposition fluxes is generally underestimated in chemistry transport models. Consequently, it has been decided to use the observed wet deposition as a basis. Wet deposition is monitored by simple methods (precipitation collectors) analysed for major anthropogenic and natural ions. As the monitoring is rather straightforward, a few hundred sites from different net-

works measure precipitation chemistry in Germany. Note that the networks of collectors for precipitation chemistry are much less dense than precipitation collectors for the national meteorological services, mainly because of the costs of chemical analysis. The density of the observations allow to make an empirical assessment of the wet deposition flux across Germany. The data we use are obtained from the UBA precipitation chemistry database. UBA collects the data form the measuring networks and includes it into it`s database. We harmonize the data and perform a quality control and quality assurance procedure to establish the annual average concentration in rain at the measurement locations. These data are used to correct the modelled rain concentration distribution towards the observed data using residual Kriging. The resulting rain water distribution is combined with a high resolution precipitation distribution (1x1 km) to arrive at the final wet deposition estimates. In this way a highly resolved map based on empirical data is obtained that benefits from the process knowledge incorporated in the LOTOS-EUROS model for nitrogen and sulphur components. The base cat-ions wet deposition is solely based on observations as the chemistry transport modelling for these components is not considered to be reliable due to insufficient knowledge on their emissions.

2.3 Empirical occult deposition (step 3)

Currently, none of the European eulerian chemistry transport models incorporates a parameterization of the occult deposition. For countries with only small areas of upland, this will not lead to significant underestimates in total deposition. However, for elevated locations it may be a substantial contribution to total deposition. Hence, it is important to simulate the process in mapping regional deposition, to avoid underestimating total deposition and exceedances of critical loads. In this study the occult deposition flux is derived by estimating the deposition flux of cloud and fog water which is combined with the pollutant concentration in the cloud water. The cloud water concentrations are deduced from the rain water concentrations under assumption that a pollutant is more concentrated in a cloud droplet than in a rain droplet. The challenge to estimate the occult deposition is to capture the variability in the cloud deposition flux which is strongly dependent on altitude, slopes and local meteorology. Therefore, we use a high resolution meteorological data available for Germany as a whole, i.e. 7x7 km^2. Note that this resolution is not able to capture high resolution variability, which means that the occult deposition reflects background values for larger regions and do not reflect the deposition at very exposed sites.

2.4 Empirical dry deposition for base cat-ions (Step 4)

Base cat-ions derive from distinct sources such as the ocean (Na^+, Mg^{2+}), soils (Ca^{2+}, K^+) and the burning of biomass (Ca^{2+}, K^+). Within the MAPESI project (Builtjes et al., 2011) the explicit modelling of the dry deposition of base cat-ions using the LOTOS-EUROS model has been tested. It was found that important emission sources of the base cat-ions such as wood combustion are very uncertain. Furthermore, the emission timing and spatial allocation of these emissions are not well known. It was concluded that at this moment these uncertainties make it impossible to model the deposition flux of base cat-ions to Germany with sufficient certainty. Hence, the dry deposition of Na^+, Ca^{2+}, Mg^{2+}, K^+ are calculated in a postprocessing procedure applying the so called 'Scavenging ratio approach'. In this approach the air concentrations are estimated from the rain water concentration maps and multiplied by the modelled effective dry deposition velocity distribution at the reference height from the chemistry transport model to arrive at a dry deposition estimate.

2.5 Total deposition estimates (step 5)

To arrive at the final result the distributions of the three fluxes are simply added. This addition takes place on the final 1x1 km^2 grid. For this purpose the fluxes for the occult and dry deposition are first resampled to this higher resolution.

Figure 9. Schematic of the assessment methodology used in this study. The scheme introduces important input data (dark blue boxes), key intermediate results (light blue boxes), calculation steps (dashed boxes) and final results (Green boxes). The arrows indicate dependencies. Some data flows are dependent on the assessed components, which are indicated.
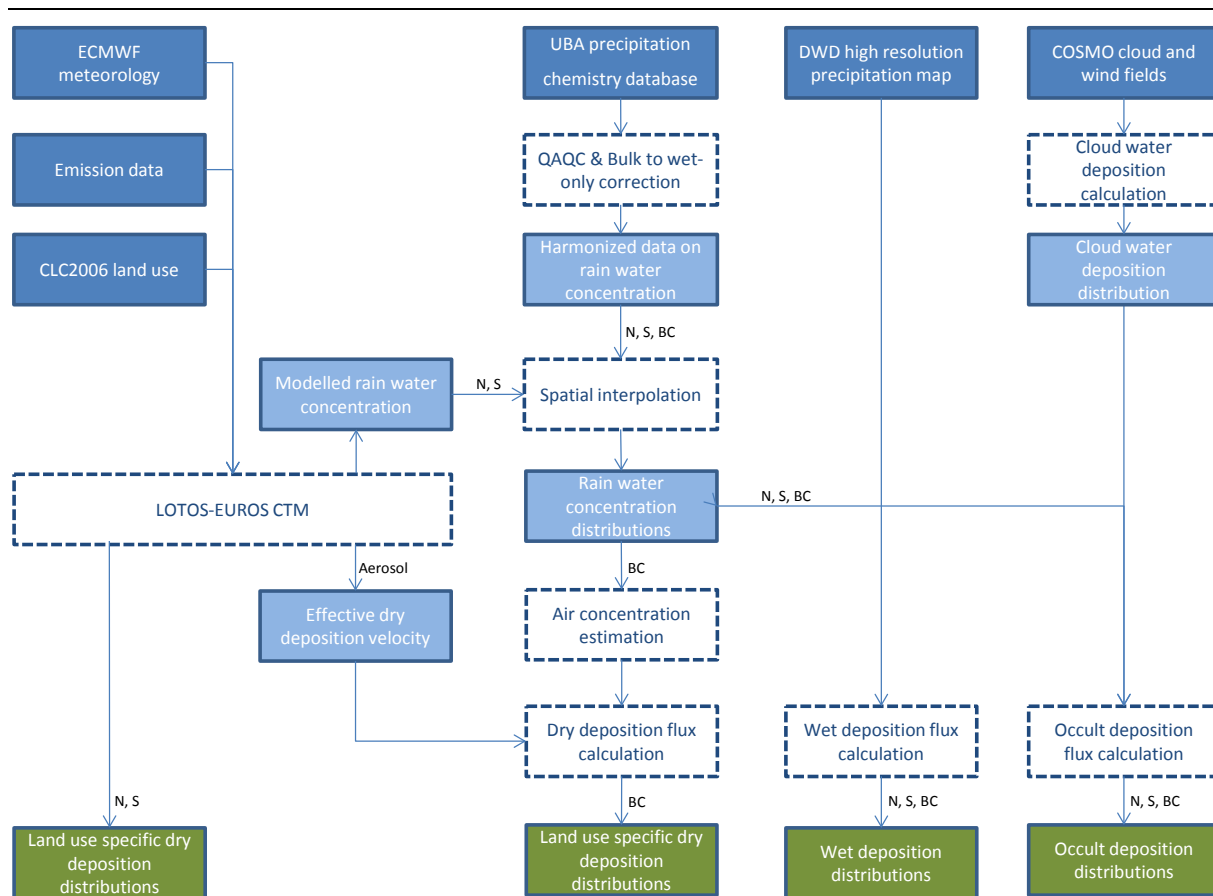
Finally, the deposition fluxes of non-sea salt components, i.e., Ca^{2+}-nss, Mg^{2+}-nss and K^+-nss, are calculated using a sea salt correction based on the assumption that all sodium derives from sea salt. The sea salt fraction of each component is calculated using the factors listed in Table 14, which represent the ratios of the components against sodium in fresh sea salt (CLRTAP (2004); see Table 2.1).

Table 14. Conversion table for sea salt fractions (CLRTAP (2004); Table 2.1)

	Ca^{2+}	Mg^{2+}	K^+	Na^+	SO_4^{2-}
eq X/eq Na^+	0.043	0.228	0.021	1.000	0.120
g X/g Na^+	0.037	0.120	0.036	1.000	0.250

3 Modelled dry deposition distributions using LOTOS-EUROS

To assess the land use specific dry deposition distributions across Germany one has to apply a modelling system. In this study we use the LOTOS-EUROS model. Below we describe the model, its application and its results for 2009.

3.1 Model description and application

3.1.1 LOTOS-EUROS Model system

The 3-D regional chemistry transport model LOTOS-EUROS is aimed at the simulation of air pollution in the lower troposphere. The model is of intermediate complexity in the sense that the relevant processes are parameterized in such a way that the computational demands are modest enabling hour-by-hour calculations over extended periods of several years within acceptable computational time. The model is a so-called eulerian grid model, which means that the calculations are performed on a fixed three dimensional grid. On this grid the concentration changes due to advection, vertical mixing, chemical transformations and removal by wet and dry deposition are performed. A sketch of such a model system is given in Figure 10. The process calculations require information about anthropogenic emissions, land use and meteorological conditions, which have to be prescribed to the model system. The results of the model are stored in output files that contain modelled air pollutant concentrations and deposition fluxes.

Figure 10.   A sketch of an eulerian chemistry transport model such as LOTOS-EUROS
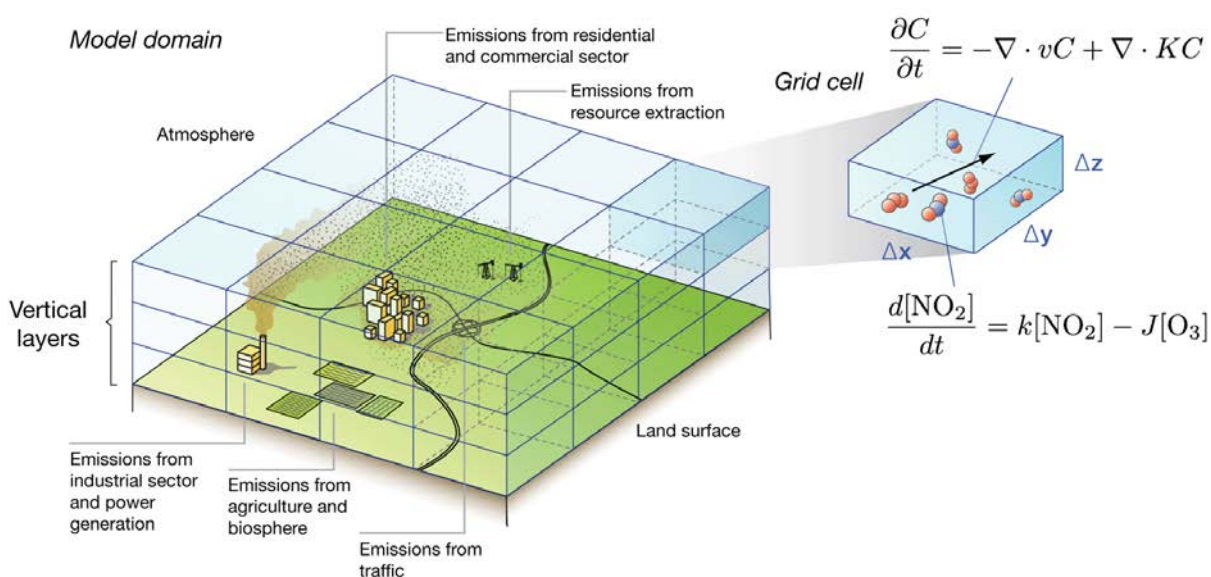
Many scientific studies have been carried out with previous (and the current) versions of the LOTOS-EUROS model studying secondary inorganic aerosol (Schaap et al., 2004b; 2011; Erisman and Schaap, 2004; Banzhaf et al., 2014), sea salt (Manders et al., 2010), particulate matter (Manders et al., 2009; Hendriks et al., 2013), ozone (Curier et al., 2012; Beltman et al., 2013), nitrogen dioxide (Schaap et al., 2013; Curier et al., 2014) and ammonia (Wichink Kruit et al., 2012a; Van Damme et al., 2014). For details of the model we refer to these publications and to the model documentation (www.lotos-euros.nl).

The LOTOS-EUROS model has a long history studying the atmospheric nitrogen and sulphur cycles. Given the complexity of the nitrogen cycle it is continuously under development. Prior to the execution of the final simulation we have consolidated all major scientific developments of the last 4 years into the LOTOS-EUROS version 1.10 as used in this study. The major features of this model version are:

- the bi-directional surface–atmosphere exchange of ammonia is accounted for following Wichink Kruit et al., 2012b). The approach is basically a parameterization based on flux measurements in the Netherlands which was incorporated into the surface–atmosphere exchange module DEPAC, i.e. DEPosition of Acidifying Compounds, as described in Van Zanten et al. (2010). Because flux measurements point into the same direction in all land use classes, the ammonia compensation point is assumed to be the same in all land use classes within a grid cell.
- The deposition of particles is represented adapting the methodology of Zhang et al. (2001).
- A new pH dependent cloud chemistry scheme is included (Banzhaf et al., 2012).
- A new scheme for in- and below-cloud scavenging of gases and particles that includes droplet saturation (Banzhaf et al., 2012).
- Secondary inorganic aerosol formation is treated by the ISORROPIA2 routine, in which the partitioning between the gas and aerosol phase is described for ammonia/ammonium and nitric acid/nitrate (Fountoukis and Nenes, 2007).
- Reaction of nitric acid with sea salt to for coarse sodium nitrate is included in a dynamical way (Wichink Kruit et al., 2012a).

For a detailed description of the deposition parameterisation including compensation point and land use specific parameters we refer to the model documentation (www.lotos-euros.nl) and Wichink Kruit et al. (2012). The impact of the developments on the modelled deposition distributions is discussed in section 8.1.1. This version of the model is state-of-the-art. The LOTOS-EUROS model is one of the few chemistry transport models that use a description of the bi-directional surface–atmosphere exchange of NH_3. In short, the new model system is shown to improve considerably as modelled concentrations and wet deposition fluxes are in general closer to observations.

3.1.2 Simulation description

For the model simulation in this study, the geographic projection is equirectangular with a grid size resolution of 0.125° longitude by 0.0625° latitude, approximately 7 by 7 km² at the latitude under consideration here. For its boundary conditions, this 'zoom' run makes use of a larger European run, with a grid size resolution of 0.5° longitude by 0.25° latitude, approximately 36 by 28 km². In the vertical, the model is based on the well mixed dynamic boundary layer concept, i.e., there are three dynamic layers and a surface layer. The lowest dynamic layer is the mixing layer, followed by two reservoir layers. The height of the mixing layer is obtained from the ECMWF meteorological input data used to drive the model. The meteorological data are obtained at the model resolution from ECMWF (i.e. interpolation performed by ECMWF procedures) and are provided on an 3-hourly basis. The data are interpolated to the hours of the day. The height of the reservoir layers is determined by the difference between ceiling and mixing layer height. A surface layer with a fixed depth of 25 m is included as part of the mixing layer to monitor ground-level concentrations. The total vertical model extend is 3.5 km above the Earth's surface.

The emissions that are used by the LOTOS-EUROS model are different for the two modelling domains. For the European background run emissions are obtained from the TNO MACC-II European emission inventory for the year 2009 and have a 0.125° longitude by 0.0625° latitude gridsize resolution (Pouliot et al., 2012; Kuenen et al., 2014).

The emissions for the zoom run over Germany are based on the PAREST emission database. This database contains sector specific emissions for the year 2005 on a regular grid with a resolution of 1/60° longitude by 1/60° latitude (about 1.2 x 1.9 km²). This emission inventory has been produced by the Institut für Zukunftsstudien und Technologiebewertung (IZT) and the Institut für Energiewirtschaft und Rationelle Energieanwendung (IER) from the University of Stuttgart within the PAREST project (Jörß et al., 2010). This is the most up-to-date inventory with a detailed spatial distribution across the whole country. To account for the emission situation in 2009-2011 the PAREST emissions for Germany are scaled by a constant factor (for each substance and sector) to the officially reported emission totals

for 2009, 2010 and 2011 as reported in 2014 by UNECE/CLRTAP (UBA, 2014). Hence, the spatial allocation is maintained as it was estimated for 2005 while the emission totals are updated. Land use is represented by the 2006 version of the Corine Land Cover database (CLC 2006). All simulations are started with a one-month spin up period prior to the year of interest, i.e. 2009.

3.2   Results

3.2.1   Modelled deposition distributions

The modelled distributions of dry and wet deposition of reactive nitrogen and sulphur are shown in Figure 11. Averaged over Germany and all ecosystems the total deposition is 908 and 268 eq ha^{-1} a^{-1} for N and S, respectively. On average, the division between dry and wet deposition is about equal. However, the ratio shows variability as in source areas for ammonia, nitrogen oxides and sulphur dioxide the dry deposition dominates. In more remote regions the wet deposition is about two times more important than the dry flux. Dry and wet deposition of N maximises in the north west of the country and in the south east, basically mirroring the distribution of animal density. Near the Alpine range in Bavaria increased wet deposition is modelled due to high precipitation amounts. Besides the impact of ammonia source areas also some of the larger cities can be recognized in the distribution. For sulphur the deposition is highest in the Ruhr area, where most of the German SO$_x$ emissions take place. In addition, some other industrial (harbour) areas can be recognized as well as the impact of shipping emission in the coastal Bundesländer of Schleswig-Holstein and Niedersachsen.

The dry deposition flux is strongly dependent on land use category through surface roughness and physic-chemical properties of the pollutants such as solubility or reactivity. In Table 15 the land use dependent dry, wet and total deposition are listed. The comparison between land use classes clearly illustrates that the higher roughness of the forest classes cause increased dry deposition compared to low vegetation classes such as grasslands. Species dependency is illustrated when comparing the sulphur dry deposition flux to water compared to those of grass and arable lands. The solubility of SO$_2$ causes the dry deposition of sulphur to be higher to water, although the surface roughness of water is lower.

Figure 11.   Annual distributions of dry (left) and wet (right) deposition for reactive nitrogen (upper panels) and sulfur (lower panels).
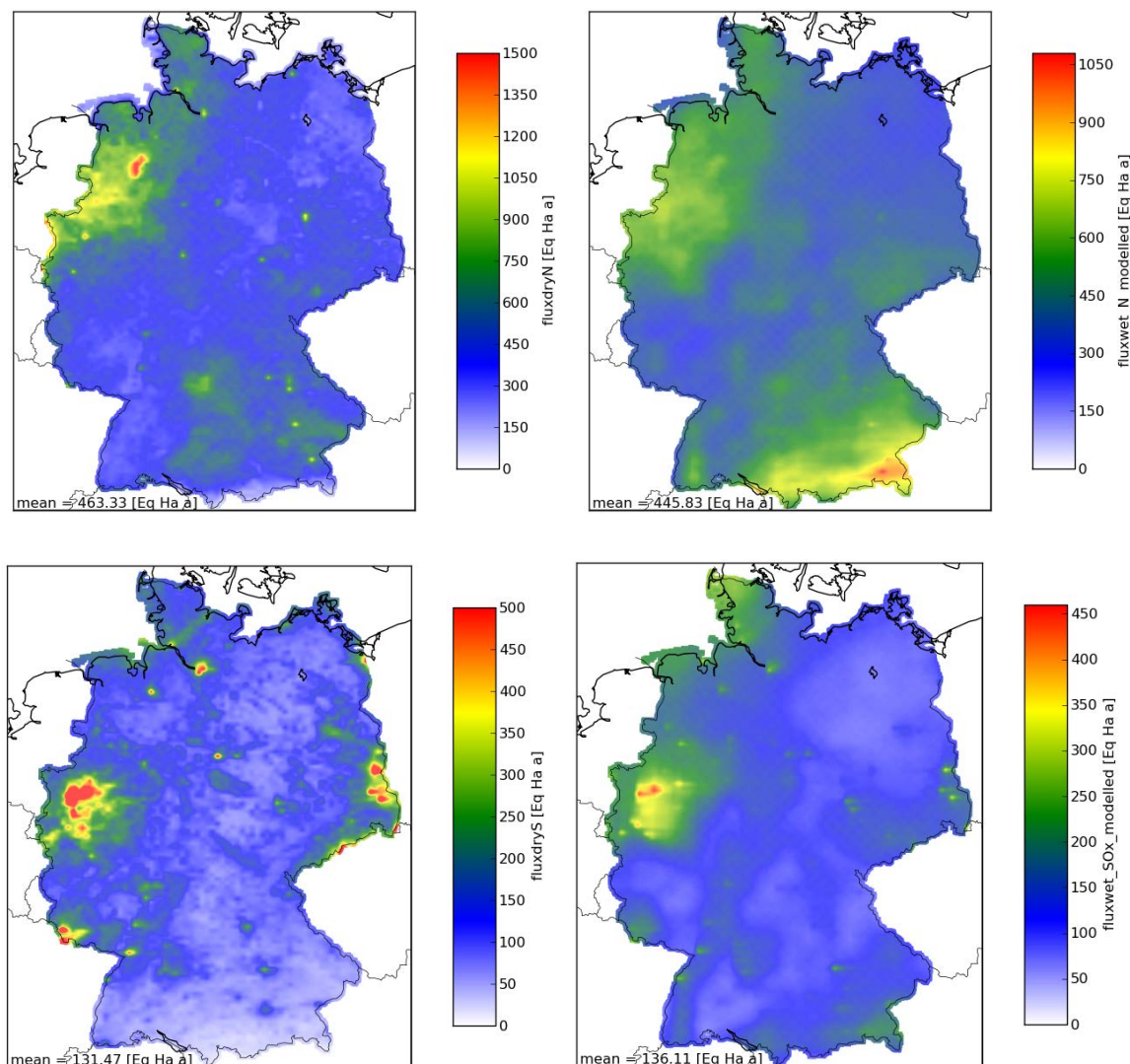
Table 15.   Overview of averaged modelled deposition fluxes (eq ha^{-1} a^{-1}) per land use category across the German territory for the year 2009.

land use	abbreviation	dry N	wet N	total N	dry S	wet S	total S
arable	ara	406	446	852	92	136	228
coniferous	cnf	666	446	1112	205	136	341
deciduous	dec	558	446	1004	203	136	339
grassland	grs	325	446	771	129	136	266
other	oth	318	446	764	62	136	198
crops	crp	467	446	913	145	136	281
semi-natural	sem	372	446	818	146	136	282
water	wat	285	446	731	127	136	263
urban	urb	672	446	1118	147	136	283
mixed forest	mix	612	446	1058	204	136	340

Table 16.   Land use dependent annual effective and average dry deposition velocity at 2.5 meter height (above zero-displacement height and roughness length) across land use types in Germany for six components in cm/s for the year 2009.

V_d	NO₂		NO		HNO₃		NH₃		SO₂		SO₄²⁻ (fine)	
[cm/s]	Eff	Ave	Eff	Ave	Eff	Ave	Eff	Ave	Eff	Ave	Eff	Ave
ara	0.10	0.15	0.03	0.02	1.20	1.04	0.71	0.82	0.32	0.46	0.08	0.09
cnf	0.15	0.24	0.03	0.02	1.63	1.52	1.23	1.83	0.75	0.91	0.16	0.20
dec	0.13	0.21	0.03	0.02	1.63	1.52	0.95	1.48	0.74	0.90	0.16	0.20
grs	0.08	0.15	0.03	0.02	1.11	0.98	0.58	0.88	0.56	0.63	0.07	0.08
oth	0.07	0.07	0.05	0.05	0.89	0.81	0.56	0.56	0.21	0.30	0.04	0.04
crp	0.13	0.18	0.03	0.02	1.42	1.22	0.81	1.03	0.66	0.76	0.10	0.11
sem	0.08	0.16	0.03	0.02	1.24	1.08	0.63	0.97	0.60	0.68	0.10	0.12
wat	0.05	0.05	0.05	0.05	0.67	0.62	0.48	0.60	0.59	0.57	0.08	0.09
urb	0.08	0.08	0.08	0.08	2.94	2.58	1.09	1.32	0.43	0.82	0.14	0.17
mix	0.14	0.23	0.03	0.02	1.63	1.52	1.09	1.65	0.75	0.90	0.16	0.20

Figure 12.   Ammonia concentration distribution (µg/m³) at 2.5m (above zero-displacement height and roughness length) (left) and effective dry deposition velocity (cm/s) (right) above coniferous forest for the year 2009.
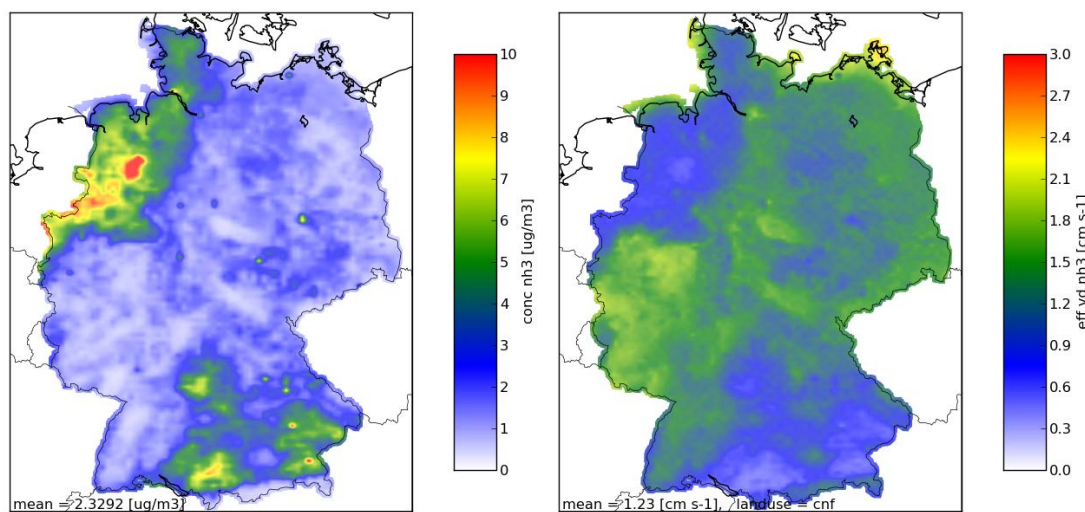
In Table 16 the average (=1/(Ra+Rb+Rc)) and effective (=annual average flux/concentration) dry deposition velocities to land use classes are summarized. Note that the effective dry deposition velocities are usually lower than those of the average velocity. This is due to the anti-correlation between the dry deposition velocity and the atmospheric concentration of most pollutants that together determine the flux. For example, NO₂ concentrations show a daytime and summer minimum, whereas the dry deposition velocity maximizes at these times. Hence, the annual effective dry deposition velocity is lower than the mean of the hourly velocities. The only exception is nitric acid, i.e., HNO₃. Nitric acid concentrations (daytime and summer maximum) correlate strongly with the dry deposition velocity leading to a higher effective than average dry deposition velocity.

For most pollutants the distribution of the annual mean and effective deposition velocities (at 2.5 m above zero-displacement height and roughness length) show little variation across Germany, although the seasonal variability in the dry deposition velocity itself is larger in the more continental south than in the north. The deposition velocity of ammonia behaves differently as it includes the impact of the compensation point. Figure 12 clearly illustrates the inverse relationship between the concentration level (left panel) and the effective dry deposition velocity for coniferous forest for ammonia (right panel). This inverse relationship is caused mainly by the compensation point. In ammonia rich areas the vegetation is saturated with ammonia to a certain degree limiting the uptake and causing re-emission of ammonia during the day. Therefore the concentrations increase whereas the flux is lower in comparison to a situation with a very low or no compensation point, and thus the effective deposition flux ($V_{d\_eff} = F/c$) becomes lower in source areas. In the large forest areas in Germany effective deposition velocities up to 2 cm/s are modelled, whereas in ammonia rich areas in Niedersachsen and Bavaria values well below 1 cm/s are modelled. In Figure 13 we compare the range of modelled annual mean dry deposition velocities across Germany to a compilation of values reported in literature (Schrader and Brümmer, 2014). The literature data have been obtained by a host of different methodologies spanning different climatic conditions. Some studies reported effective deposition velocities and others the mean or median values. Moreover, the modelled deposition velocities refer to 2.5 m height, whereas the literature data often do not specify the representative height. Despite these uncertainties and the tentative nature of the comparison the results show that the modelled dry deposition velocities compare well with literature values.

Figure 13.   Comparison between the range of annual mean dry deposition velocities (cm/s) for ammonia across Germany and the range average of ammonia deposition velocities reported in literature as compiled by Schrader and Brümmer (2014).
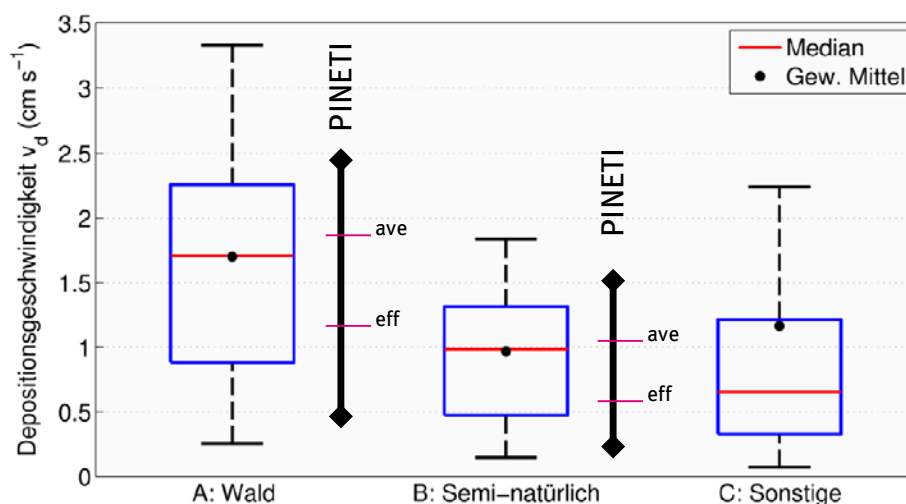
3.2.2   Evaluation of modelled concentration and deposition distributions

In Figure 14, the distributions of the NO_2, HNO_3, NO_3^-, NH_3, NH_4^+, SO_2 and SO_4^{2-} concentrations over Germany are shown. It is clearly visible that the concentration distributions of NH_4^+, NO_3^- and SO_4^{2-} show a good correspondence with the concentration distributions of NH_3 and SO_2. NH_3 is mainly occurring in the agricultural intensive northwest and southeast of Germany, while SO_2 is mainly occurring in the industrial Ruhr area. The abundance of these precursor gases leads to elevated secondary inorganic aerosol levels in these areas. Note that the HNO_3 concentration distribution shows reduced levels in the ammonia rich areas, indicating that most of the HNO_3 is converted into NO_3^- aerosol.

In this section we present results of the model evaluation against observations. Unfortunately, concentration data on total ammonia, total nitrate and sulphate from the UBA network used in previous studies are not available for 2009 anymore. Hence, we concentrate the concentration evaluation on nitrogen dioxide and sulphur dioxide. An additional effort to evaluate the model results against ammonia measurements is reported in section 8.2.1. In addition, we provide a comparison against the available wet deposition measurements.

3.2.2.1 Air concentrations

Data from the UBA air quality database are used here to compare to our model results. For this comparison a rigorous selection of the stations is needed, as effects of local sources need to be excluded as far as possible. Hence we used only stations classified as rural background stations, located below an altitude of 1000m and providing a data coverage of more than two thirds for 2009. In addition we excluded stations with a minimum value in the whole time series above 2 µg m^{-3} and stations showing strong indications for a pronounced influence of local sources (this was assumed when NO_2 concentrations exceed 20 µg m^{-3} on most days of the year). The subsequent comparisons were performed with the remaining 31 stations for SO_2 and 45 stations for NO_2.

In Figure 15 the comparison of the modelled and observed annual average concentrations are shown. The stations have received symbols according to the state they are located in. For NO2 there are many stations that show a close correspondence to observed values near the one-to-one line. However, there are also a number of stations for which the modelled values are about 2-4 µg m^{-3} lower than those observed. The model tends to underestimate the observed NO2 concentrations by on average 22%. Overall the gradient of NO2 over the country is addressed well. For SO2 the same conclusion can be drawn, albeit that on average a small overestimation is observed. As the modelling of all the processed including deposition occurs on an hourly time resolution it is interesting to see if the model reproduces the seasonality and variability on observation stations. Therefore, in Figure 16 the time series comparison is shown for seven stations throughout Germany. It can be observed that the model captures the seasonal variability in both components. Moreover, on a short time scale many of the episodes with high concentrations are captured. The major episode of nitrogen dioxide in January is captured less well which may be due to very stable conditions in part of Germany. As the meteorological input is on a three hourly basis and emission input is deduced from annual numbers the exact timing of the plumes is often wrong by a few hours. Hence, we calculated the temporal correlation coefficient on the basis of daily averages. The coefficient's are very reasonable with values of 0.71 for NO2 and 0.59 for SO2 (Table 17). In short, we feel that the distributions of nitrogen dioxide and sulphur dioxide on rural background stations is simulated satisfactorily.

Figure 14.   Concentration distributions (µg/m^3) of NH$_3$, NH$_4^+$, NO$_2$, NO$_3^-$, HNO$_3$, SO$_2$ and SO$_4^{2-}$ over Germany in 2009.
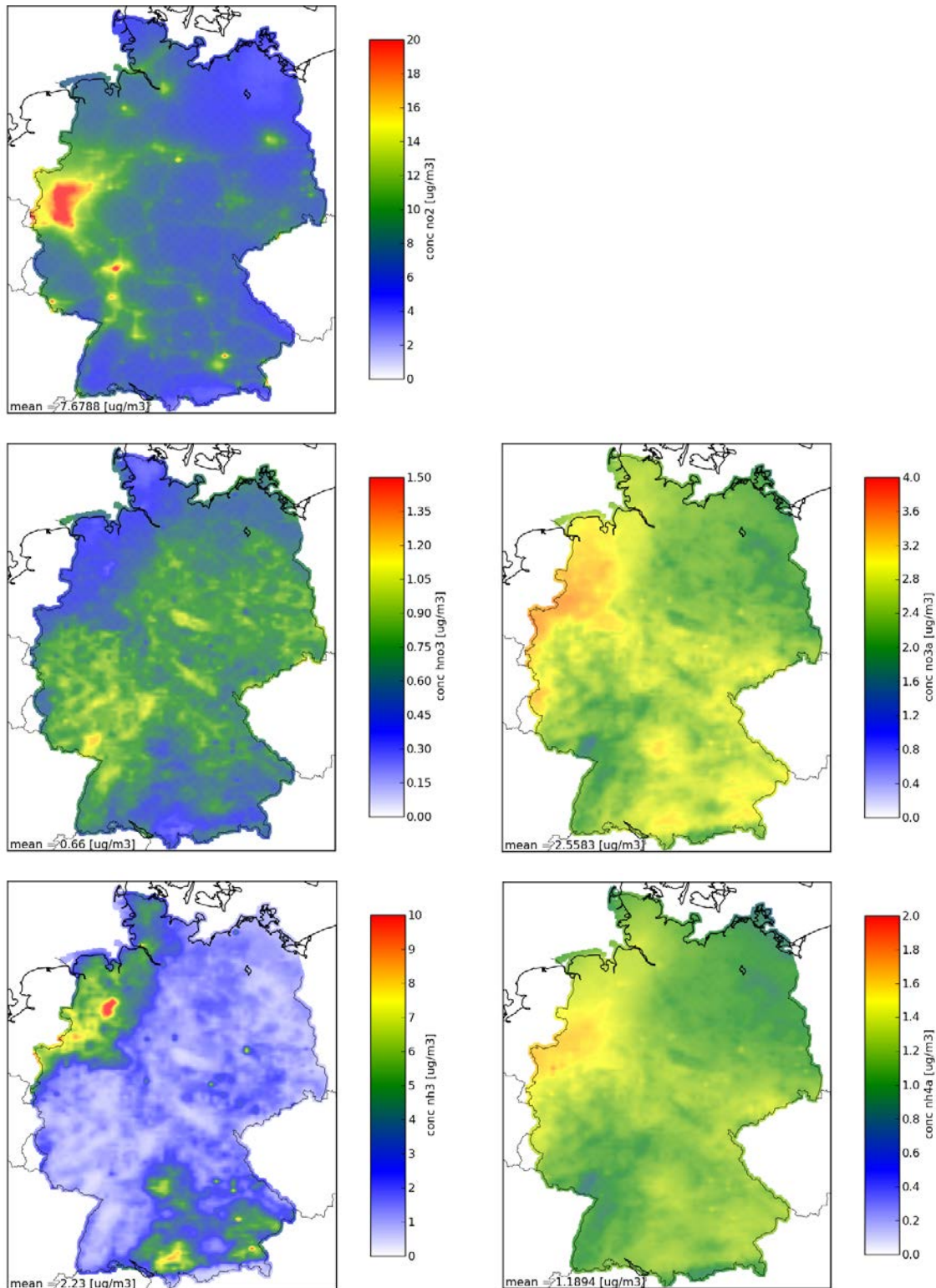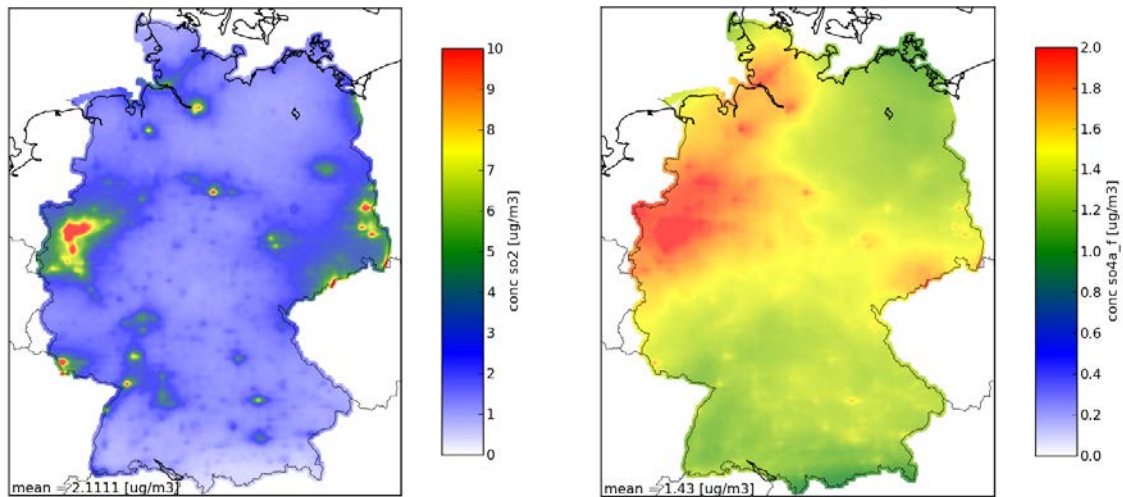
Table 17.   Summary of the statistical model evaluation for SO_2 and NO_2 for the year 2009. The data represent the averages over all N stations. We present the observed and modelled mean concentration as well as the variability expressed as a standard deviation (STD). Furthermore, the bias, root mean squared error (RMSE) and temporal correlation coefficient (COR) are given. The evaluation was performed with time series of daily means.

	N	$MEAN_{OBS}$	$MEAN_{MOD}$	STD_{OBS}	STD_{MOD}	BIAS	RMSE	COR
SO_2	31	2.1	2.4	2.0	2.3	0.26	2.2	0.59
NO_2	45	9.0	7.4	6.5	4.8	-1.5	5.1	0.71

Figure 15.   Comparison between annual averaged measured and modelled concentrations ($\mu g/m^3$) for NO_2 (left) and SO_2 (right) for the year 2009
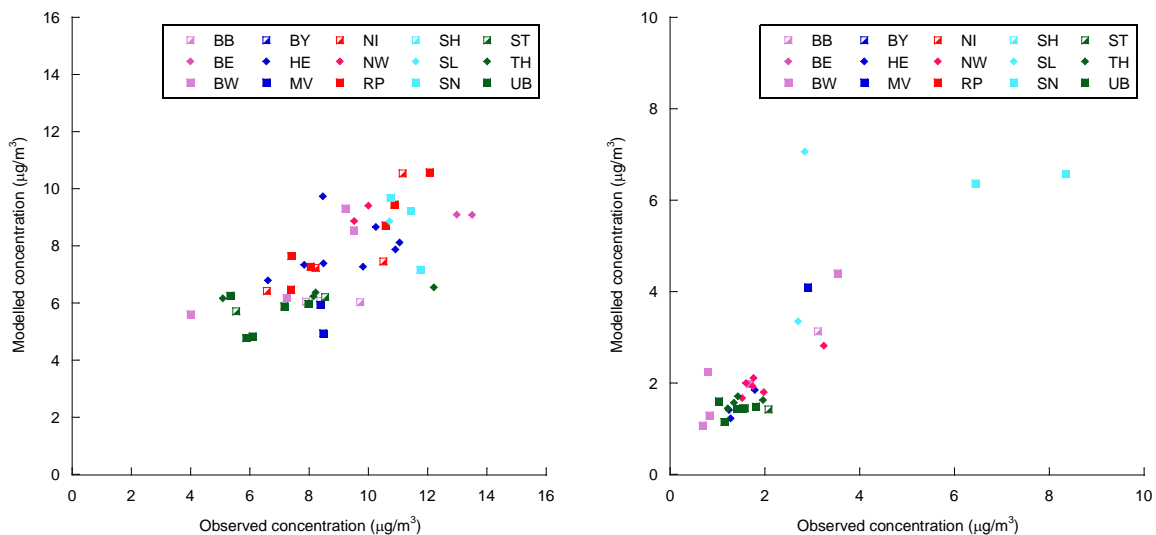
Figure 16.   Comparison between measured and modelled concentration (μg/m³) time series for NO₂ (left) and SO₂ (right) for the year 2009
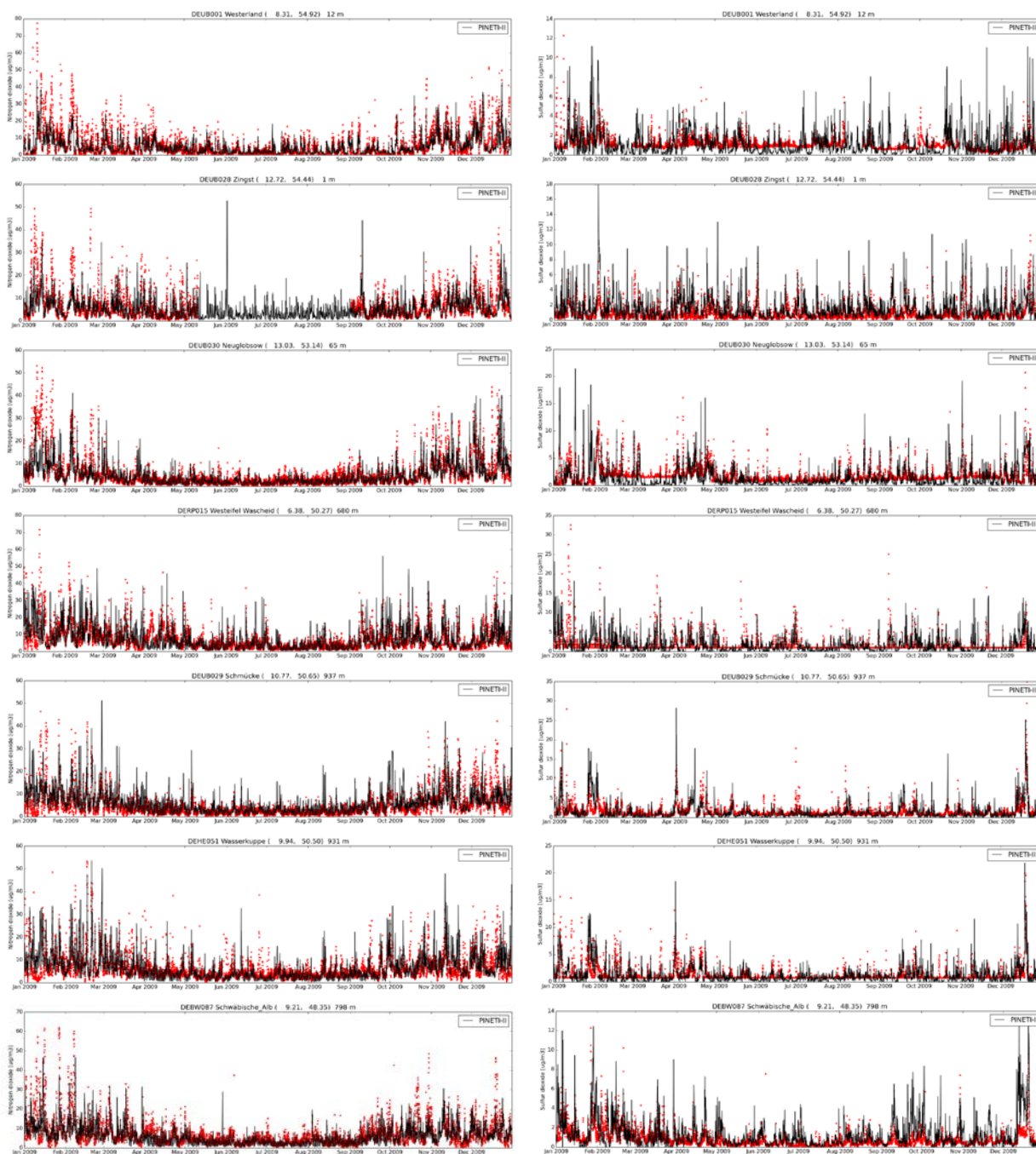
3.2.2.2   Wet deposition

The LOTOS-EUROS results are not used for the estimation of the wet deposition in this study. However, it is important to also compare the modelled wet deposition fluxes to observations as it provides information on the pollutant budget in the model. Hence, for the evaluation of the wet deposition fluxes of LOTOS-EUROS we compare to the data of 150 stations used for the empirical assessment of the wet deposition flux (see section 4.2). The comparison listed in Table 18 shows that the model underestimates the wet fluxes for all components. The underestimation is lowest for ammonium (21%). Nitrate and sulphate show similar underestimations, 38 and 40% respectively. In absolute terms the underestimation is about 140 eq ha⁻¹ yr⁻¹. The origin of these biases especially for nitrate deserves further attention.

Table 18.   Comparison of wet deposition fluxes (eq ha^{-1} yr^{-1}) averaged over all available stations for the year 2009. The bias is provide in an absolute and relative sense.

Variable	Observed	Modelled	Bias	Relative bias (%)
NH$_x$	295	234	-61	-21
NO$_y$	226	139	-87	-38
SO$_x$	176	98	-78	-44

3.3   Conclusion

The LOTOS-EUROS model version 1.10 used in this study consolidates state-of-the-art parameterizations for the nitrogen and sulphur cycles in the atmosphere including the compensation point for ammonia. In general the LOTOS-EUROS model results compare favourably with available measurement data albeit that both the wet deposition fluxes and nitrogen dioxide levels are underestimated. From the model calculations only the dry deposition fluxes are a part of the final deposition assessment. The average numbers for Germany for the year 2009 are summarized in Table 19. Furthermore, the modelled distributions of rain water concentrations and aerosol effective dry deposition velocity are used in the assessment of the wet and occult deposition described below.

Table 19.   Overview of the results of the modelled dry deposition fluxes for Germany as a whole for the year 2009

Component	Unit	Dry deposition
SO$_x$-S	eq ha^{-1} yr^{-1}	120
SO$_x$-S-nss	eq ha^{-1} yr^{-1}	115
NH$_x$-N	eq ha^{-1} yr^{-1}	337
NO$_y$-N	eq ha^{-1} yr^{-1}	131
N	eq ha^{-1} yr^{-1}	467

4 Empirical assessment of wet deposition distributions

4.1 Overall approach

Traditionally, the assessment of wet deposition fluxes to ecosystems in Germany is performed with an empirical approach making use of observed wet deposition fluxes at a large number of stations. In this study we derive rain water concentrations at the measurement locations and interpolate these data across Germany to arrive at a nationwide distribution. The distribution of the concentration in rain water is then multiplied with a high resolution precipitation map to arrive at the wet deposition estimates.

$$F_{wet} = C_{rain\ water} * Precipitation\ amount$$

The assessment is based on annual average data as the underlying data do not allow for a higher time resolution. Below, we provide more detail for the procedures followed to assess the wet deposition fluxes and present the results for 2009.

4.2 Wet deposition measurement data

The concentrations of the different components in precipitation in Germany are measured by an extensive countrywide measurement network maintained by various national and regional monitoring programs. The list of available stations is provided by Wichink Kruit et al (2014) and we like to acknowledge again the kind assistance by the network operators. The national UBA network consists of only 11 sites, evenly distributed throughout the country. The various regional networks add 249 stations to the database. Note that the UBA network samples on a weekly rhythm, whereas the regional networks may operate at a weekly, two-weekly, four-weekly or monthly basis. The sampling strategies of the regional networks are not synchronised. Currently, the wet deposition database is centrally maintained at UBA, to which all operators provide their data. We have used an extract of this database from November 2013 for our analysis. Precipitation amount, QAQC flags and concentrations of SO_4^{2-}, NO_3^-, NH_4^+, Mg^{2+}, Na^+, Ca^{2+}, K^+, Cl^- as well as pH in rain water have been made available to us.

At the available stations a variety of samplers are used to quantify the wet deposition. Within these samplers two types can be differentiated, wet-only and bulk deposition samplers. Bulk samplers collect precipitation in a bucket, which is open all the time. In most cases a net prevents leaves etc. from falling into the funnel. This sampling method has a slight tendency to cause an overestimation of the wet deposition, because it is susceptible to dry deposition during dry conditions. In contrast, wet-only samplers collect the precipitation in a funnel, which is only open when it rains. A sensor registers whether it is raining and the lid is automatically opened at the beginning of a rain event and closed at the end. Within Germany the majority of the data is obtained with bulk samplers as only 40 out of the 260 stations sample with wet only samplers. Hence, to use the information of bulk samplers in our analysis we need to correct the data for the dry deposition into the funnels. The correction is based on earlier investigations in which measurements with wet-only samplers and bulk samplers were performed simultaneously (Gauger et al., 2000, 2008). The bulk measurements are reduced to wet-only inputs by means of mean correction factors as listed in Gauger et al. (2008). The bulk to wet-only correction is performed for those stations that passed our QAQC procedure.

4.3 Quality Assessment and Quality Control

Although the independent networks have performed quality control procedures the dataset is inhomogeneous. Hence, we perform our own QAQC protocol and data selection procedure. We require a minimum valid data coverage of 40% for a given year to be included in further analyses. There are several reasons for non-complete coverage at a measuring station, i.e., no data reported, insufficient or no precipitation, large deviation in ion balance or outliers. We check each time series for these issues to select the stations used for the spatial interpolation procedure. The data limit and the factors influencing the data availability are discussed in more detail below.

In the mapping procedure the annual average concentration in the precipitation is required. This concentration is simply computed as the total annual flux divided by the total annual precipitation. In establishing a criterion with respect to the data availability a compromise has to be found between including as many stations as possible and maintaining high data quality. Hence a data availability of 40% is chosen as the cut-off-criterion which limits the number of excluded stations, while the average of this 40% is still representative to the real annual average. The assumption, that the annual average value for a station with more than 40% of valid data is representative for the annual average value for this station, is illustrated with different subsets of a dataset with 52 weekly measurements in Neuglobsow (see Figure 17). The figure shows the annual average concentration in precipitation for 1000 random subsets of the data for 5 different data availabilities, i.e., 100%, 80%, 60%, 40% and 20%. The standard deviation for these 1000 different subsets is represented by the error bars. The figure shows that the uncertainty in the annual mean concentration increases if data availability is smaller. For example, if a random subset of 20% of the data would be used to calculate the annual mean concentration for SO_4, the answer will be between 1.0 and 1.4 mg/l, with a most likely answer of 1.2 mg/l. If we increase data availability to 40%, the uncertainty reduces by a factor of 2, i.e., 1.2 ± 0.1 mg/l. The maximum error that we make for the annual mean concentration in the precipitation for a data availability of 40% is in the order of 10-20% depending on the component and station considered, e.g., the uncertainty in the K^+ concentrations is much more uncertain than that of SO_4^{2-}.

Figure 17.   Uncertainty in the annual mean concentration in precipitation for different percentages of data availability (x-axis) for 9 ion components at UBA station Neuglobsow.
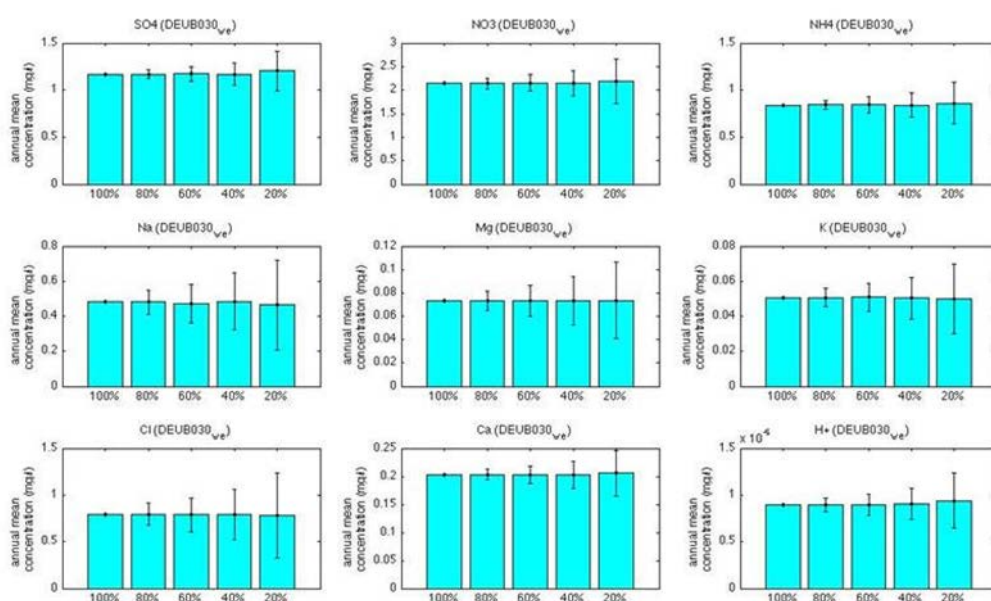
To assess the percentage of usable station data for the assessment of an annual mean concentration we first classify all samples into valid or a number of non-validity or non-availability classes. We discriminate between:

No data: No observation is present for rain or chemical analysis without a specified reason

No rain: No rain sampled

Tiny rain: Not enough rain to perform a chemical analysis

Ion balance: The net ion balance exceeds ±20%

Outlier: Failed outlier test

The first three flags are reported. Discussions with network operators has highlighted that under certain conditions the no data flag could be misleading. In occasions that the station is not accessible or the sample is frozen samples are not changed. This means that the sample is collected in the next collection round and the sample is flagged with no data although the period was covered. This feature does not happen often but it may be important for some sites in mountainous areas during winter.

The ion balance is calculated for all samples. The net ion-charge of the concentrations should be close to zero, thus no bias into positive or negative charges. If the net ion-charge exceeds ±20%, the measurement is rejected. The ion balance (IB) is described by the quality assurance handbook of the UBA monitoring network (2004), according to EMEP (EMEP, 1996) and WMO-GAW report 160 (2004), according to the following equation:

$$IB[\%] = \frac{(NH_4^+ + Ca^{2+} + Mg^{2+} + K^+ + Na^+ + H^+) - (SO_4^{2-} + NO_3^- + Cl^-)}{(NH_4^+ + Ca^{2+} + Mg^{2+} + K^+ + Na^+ + H^+) + (SO_4^{2-} + NO_3^- + Cl^-)} \cdot 100$$

The concentrations are given in [meq/l]. To be able to calculate the ion balance all relevant components need to be available from the analysis of precipitation. In case one or more of the relevant components are missing, the specific measurement event or even the whole data set cannot be used for the purpose of this project, as a quality check is not possible.

To remove outliers a statistical outlier test is performed for the time series of each station. The algorithm used here is an implementation of the Grubbs test (Grubbs, 1969). The procedure is iterative in the sense that the procedure is repeated after identifying and removing an outlier until no outliers are found anymore, or too many entries from the series are removed. As we log-transform the data in the interpolation scheme, the procedure is applied to the time series of log-concentrations.

In Figure 18 the results of the QAQC procedure is provide for nitrate observations. In general, the coverage is not so much affected by no data, no rain or tiny rain as these cover mostly less than 10% of the data. Only for no data a number of sites show values of around 20% or higher. The outlier test shows a similar picture as the no data flag. All in all, most data flagged invalid are due to the ion balance check. For the national and regional monitoring networks, the amount of data that is rejected due to ion-imbalance ranges 0-60% (bottom-left panel in Figure 18).

Figure 18.   Fractions of nitrate concentrations in the data from the national and regional monitoring networks that were rejected for a given reason in the dataset of the year 2009. The lower right plot shows the fraction of data that is considered to be valid for usage in the Kriging procedure.
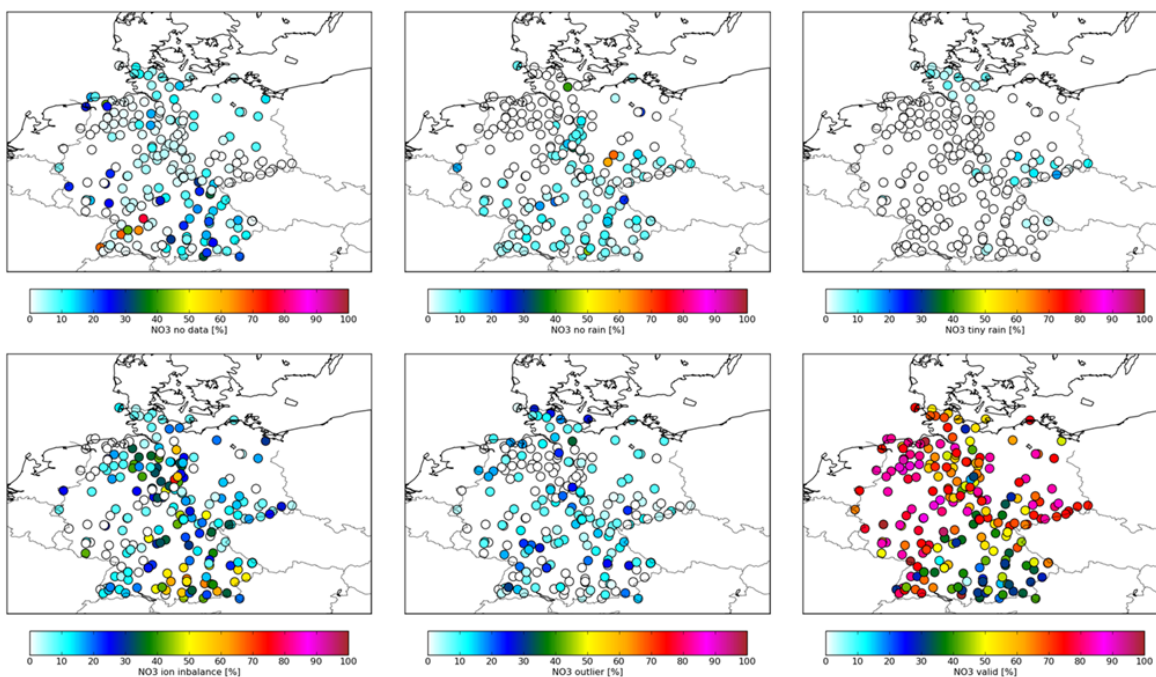
Figure 19. Illustration of the procedure of the spatial interpolation for NH₄. The panels show the measured concentrations on top of the LOTOS-EUROS distribution (A), the log-transformed data (B), the kriged residual (C), the new distribution, log-transformed (D) and the final rain water concentration distribution (E)
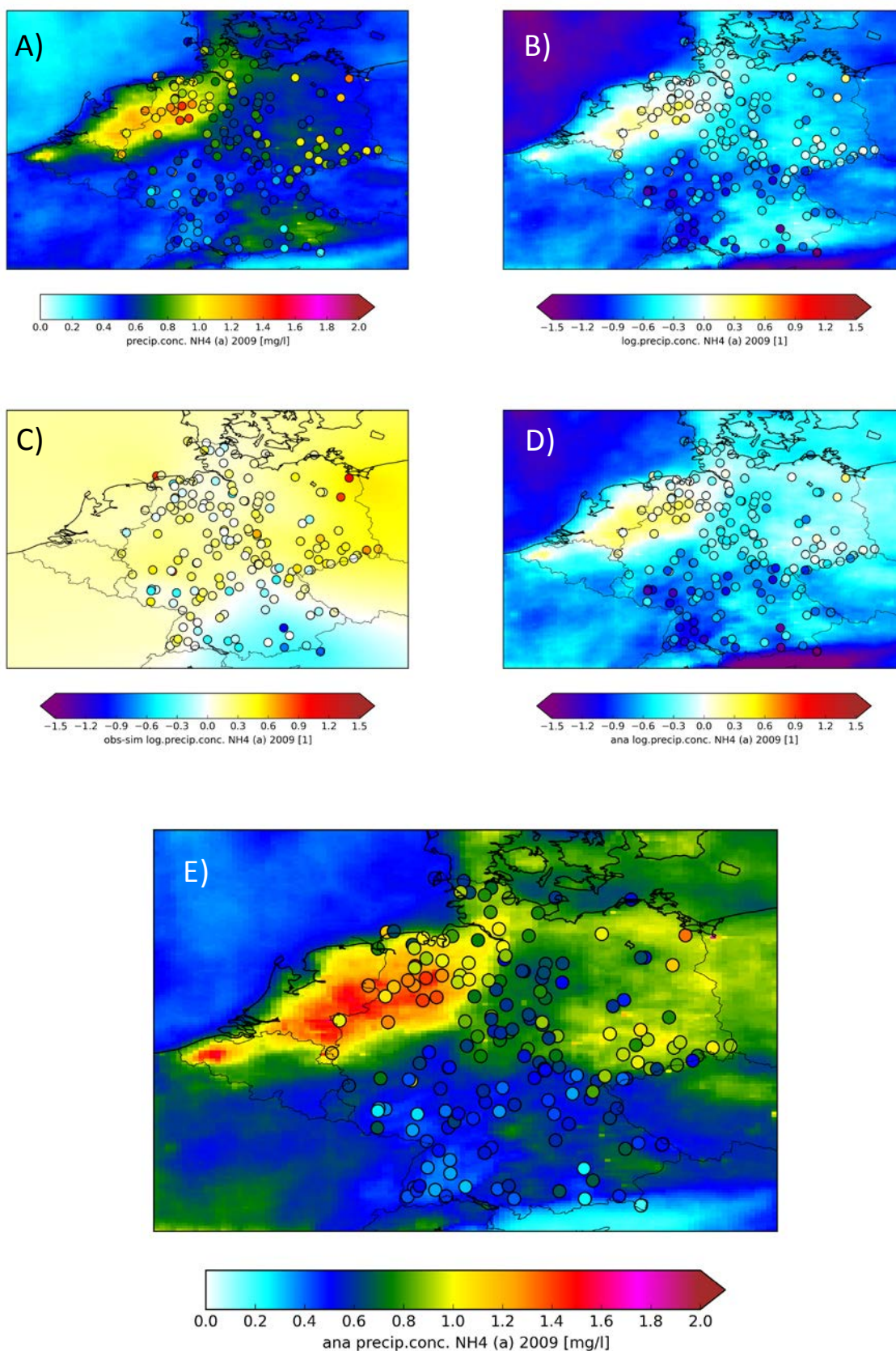
4.4   Spatial interpolation

Within this study we used the residual Kriging methodology developed by Wichink Kruit et al. (2014) to generate the rain water concentration distribution across Germany for 2009, 2010 and 2011. Within this procedure the difference between the residual between the observations and an a-priory distribution is interpolated. When available, the a-priory distribution is the modelled average rain water concentration from the LOTOS-EUROS model. This means that for the nitrate, ammonium, sulphate and sodium LOTOS-EUROS distributions are used, whereas for the other base cat-ions a constant field is used which means that ordinary Kriging is performed. The advantage of using LOTOS-EUROS distributions as a-priory is that we use process knowledge in the interpolation, which resulted in better validation statistics (Wichink Kruit et al., 2014).

The residual Kriging procedure is illustrated in Figure 19 for ammonium concentrations in rain water. In A) the measured concentrations are plotted on top of the modelled LOTOS-EUROS distribution. The observations and model results show many similarities as the main gradients are captured by the model. In general the modelled concentrations in rain water tend to be lower than observed in the northern part of the country, whereas in Bavaria the modelled concentrations tend to be slightly above is the observed values. In an absolute sense the underestimation is largest in the east of the country. After the log transformation (B) the residual between the observed and modelled concentrations are kriged (C). The kriged distribution is used to correct the modelled distribution towards the measurements (D). After the statistical treatment the data are log-transformed again to obtain the final concentration distribution (E). The final distribution shows a much better agreement with the observed data. As there is considerable variability between observed concentrations at stations at distances close to each other there remains a residual between the observed and optimized distribution. In Figure 20 a comparison between the kriged distribution values and the observed concentrations at the measurement locations is shown for ammonium, nitrate and sulfate. For ammonium the differences can be as large as 25%, whereas the differences for nitrate and sulfate are much smaller (~10%). The latter can be explained by the much smaller gradients across Germany observed in the rain water concentrations for nitrate and sulfate.

Figure 20.   Comparison between the kriged rain water concentration distribution values and the observed concentrations (mg/l) at the measurement locations for ammonium, nitrate and sulfate
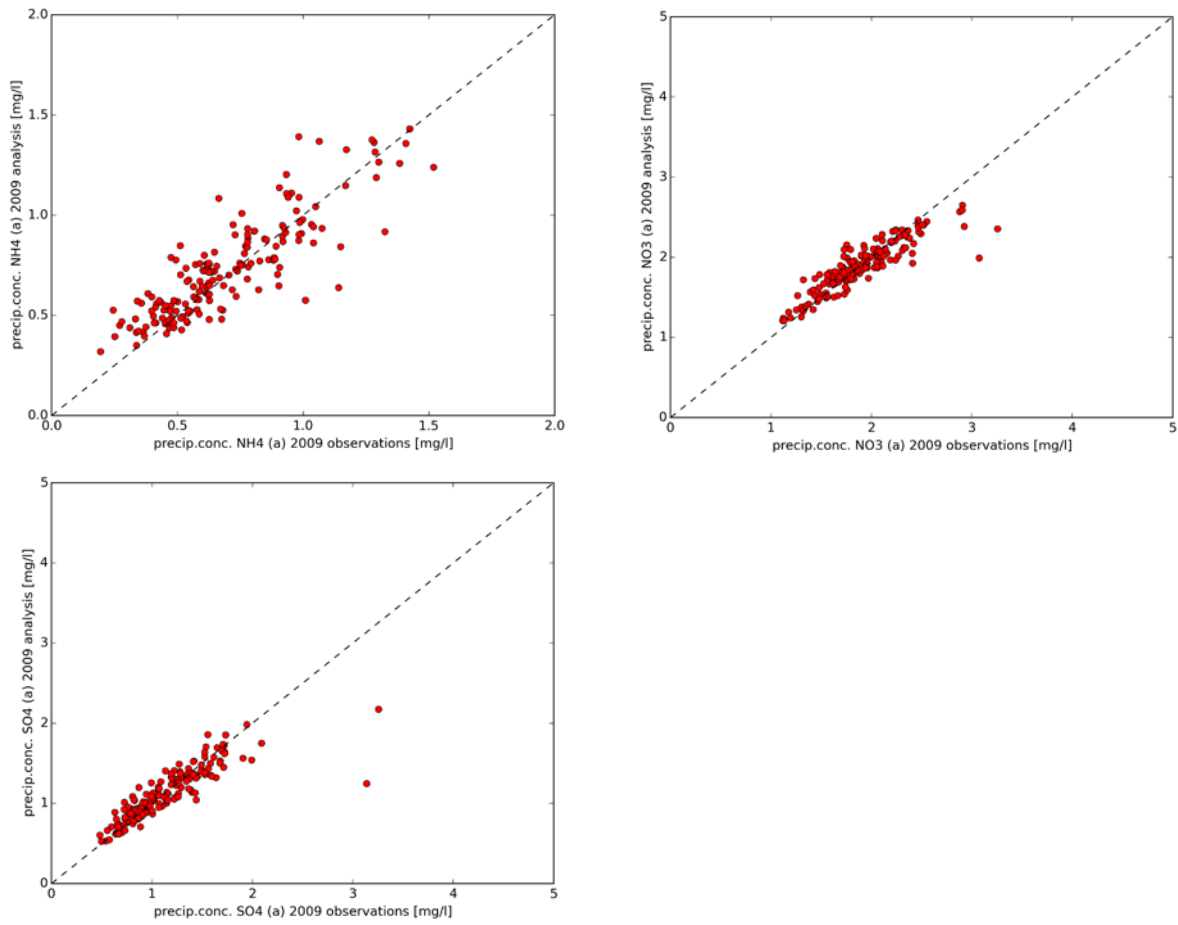
Figure 21.   2009 precipitation distribution from LOTOS-EUROS and the combined precipitation distribution with the high resolution DWD dataset for Germany (mm/yr)
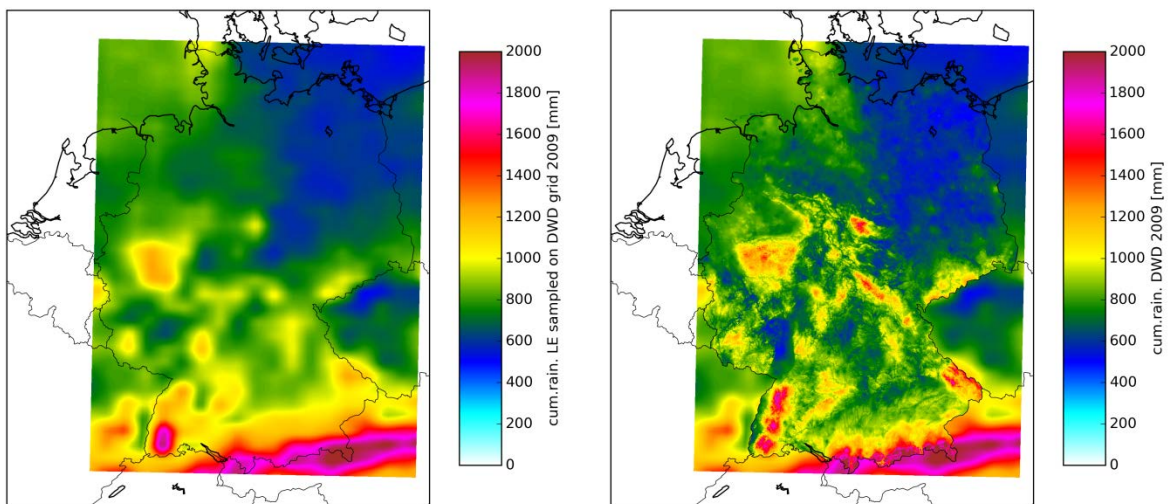
4.5 Wet deposition estimates

The final wet deposition distributions are obtained by multiplying the interpolated rain water concentration field with the precipitation distribution on a 1x1km² grid. These data were obtained from UBA and derive from the DWD (Figure 21). Table 20 summarizes the averaged estimates of wet deposition fluxes across the German territory for reactive nitrogen, sulphur and base cat-ions. On average the total N wet deposition amounts to 575 eq ha^{-1} a^{-1} while the average estimate for S amount to 187 eq ha^{-1} a^{-1}. Figure 22 shows the corresponding annual wet deposition distributions. As for the dry deposition the wet deposition of N maximises in the north west and the south east of the country as these are the areas with the highest animal husbandry density. The wet deposition of sulphur is highest in the Ruhr Area where the highest German SOx emissions occur. Furthermore, due to shipping emissions coastal areas in north-western Germany and harbour areas like e.g. Hamburg can be recognized in the sulphur wet deposition distribution. However, other than for the dry flux, which only peaks in areas with high emissions, the wet flux of all components is also increased in areas with high precipitation amounts, i.e. mountainous areas like the alpine region, the Black Forest, the Erz Mountains and the Harz Mountains. This is connected to the fact that the oxidation in cloud water and gas to particle conversion provides a means of long range transport of S and N.

The base cat-ions which are solely or mainly connected to sea salt like Na$^+$ and Mg$^+$ peak at the North Sea coast. Note that while for wet flux of S and N components the LOTOS-EUROS distributions were used the wet flux of the base cat-ions is derived solely using the observations. The base cat-ions distributions shown in Figure 22 are not corrected for sea salt contribution. The average estimates for the sea salt corrected base cat-ions wet deposition fluxes performed as described in chapter 2 are presented in Table 20.

Table 20.   2009 Overview of averaged estimates of wet deposition fluxes across the German territory for reactive nitrogen, sulphur and base cat-ions.

Component	Unit	Wet deposition
Ca^{2+}	eq ha^{-1} yr^{-1}	72
Ca^{2+}-nss	eq ha^{-1} yr^{-1}	66
K$^+$	eq ha^{-1} yr^{-1}	25
K$^+$-nss	eq ha^{-1} yr^{-1}	22
Mg^{2+}	eq ha^{-1} yr^{-1}	41
Mg^{2+}-nss	eq ha^{-1} yr^{-1}	11
BC-nss	eq ha^{-1} yr^{-1}	99
Na$^+$	eq ha^{-1} yr^{-1}	147
SO$_x$-S	eq ha^{-1} yr^{-1}	187
SO$_x$-S-nss	eq ha^{-1} yr^{-1}	170
NH$_x$-N	eq ha^{-1} yr^{-1}	327
NO$_y$-N	eq ha^{-1} yr^{-1}	248
N	eq ha^{-1} yr^{-1}	575

Figure 22.   2009 Overview of wet deposition distributions (eq ha^{-1} a^{-1}) for ammonium, nitrate, total Nr, sulfate, sodium, magnesium, potassium and calcium
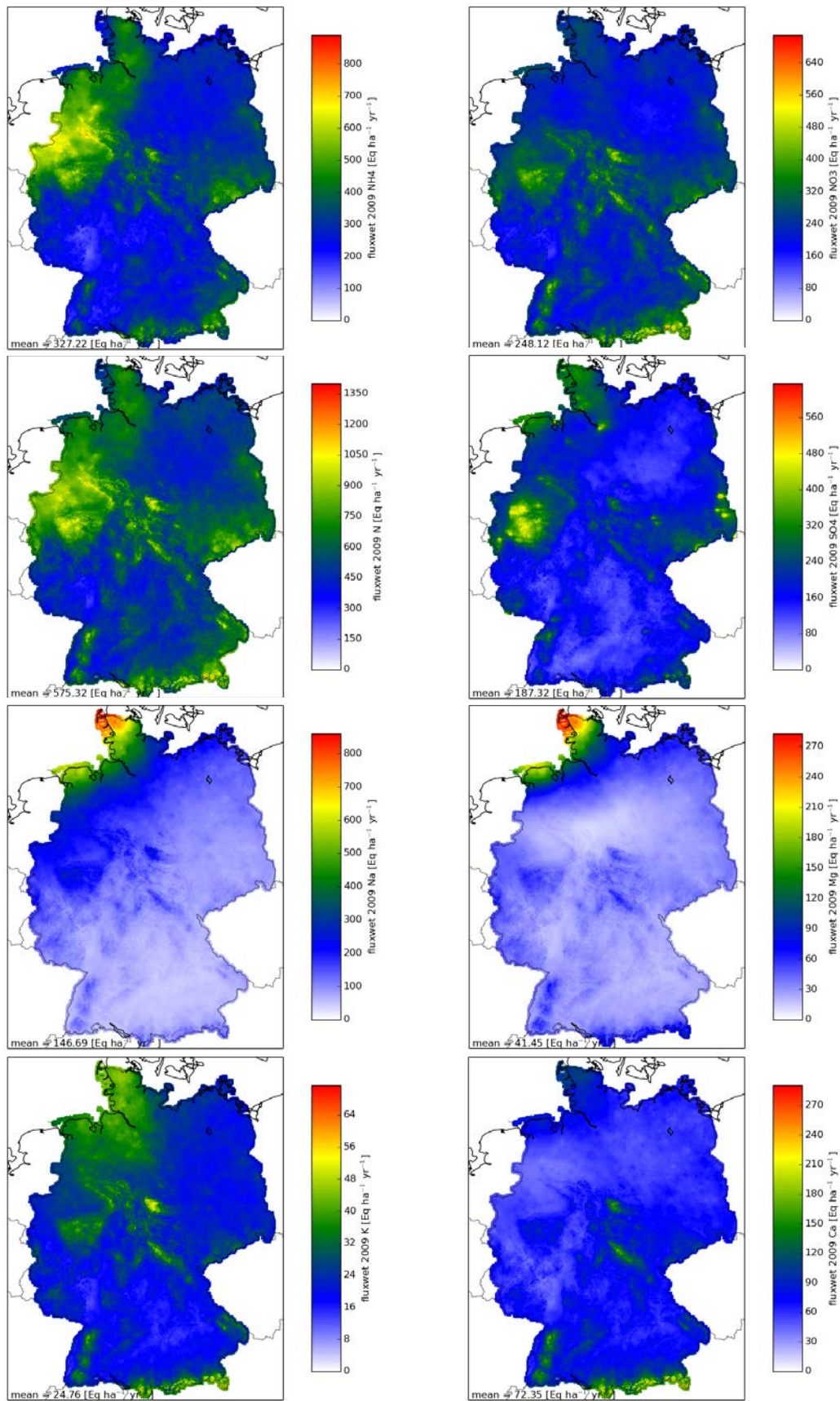
5 Empirical assessment of occult deposition distributions

Nutrient or pollutant input in ecosystems by deposition of fog or cloud droplets is called occult deposition. The occult deposition computed within this work refers to input by orographic clouds, which is the result of condensation processes in moist air lifted by mountains (= orographic cloud) or by intrusion of mountaintops into a low level cloud deck (Bleeker et al., 2000). In former projects (Builtjes et al., 2011; Wichink Kruit et al., 2014 (Teilbericht 1)) the occult deposition flux was estimated following the approach by Bleeker et al. (2000). An evaluation of this approach (Wichink Kruit et al., 2014 (Teilbericht 3)) has resulted in a proposal to update the methodology, which was consolidated within this assessment. The computation of the occult deposition flux is performed here following the approach by Katata (2008; 2011). Below we describe the methodology and present the results.

5.1 Methodology

Generally, the occult flux F_{occult} is derived by the multiplication of the deposition flux of fog water F_{Fog} and the pollutant concentration in the fog water C_{Fog}:

$$F_{occult} = F_{Fog} \cdot C_{Fog}$$ (Equation 1)

5.1.1 Fog or cloud water deposition flux

The revised calculation of fog water deposition (F_{Fog}) follows the approach by Katata et al. (2008; 2011). In Katata et al. (2008) a simple linear equation for the fog/cloud deposition velocity v_d based only on horizontal wind speed has been derived from numerical experiments using a detailed multi-layer land surface model that includes fog/cloud water deposition onto vegetation (SOLVEG). In Katata et al. (2011) the formulation was incorporated into the state-of-the-art meteorological model WRF and the calculated flux was validated.

Following Katata et al. (2008) the fog/cloud water deposition velocity can be calculated with

$$v_d = A \cdot U$$ (Equation 2)

where A is the slope of v_d that depends on vegetation characteristics (nondimensional), and U the horizontal wind speed over forest canopies [m s^{-1}].

A is calculated by:

$$A = 0.0164 \cdot \left(\frac{LAI}{h}\right)^{-0.5}$$ (Equation 3)

where LAI is the Leaf Area Index and h the canopy height [m]. The calculations of A using Equation 3 agreed with observations in various cloud forests with LAI/h > 0.2 (Katata et al.,2008) and it was stated that Equation 3 can be widely used to predict cloud water deposition on forests with LAI/h > 0.2.

Using v_d the flux of fog water deposition F_{Fog} [kg m^{-2} s^{-1}] is calculated using:

$$F_{Fog} = v_d \cdot \rho \cdot q_c = A \cdot u \cdot \rho \cdot q_c$$ (Equation 4)

where ρ is the air density [kg m^{-3}], u and q_c are the horizontal wind speed [m s^{-1}] and the liquid water content [kg water kg air^{-1}] at the lowest atmospheric model layer, respectively. The accuracy of Equation 4 in the amount of fog deposition has been validated with data on turbulent fog flux over a coniferous forest in Germany (Klemm and Wrzesinsky, 2007) with a prediction error of 13% (Katata et al., 2011).

The meteorological input to calculate the occult deposition flux within PINETI-2 was taken from the COSMO-EU model (Doms et al., 2011) which is the operational weather prediction model of the German Weather Service (DWD). COSMO-EU was chosen as it provides the meteorological fields over Germany on a rather high grid resolution of ca. 7x7 km². Hourly data of the meteorological fields were used to calculate the annual fog water deposition flux based on Equation 4 with

$$F_{Fog(annual)} = \sum_t v_d(t) \cdot \rho(t) \cdot q_c(t) = A \cdot \sum_t u(t) \cdot \rho(t) \cdot q_c(t) \qquad \text{(Equation 5)}$$

where ρ is the air density [kg m^{-3}], q_c is the liquid water content [kg water kg air^{-1}] at the lowest atmospheric model layer (about 10 m above the ground level) and u the horizontal wind speed at 10 m [m s^{-1}]. The elevation of u may be different from that of U in Equation 2 in some case, but this does not cause a significant error in representative wind speed according to the logarithmic wind profile in the surface boundary layer (Katata et al., 2011).

The approach following Katata (2008;2011) as described above is based on experimental data in forests and hence, provides an estimation of fog water deposition on forests only. Furthermore, the input on vegetation by fog is much more relevant for forests than for other land use categories as e.g. for grassland as the area of incidence is largest for forests when they filter the air mass passing through including fog or clouds. Hence, available studies on the occult input on vegetation are limited on forests and therefore fog water deposition on land use categories other than forest categories are neglected within PINETI-2. The fog water deposition was calculated for the forest land use categories

- Coniferous forest (LAI=6; h=20 m)

- Deciduous forest (LAI=5; h=20 m)

- Mixed forest (LAI=5.5; h=20 m)

over Germany. The meteorological years used to derive the fog water deposition fluxes were 2009, 2010 and 2011.

5.1.2 Concentration in fog water

In PINETI-2 the annual mean pollutant concentration in fog water (C_{Fog}) was estimated from the annual mean concentration in rainwater using so called enrichment factors (=EF) to extrapolate the fog chemistry from the rain chemistry by:

$$C_{Cloud} = C_{Rain} \cdot EF \qquad \text{(Equation 6)}$$

Hereby the annual mean concentrations in rainwater per species stem from the krigged concentration fields derived for the calculation of the wet deposition flux. The enrichment factors for the different species were derived from a number of field studies in which fog and rain chemistry were measured simultaneously. Table 21 summarizes the included studies and enrichment factors. As the table shows the enrichment factors are greater than unity for all species which indicates that within all available studies and for all species the concentration in fog water was higher than in rain water. This can be explained by a lower dilution in fog/cloud droplets as these are smaller than rain droplets and contain less water. From these studies the mean enrichment factor was built for each species to be used in PINETI-2. The final enrichment factors per species are shown in Table 22.

Table 21 Studies used to derive the enrichment factors per pollutant to calculate the concentration in fog water from the concentration in rain water

Study	Location	Country	Height a.s.l. (m)	Investigation period	dominant fog type	EF SO4	EF NO3	EF NH4	EF H+	EF Na	EF Cl	EF Mg	EF Ca	EF K
Fowler et al. 1995	Dunclair Heights (UK)	UK	600	1993-1994	advection of clouds	5.40	7.00	7.50						
Fowler et al. 1995	Halladale (UK)	UK	337	1993	advection of clouds	8.00	12.80							
Fowler et al. 1995	Great Dun Fell (UK)	UK	847	1993	advection of clouds	5.00	13.80	5.10						
Inglis et al., 1995	Holme Moss (UK)	UK	600	1994	advection of clouds	4.60	6.60	4.20						
Crossley et al., 1992	Castleaw (UK)	UK	450	1986	advection of clouds	12.00	7.60	10.50						
Reynolds et al., 1996	Llyn Brianne (UK)	UK	520	1989-1990	advection of clouds	7.50	7.50	8.50	3.50	11.00	11.00	11.00	5.00	6.50
Brantner et al., 1994	Mt. Sonnblick (A)	A	3106	1991	orographic fog (clouds)	3.00	2.00	5.00	3.00					
Collett et al., 1993	Mt. Rigi (CH)	CH	1325	1990-1991	orographic fog (clouds)	2.30	2.60	2.70						
Bormann et al., 1989	Douglas Island (US)	US	800	1984-1985	advection of clouds	5.60	7.00	3.50	3.00	4.80	6.30	5.50	5.00	5.30
Bormann et al., 1989	Marys Peak (US)	US	1245	1984-1986	orographic fog (clouds)	2.70	3.40	4.60	2.00	0.90	0.70	0.90	1.40	1.20
Miller et al., 1993	Whiteface Mountain (US)	US	1050	1986-1989	advection of clouds	3.30	2.70	5.10	2.60	2.10	2.20	1.50	1.30	2.50
Vong et al., 1997	Cheeka Peak (US)	US	460	1993	advection of clouds	6.50	5.60	3.00	5.70	6.90	7.70			3.00
Schemenauer et al., 1995	Mont Tremblant (CAN)	CAN	610.00	1985-1991	advection of clouds	4.00	3.90	5.90	2.60	2.10	2.20	3.50	3.80	3.20
Zier et al., 1992	Erzgebirge (D)	D	877.00	1987.00	advection of clouds	8.50	11.00	18.50						
Dasch et al.. 1988	Clingmans Peak (US)	US	2025.00	1986.00	orographic fog (clouds)	13.00	13.00	14.00						
Thalmann et al. 2002	Waldstein (D)	D	786	27.06.-05.12.2000	advection of clouds	18.00	24.00	25.00	16.00	5.00	8.00	11.00	7.00	7.00
Klemm et al., 2007	Waldstein (D)	D	775	17.04.2001-18.03.2002	advection of clouds	11.80	12.70	18.10			6.10			
Burkhard et al. 2003	Lägeren (CH)	CH	690	21.09.2001-10.04.2002	atmos. instability fog	11.00	23.00	25.00	10.00	3.00	3.00		6.00	
Herckes et al. 2002	Strengbach, Vogesen (F)	F	1146	01.03.1998-31.07.1998	orographic fog (clouds)	7.00	5.00	4.50	51.00	10.00	8.00	6.00	8.00	9.50
Lange et al., 2003	Erzgebirge (D)	D	880	01.12.1997-01.06.1998	advection of clouds/fog	6.50	6.50	6.50		6.50	6.50	2.50	6.50	20.00
Skybova, 2006	Beskydy Mountain (CZ)	CZ	1324	01.05.2003-01.04.2004	orographic fog (clouds)	2.00	4.10	3.60		1.00	1.40	2.40	3.70	1.40
Beudert et al., 2012	Großer Falkenberg (D)	D	1314	01.09.-05.12.2011	advection of clouds/fog	13.72	16.15	18.20	2.42	7.11	4.30	7.63	6.33	2.53
Aleksic et al. 2009	Whiteface Mountain (US)	US	1483	1993-2006	advection of clouds/fog	6.50	5.40	9.50	5.00	3.80	4.30	6.70	6.40	5.30
Zapletal et al. 2007	Cervenohorske (CZ)	CZ	1013	1999-2002	advection of clouds/fog	1.46	4.50	4.30	1.26	1.97	1.00		7.92	2.27
Acker et al., 1998	Mt. Brocken	D	1142	1993-1996	advection of clouds/fog	4.88	7.63	8.10	3.66	3.71	2.92	4.03	2.90	1.85

Table 22   Mean enrichment factors per species

Species	Mean enrichment factor
SO_4^{2-}	6.97
NO_3^-	8.62
NH_4^+	9.20
H^+	7.98
Na^+	4.66
Mg^{2+}	5.22
Ca^{2+}	5.09
K^+	5.11
Cl^-	4.73

Finally the occult deposition flux per species was derived by inserting the annual mean concentration in cloud water per species of the specific year and the annual fog water deposition flux of the year 2009 in Equation 1.

5.2   Occult deposition maps

Figure 23 shows maps of the 2009 occult deposition distribution for reactive nitrogen, sulphur and the base cat-ions. The spatial distribution of the occult flux across the German territory is very similar for all components. This is because the fog/cloud water deposition flux determines the distribution of the occult flux. The fog/cloud water deposition calculated as proposed by Katata et al. (2008; 2011) is determined by the liquid water content (LWC) near the surface and the horizontal wind speed. The horizontal wind speed peaks in coastal areas and elevated areas, i.e. mountainous regions. In the latter areas also the LWC near the surface peaks. Hence, over Germany the occult input is highest for the low mountain ranges. Through this approach the alpine regions are less affected as near surface clouds are often associated with very low wind speeds.

Table 23 summarizes the averaged estimates of the occult deposition fluxes across Germany for S and N and the base cat-ions. For total N and S deposition the 14 eq ha^{-1} a^{-1} and 4 eq ha^{-1} a^{-1}, respectively, represent a small contribution to the total deposition averaged over Germany. However, locally the occult input may account for up to 20-30% of the assessed total deposition, e.g. Erz Mountains. Note that the data in Figure 23 and Table 23 were obtained using the actual land use distribution in order to be consistent with the other chapters. As the occult deposition is only assessed for the forest land use classes the contribution of the occult input is considerably higher to those land use classes (roughly a factor 3).

Table 23.   Overview of averaged estimates of 2009 occult deposition fluxes across the German territory for reactive nitrogen, sulphur and base cat-ions. Data are obtained using the CORINE-2006 land use distribution.

Component	Unit	Occult
Ca^{2+}	eq ha^{-1} yr^{-1}	1
Ca^{2+}-nss	eq ha^{-1} yr^{-1}	1
K^+	eq ha^{-1} yr^{-1}	0.3
K^+-nss	eq ha^{-1} yr^{-1}	0.3
Mg^{2+}	eq ha^{-1} yr^{-1}	0.5
Mg^{2+}-nss	eq ha^{-1} yr^{-1}	0.1
BC-nss	eq ha^{-1} yr^{-1}	1
Na^+	eq ha^{-1} yr^{-1}	2
SO_x-S	eq ha^{-1} yr^{-1}	4
SO_x-S-nss	eq ha^{-1} yr^{-1}	3
NH_x-N	eq ha^{-1} yr^{-1}	8
NO_y-N	eq ha^{-1} yr^{-1}	6
N	eq ha^{-1} yr^{-1}	14

Figure 23.   Overview of 2009 occult deposition distributions (eq ha⁻¹ a⁻¹) for ammonium, nitrate, total Nr, sulfate, sodium, magnesium, potassium and calcium
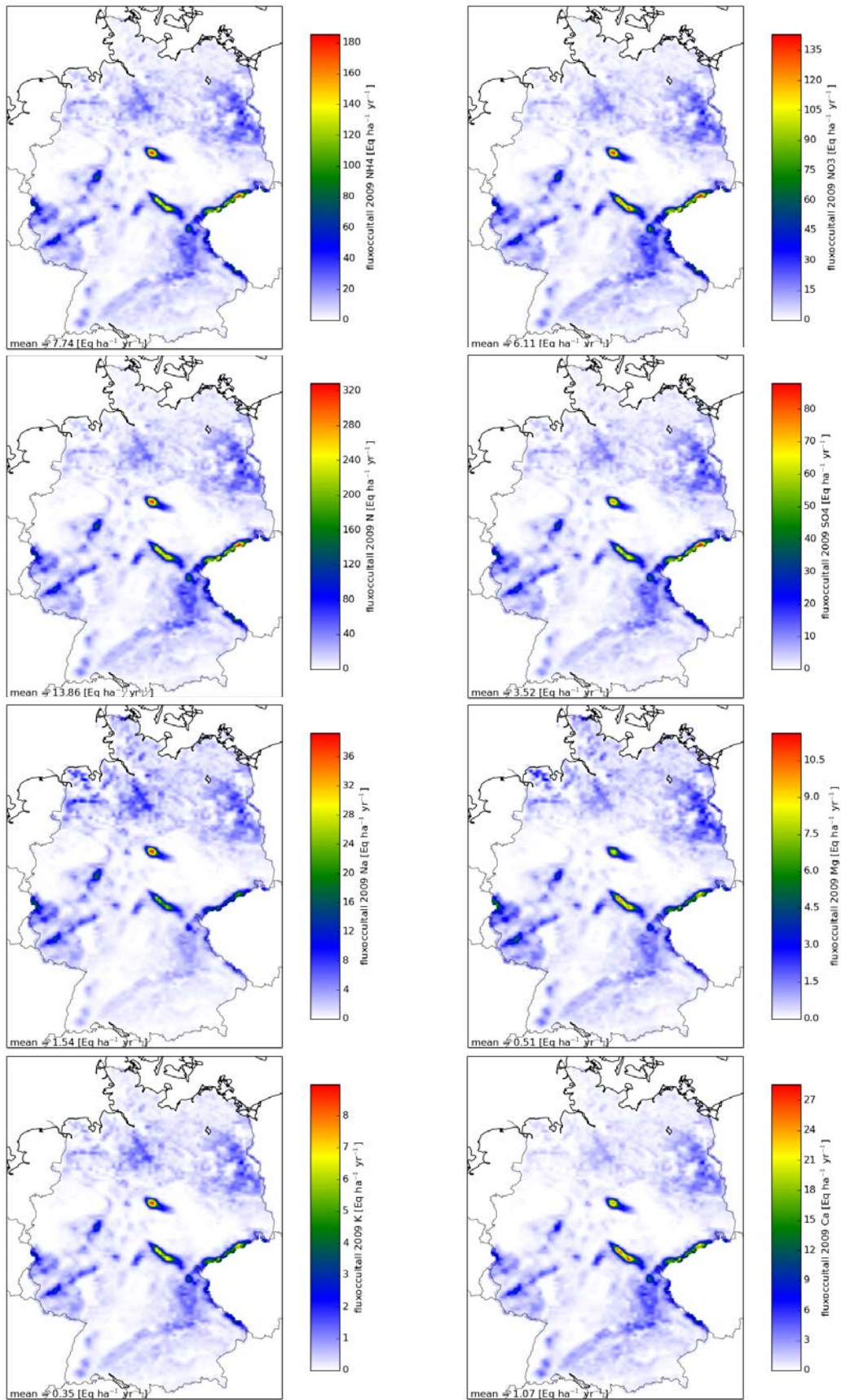
6 Empirical assessment of base cat-ion dry deposition distributions

As there are currently no reliable chemistry transport modelling results available for the base cat-ions, the dry deposition of Na^+, Ca^{2+}, Mg^{2+}, K^+ is calculated in a post-processing procedure. This estimation procedure has been used in a number of earlier projects (e.g. Wichink Kruit et al., 2014a; Builtjes et al., 2011).

6.1 Methodology

The dry deposition flux F_{dry} is derived through the multiplication of the atmospheric species concentrations C_{air} and the dry deposition velocity v_d:

$$F_{dry} = C_{air} \cdot v_d$$

The land use specific deposition velocity is obtained from the LOTOS-EUROS model calculations. Here we use the effective deposition velocity for coarse particles as most of the base cat-ion emissions (and deposition) are associated to the coarse particle mode. The exception is K^+ as this is also a (wood) combustion related tracer. Half of the K^+ mass is assumed to be in the fine particle mode.

The atmospheric concentrations C_{air} are estimated applying the so called 'Scavenging ratio approach' following Draaijers et al. (1996). By means of this approach, the atmospheric concentrations of the base cat-ions are derived from the species concentrations in rainwater as obtained from the interpolation of the precipitation chemistry data (see above). The atmospheric concentrations (C_{air}) [µg m⁻³] can be derived from the concentrations in rainwater (C_{rain}) [mg l⁻¹] by

$$C_{air} = \frac{(C_{rain} \cdot \rho)}{188 \cdot e^{0.227 \cdot MMD}}$$

with the air density ρ, and

$$MMD = A \cdot C_{rain} + B.$$

MMD stands for 'Mean Mass Diameter' [µm] and the best-fit-constants A and B describe the ratio between the MMD and the concentration in rainwater C_{rain} (Draaijers et al., 1996) resulting from simultaneous measurements of ambient concentrations and concentrations in precipitation of the involved species. Hence, A and B are species specific and are given in Table 24.

Table 24   Species specific best-fit parameters A and B following Draaijers et al. (1996)

Species	A	B
Na^+	0.574	6.082
Mg^{2+}	2.778	5.694
Ca^{2+}	1.52	6.316
K^+	2.74	4.096

6.2 Results

Figure 24 shows maps of the 2009 dry deposition distribution of the base cat-ions derived using the 'Scavenging ratio approach' as described above. Dry deposition input is significantly smaller than wet input for all components as for particles wet deposition is the most effective removal process. This is especially true for K as these are assumed to be smaller particles as combustion is the largest source of potassium. The base cat-ions which are solely or mainly connected to sea salt like Na^+ and Mg^+ peak at the North Sea coast. The forest areas and mountainous areas have increased deposition due to increased v_d in those regions.

Table 25.   Overview of averaged estimates of dry deposition fluxes across the German territory for base cat-ions. Data are obtained using the actual land use distribution.

Component	Unit	Dry
Ca^{2+}	eq ha^{-1} yr^{-1}	17
Ca^{2+}-nss	eq ha^{-1} yr^{-1}	16
K^+	eq ha^{-1} yr^{-1}	5
K^+-nss	eq ha^{-1} yr^{-1}	4
Mg^{2+}	eq ha^{-1} yr^{-1}	11
Mg^{2+}-nss	eq ha^{-1} yr^{-1}	3
BC-nss	eq ha^{-1} yr^{-1}	23
Na^+	eq ha^{-1} yr^{-1}	37

Figure 24.   Overview of 2009 dry deposition distributions (eq ha^{-1} a^{-1}) for sodium, magnesium, potassium and calcium.
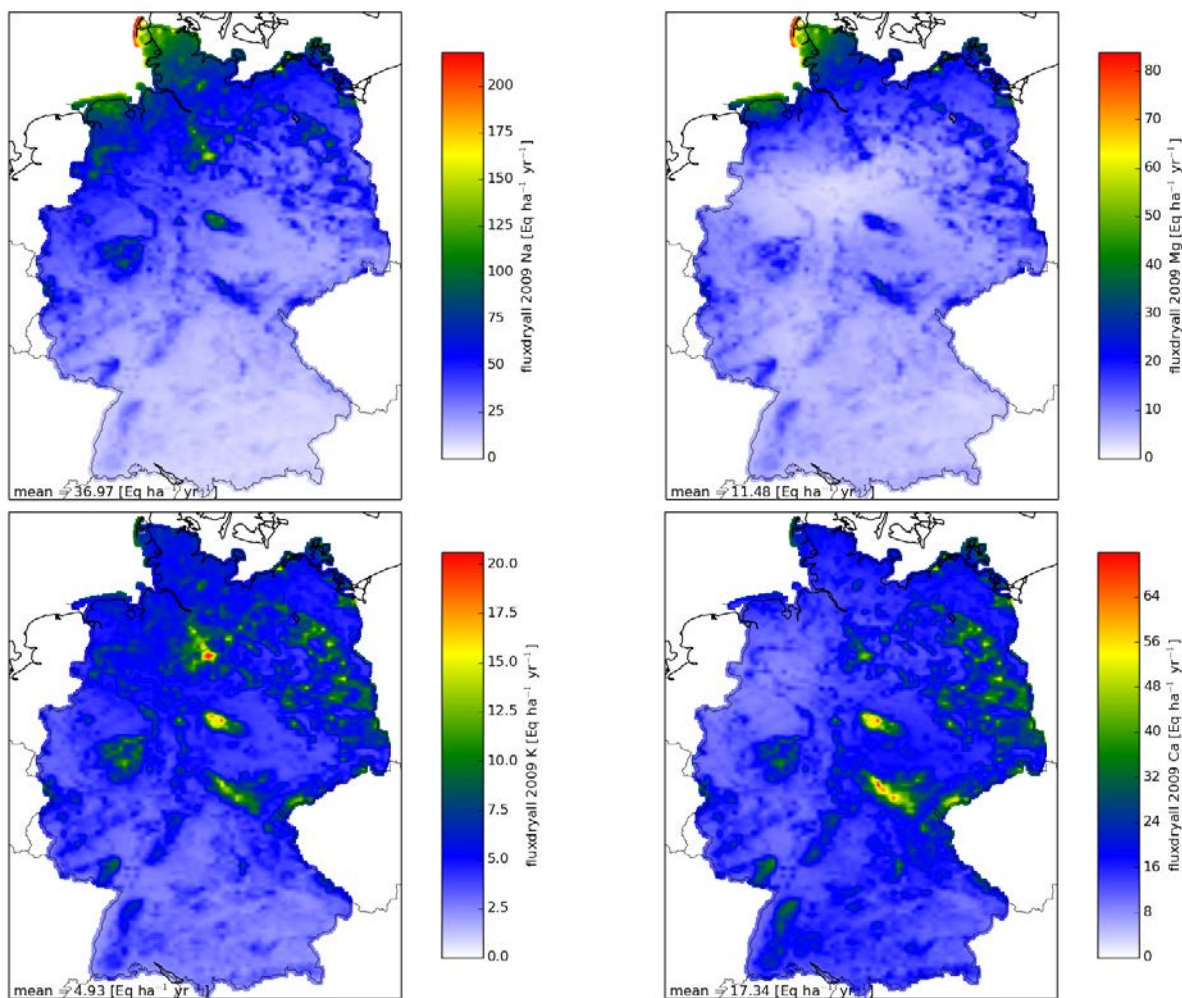
7 Total deposition

The total deposition is obtained by summing the fluxes for dry, wet and occult deposition. Figure 25 shows the resulting 1 x 1 km² total deposition fields per component over Germany in 2009. The total deposition values are given for Germany as a whole. The country average total depositions of the different components in Germany in 2009 is summarized in Table 26. In this table the summation over the three pathways is provided. The total N deposition amounts to 1057 eq ha⁻¹ a⁻¹ on average across the country while the average estimate for Sulphur deposition without sea-salt fraction (S_nss) amounts to 288 eq ha⁻¹ a⁻¹. As previously indicated for the separate fluxes the total N deposition maximises in the North West and the south east of the country as these are the areas with most intensive agriculture. Note that the deposition of oxidized and reduced nitrogen show distinctly different patterns. Oxidized nitrogen becomes an important contributor to total N deposition away from the agricultural areas and contributes more than half to the total N deposition in areas such as the black forest. The total deposition of sulphur is highest in the Ruhr Area, although away from this source areas the mountainous areas show secondary maxima.

The base cat-ions which are solely or mainly connected to sea salt like Na^+ and Mg^+ peak at the North Sea coast. Potassium shows a more anthropogenic signature with highest fluxes in the areas with highest precipitation. Finally, calcium shows a mixed picture as both anthropogenic source and sea salt are important contributors to it concentrations in coastal regions.

Table 26. Overview of averaged estimates of total deposition fluxes across the German territory for reactive nitrogen, sulphur and base cat-ions in 2009. Data are obtained using the CORINE-2006 land use distribution.

Component	Unit	Wet	Dry	Occult	Total
Ca^{2+}	eq ha⁻¹ yr⁻¹	72	17	1	91
Ca^{2+}-nss	eq ha⁻¹ yr⁻¹	66	16	1	83
K^+	eq ha⁻¹ yr⁻¹	25	5	0.3	30
K^+-nss	eq ha⁻¹ yr⁻¹	22	4	0.3	26
Mg^{2+}	eq ha⁻¹ yr⁻¹	41	11	0.5	53
Mg^{2+}-nss	eq ha⁻¹ yr⁻¹	11	3	0.1	14
BC-nss	eq ha⁻¹ yr⁻¹	99	23	1	123
Na^+	eq ha⁻¹ yr⁻¹	147	37	2	185
SO_x-S	eq ha⁻¹ yr⁻¹	187	120	4	311
SO_x-S-nss	eq ha⁻¹ yr⁻¹	170	115	3	288
NH_x-N	eq ha⁻¹ yr⁻¹	327	337	8	672
NO_y-N	eq ha⁻¹ yr⁻¹	248	131	6	385
N	eq ha⁻¹ yr⁻¹	575	467	14	1057

Table 27.   Overview of averaged estimates of deposition fluxes per land use category across the German territory for reactive nitrogen and sulphur in 2009.

Land use	Code	total N [eq ha⁻¹ yr⁻¹]	total S_nss [eq ha⁻¹ yr⁻¹]
Grassland	grs	901	291
Semi-natural	sem	948	301
Arable	ara	982	247
Permanent crops	crp	1043	315
Coniferous forest	cnf	1287	358
Deciduous forest	dec	1183	356
Mixed forest	mix	1235	357
Water	wat	861	291
Urban	urb	1248	283
Other	oth	894	221

Figure 25. Overview of total deposition distributions (eq ha^{-1} a^{-1}) for ammonium, nitrate, total Nr, sulfate, sodium, magnesium, potassium and calcium in 2009
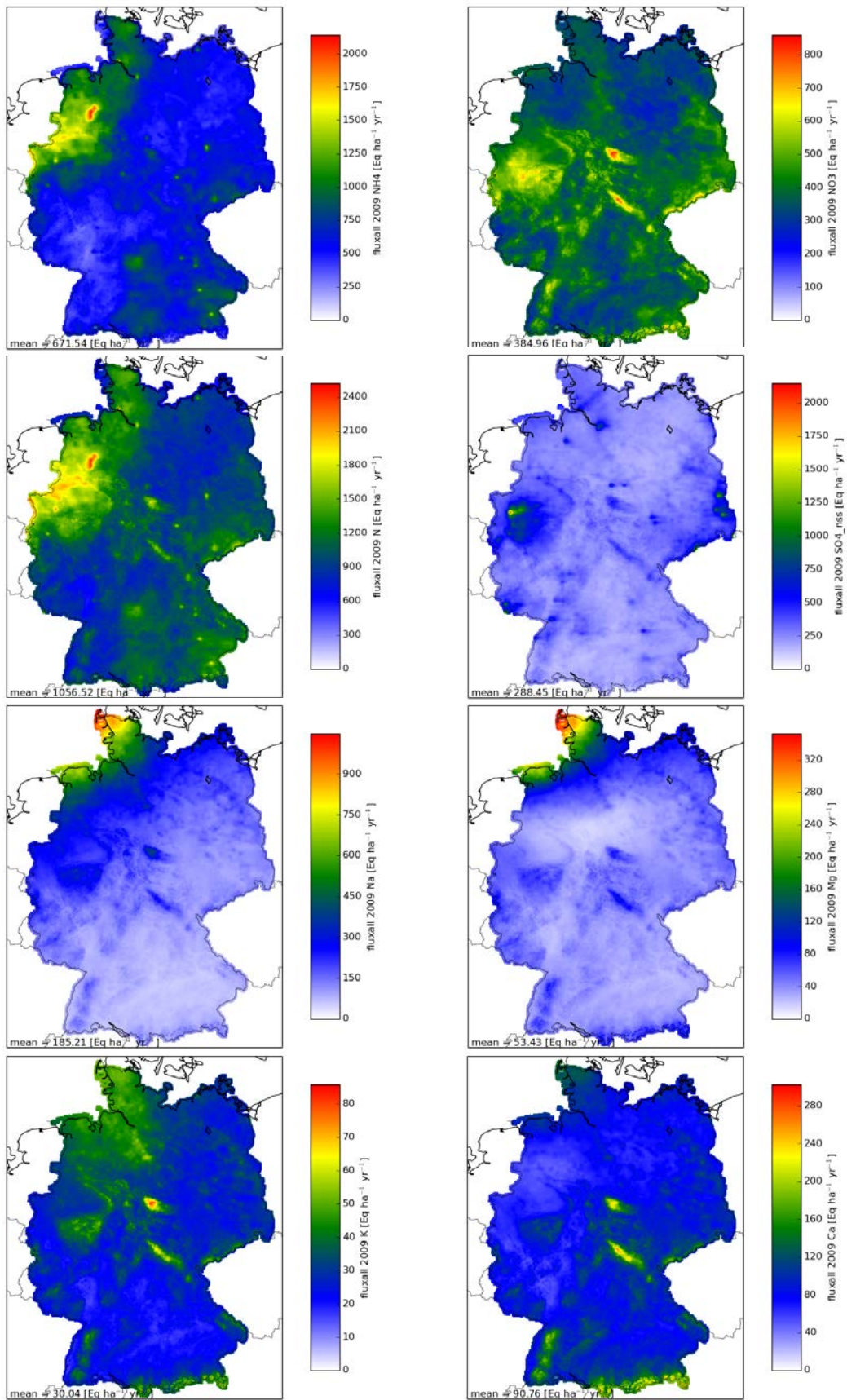
8   Evaluation of the results

8.1   Comparison to previous studies

8.1.1   Comparison to earlier assessments for Germany

In Figure 26 we compare the new estimate for the total N deposition over Germany to the results of two previous studies. The two studies are the projects MAPESI (Builtjes et al., 2011) and PINETI (Wichink Kruit et al., 2014a). The comparison shows that the assessment of total deposition across Germany has been lowered by 27% from MAPESI to PINETI-2. These differences are largely determined by improvements of the methodology towards the state of the science. As a consequence of the PINETI and PINETI-2 projects the deposition is lowered in two (almost equal) steps:

1. Within PINETI the methodology to assess the wet deposition is been updated. Moreover, the occult deposition flux has been assessed to be much smaller than in earlier studies. These changes resulted in a 13 % lower total deposition flux than in MAPESI. For a discussion on these differences we refer to Wichink Kruit et al. (2014a).
2. Within the results presented in this study (PINETI-2), the dry deposition estimates are lower than in PINETI and MAPESI. This is a consequence of methodological updates in the LOTOS-EUROS model version that has led to a better representation of the nitrogen budget. Below we explain this feature in more detail.

Hence, for all deposition pathways new developments have been included leading to lowered total deposition assessment compared to MAPESI.

Figure 26.   Comparison of the 2009 total N deposition from this study (PINETI-2) and the final assessment in the MAPESI project for 2005 and in the PINETI project for 2009.
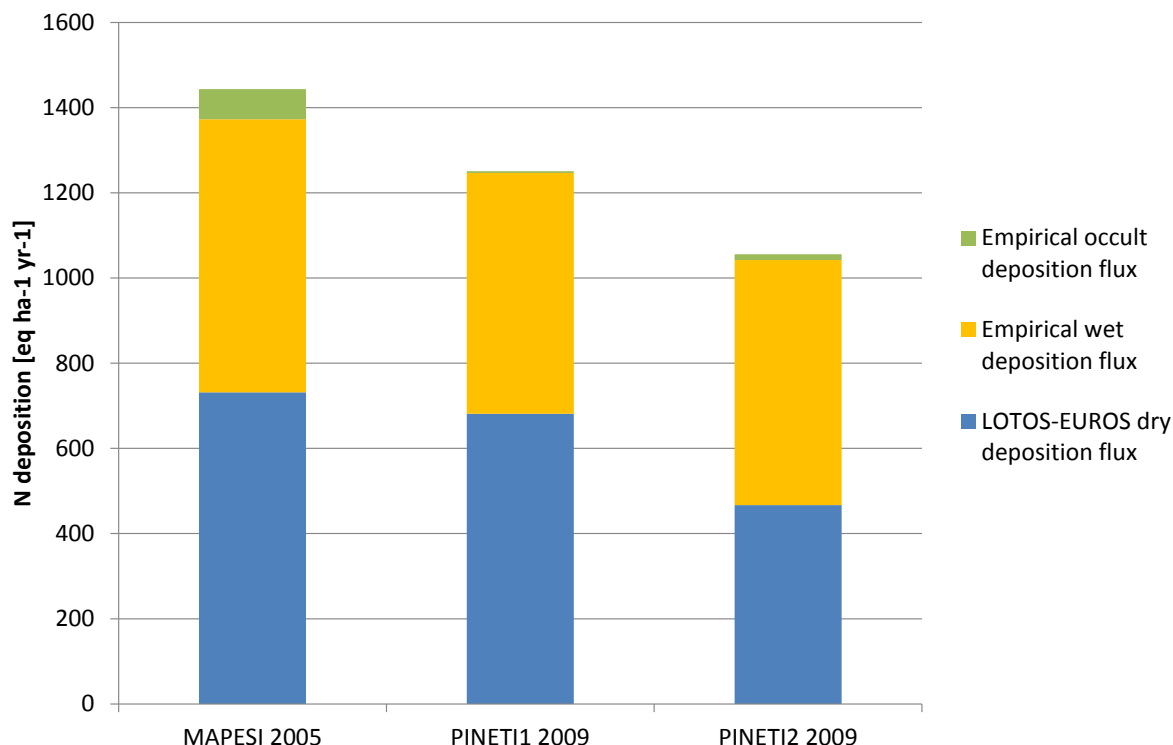
To explain the differences between PINETI-2 and PINETI we recall that in the last years important developments have been made in LOTOS-EUROS for the modelling of the budget of nitrogen and sulfur components. These developments have been consolidated into one new model version of LOTOS-EUROS, v1.10. The most relevant improvements are:

- the introduction of the compensation point for ammonia,

- the co-deposition effect between ammonia and sulfur dioxide,

- a new description for the dry deposition of aerosols,

- A pH-dependent formation of sulfate in clouds

- Below and in-cloud scavenging that takes droplet saturation into account

- Update of the deposition and land use related parameters

Here we have a look at the impact of the model developments with a focus on the compensation point. Wichink Kruit et al. (2012) describes the implementation of the compensation point for ammonia into LOTOS-EUROS through DEPAC v3.11 in detail. The land use independent compensation point in each cell is calculated using the ammonia concentration of the previous month (Stomata) and previous hour (external leaf) (as a proxy for the NH_3 deposition) combined with the empirical relations for the emission potentials for the stomata and the external leaves following Wichink Kruit et al. (2010). Recent validation study showed that these relations were also applicable to a forest stand in the Netherlands. Inspection of the modelled atmospheric concentration for ammonia showed that the modelled life time of ammonia increased and concentrations in source areas increased significantly.

We illustrate the impact of including the compensation point for ammonia in DEPAC v3.11 by replacing it with DEPAC v3.3, which was used in the PINETI-1 model version (COMP-OFF). In Figure 27 we show the impact of neglecting the ammonia compensation point for the deposition to coniferous forest and wet deposition. In the PINETI-II simulation the compensation point for ammonia causes lower deposition within the major source regions in the northwest and southeast of the country. As a consequence, the concentrations of ammonia increase causing more effective wet deposition as well as larger transport distances. The latter results in increased dry deposition fluxes of N in the central part of the country including the forested areas of the black forest and, Harz of about 10-20 %. Wet deposition is increased everywhere, but mostly in the source areas.

Figure 27.   Relative difference in dry (left) and wet (right) reduced nitrogen deposition to coniferous forest due to the incorporation of the compensation point of ammonia. Note that the color scales are not the same.
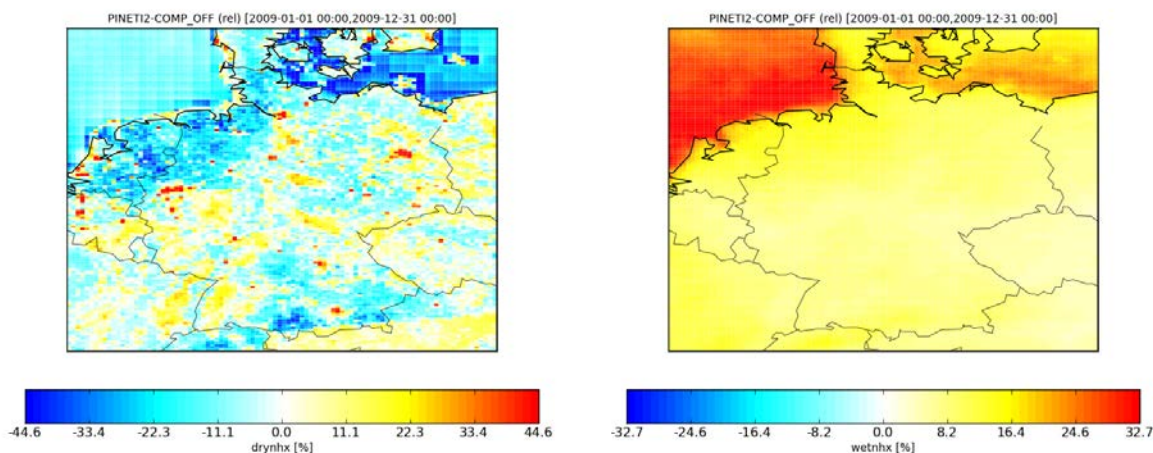
Figure 28.   Relative difference between PINETI 1 and PINETI2 modelled deposition fields across Germany for total nitrogen.
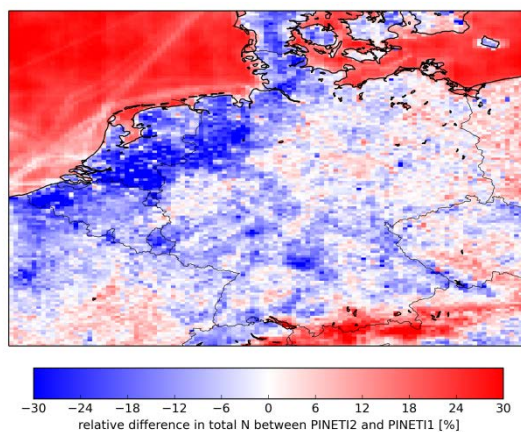
The spatial map of the differences in total N deposition between the two model versions shows that for nitrogen the spatial signature is dominated by the impact of the compensation point (Figure 28). The ammonia emission regions show the largest reduction in total N deposition, whereas the natural areas show increased deposition through the longer atmospheric life time and transport distance. In the alpine area the shift to wet deposition causes higher total N deposition fluxes. Differences between land use classes are further explored in Figure 29 where we compare the contrast between the land use classes in terms of dry deposition fluxes of nitrogen. Clearly, the PINETI-2 model version has a larger contrast between the land use classes with high and low roughness. For example, coniferous and deciduous forest receive respectively about 100 and 70% more dry deposited nitrogen than grassland versus 60 and 40% in the old model version.

Figure 29.   Comparison of the normalized dry deposition fluxes of each land use class by that to grass land for PINETI-1 and PINETI-2.
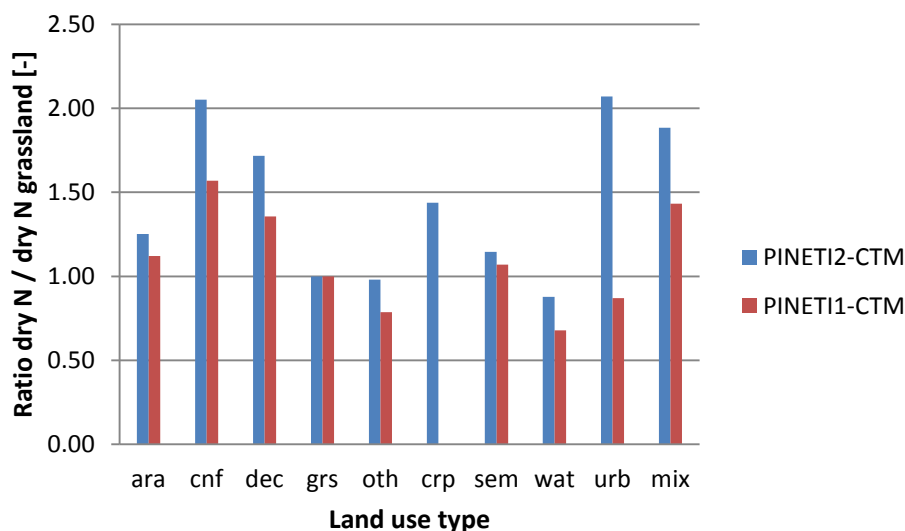
The total modelled deposition is rather insensitive to the change in model parameterizations. This is also illustrated in Figure 30, where a comparison is made between the modelled total N deposition for MAPESI-2005 (LOTOS-EUROS v1.5), PINETI-2009 (LOTOS-EUROS v1.7) and PINETI-2-2009 (LOTOS-EUROS v1.10) and the emissions used in these simulations. The reduction in the modelled total N deposition between 2005 and 2009 can be largely explained by the reduction in nitrogen emissions (NO_x and NH_3) between 2005 and 2009 (green bars in Figure 30). Although the total deposition is rather insensitive to the model parameterizations, the inclusion of the new process descriptions reduces the dry deposition efficiency and leads to increased wet deposition fluxes for Germany on average. This led to a considerable shift from modelled dry to wet deposition, especially for reduced nitrogen. In comparison, a small decrease of about 5% in the total N deposition is observed. The shift from dry to wet deposition in LOTOS-EUROS is beneficial in comparison to observations as it reduced the bias between modelled and observed wet deposition fluxes considerably. The shift has a strong impact on the assessment of the total deposition of N across Germany due to the practice that the wet deposition fluxes are estimated empirically. In practice, the empirical wet deposition fluxes replace the modelled values by LOTOS-EUROS. The mass balance as observed for Germany as a whole in LOTOS-EUROS is basically violated by this practice. The newly modelled wet deposition fluxes by LOTOS-EUROS are closer to the observed once compared to earlier projects (compare the orange and red bars in Figure 26 and Figure 30) which yields a smaller correction for the wet deposition and thus a lower total deposition estimate.

Note that within Germany the update of the model parameterizations also causes redistribution from source areas towards natural areas leading to a smaller decline in the assessed total deposition compared to previous projects in the large forest areas in Germany. Hence, the reduction shown in Figure 26 is not a homogeneous reduction across the German territory.

Figure 30.   Comparison of modelled total N deposition in 2005 and 2009 and total N emissions in 2005 and 2009.
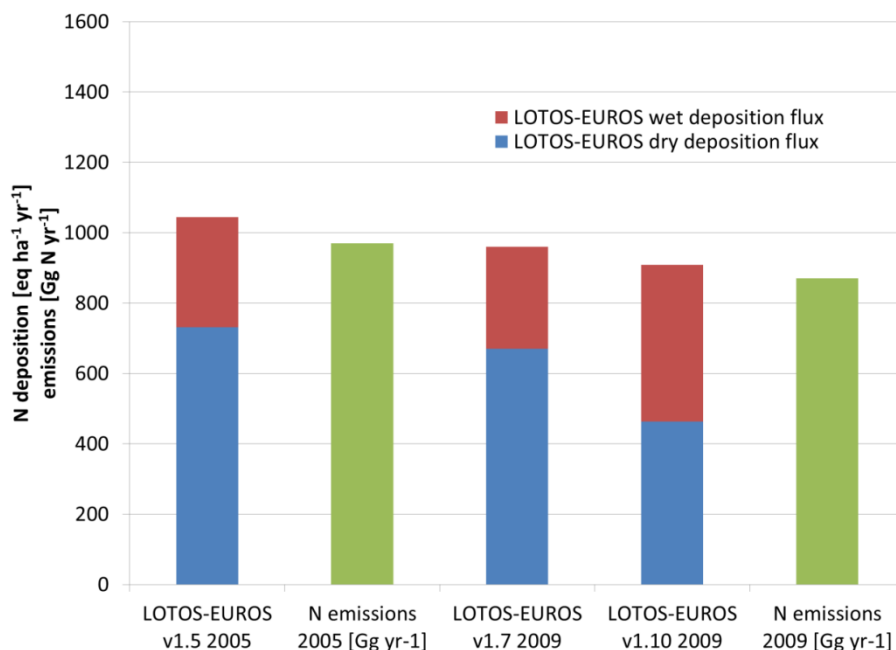
8.2   Underpinning the new deposition estimates

In short, the better representation of the wet deposition flux in LOTOS-EUROS reduces the assessed total deposition considerably. To further underpin the new total deposition estimates we have performed additional efforts to compare our results to:

- a compilation of ammonia observations in Germany

- deposition estimates for monitoring sites

- deposition assessments of EMEP for Germany

- background deposition maps in the Netherlands

- canopy budget calculations at ICP Level 2 sites

These comparisons are described below.

8.2.1   Comparison to ammonia observations

Ammonia plays a key role in the atmospheric nitrogen cycle. The first activity to focus on was to try to evaluate the model for ammonia. Unfortunately, it is a gas which is not easy to measure. Methodologies to monitor ammonia on an hourly basis are costly and require high level technical skill. Hence, these techniques are not often used to monitor ammonia and high resolution data are sparse. Alternatively, one could measure ammonia with passive samplers. These samplers are easy to use and cheap, but yield only average concentrations over a longer time interval (of a week or month). We have contacted specialists from the field to enquire if passive sampler data for ammonia were present. For 6 networks stations with data were obtained for the years 2009-2011. Most networks provided data for 2010 and 2011, leaving 2009 less covered. Hence, we have averaged the concentrations over the 2009-2011 period to compare to our modelled ammonia distribution. Five stations with concentrations far above 7 µg/m^{3} were removed from the analysis as they were considered hot spot locations. Figure 31 shows the result of this exercise. On average, the model tends to underestimate the observed concentrations slightly and yields an explained spatial variability of 50%. Hence, the model is able to reproduce a

large part of the variability and large scale gradients across Germany. Within a region, e.g. Niedersachsen, still considerable spread around the 1:1 line is observed. Improvements of the comparison are foreseen when the underlying emission data for ammonia are further detailed. Overall, the model performance for a regional assessment is very promising. In a next step is seems logical to also investigate the seasonal cycles and search for high resolution observational data sets. As ammonia levels are highly variable more detailed emission information is anticipated to improve the comparison further.

Figure 31.   Comparison between modelled annual average ammonia concentrations and passive sampler observations averaged over 2009-2011.
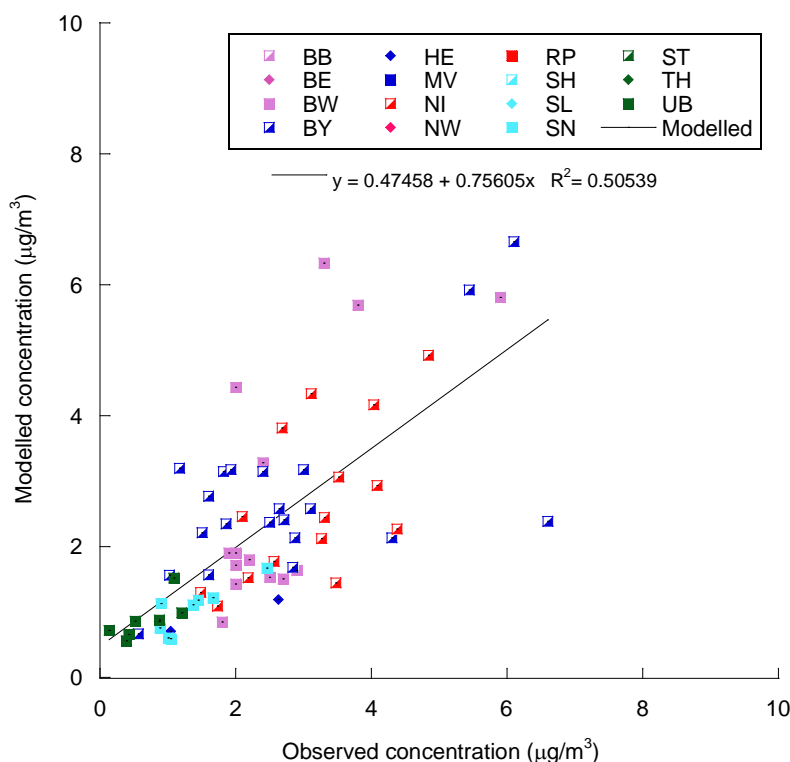
8.2.2   Comparison of total nitrogen deposition at monitoring sites

In Table 28, the total N deposition results of the MAPESI project for 2007 and the PINETI-2 project for 2009 are compared with the estimates at two intensive monitoring site and one research site. The sites are Forellenbach (Bavarian Forest; Beudert and Breit, 2014), Neuglobsow (Brandenburg; Schulte-Bisping and Beese, 2016) and Bourtanger Moor (Lower Saxony; Mohr et al., 2013). Forellenbach is an Integrated Monitoring site (ICP Integrated Monitoring) and is located in the Southeast of Germany in the Bayerischer Wald. Neuglobsow is also an Integrated Monitoring site and is located in the Northeast of Germany. Bourtanger Moor is a Nature2000 area that is located in the Northwest of Germany, close to the border with the Netherlands. Note that the total N deposition at these stations is determined with different methodologies. For Forellenbach and Neuglobsow the PINETI-2 estimates are 10-20 % higher than estimated based on the local observations. For these sites the MAPESI data show values of a factor 2 above the local assessments. At Bourtanger Moor, a variety of methods to determine total N deposition was explored at different locations in the nature area (Mohr et al., 2013) and a large range of total N deposition estimates was found, i.e. values were in a range from roughly 16 till 35 kg ha^{-1} yr^{-1}. Our PINETI-2 estimate for Bourtanger Moor using semi-natural vegetation is 20 Kg N ha^{-1} yr^{-1}, which is within the observed range although slightly lower than the average of all observations of 25 Kg N ha^{-1} yr^{-1}. The corresponding MAPESI estimate was 38 Kg N ha^{-1} yr^{-1}, above the maximum estimate based on the observations.

In short, for these locations it appears that the PINETI-2 values are much more in line with the central estimates based on observations than the rather high total N depositions that were calculated in the MAPESI project for 2007. Unfortunately, the number of intensive monitoring stations is rather low, which highlights the need for additional locations where dry deposition fluxes are determined.

8.2.3 Comparison to deposition assessments from EMEP

In Figure 32, the spatial distributions of the best estimate of the total NOy and total NHx deposition over Germany for 2009 from the PINETI-2 project (upper panels), the officially reported results from EMEP for 2009 (middle panels) and the recalculated results (in 2013) from EMEP for 2009 (lower panels) are shown. Note that the PINETI-2 results are in eq ha^{-1}, while the EMEP results are in mg N m^{-2}. Also note that the color bars in the EMEP figures are not equal, so that it looks like the total reduced nitrogen deposition between EMEP and EMEP_rec2013 increases, while the average value of EMEP_rec2013 is lower. The green arrows on the color bars in the EMEP figures indicate the average value of the EMEP calculation over Germany, while the black arrows indicate the average value of the best estimate from the PINETI-2 project over Germany. The figures show that the spatial distributions of the NOy and NHx deposition in the EMEP model and the best estimate from the PINETI-2 project are rather similar, although it is obvious that the best estimate from the PINETI-2 project is much finer in resolution than the EMEP results. In Table 29 the country average values of the individual panels of Figure 32 are summarized. If we consider the NOy and the NHx contributions to the total N deposition, it is worth mentioning that the recalculated EMEP results for NOy are approximately 22% higher than the originally reported values for 2009 by EMEP. These differences are due to changes in the model code (EMEP, 2012). The modifications in the EMEP model resulted in the increase of both dry and wet NOy deposition in Germany. Hence, also the EMEP results show important impacts due to methodological changes over time. The PINETI-2 results are 10% larger and 10% smaller than the EMEP and EMEP_rec2013 results, respectively. The total NHx deposition is 5% smaller than EMEP and very close to EMEP_rec2013. The total N deposition in the best estimate from the PINETI-2 project is 0.5% and 4% smaller than the values that are calculated by the EMEP and EMEP_rec2013 model, respectively. Altogether, the comparison between the best estimated total N deposition in PINETI-2 and the reported total N deposition by EMEP is remarkably good.

Table 28.   Comparison of best estimate results of MAPESI for 2007 and PINETI-2 for 2009 with monitored total N deposition (kg N ha^{-1} yr^{-1}) at three sites across Germany: Forellenbach (Beudert and Breit, 2014), Neuglobsow (Schulte-Bisping and Beese, 2016) and Bourtanger Moor (Mohr et al., 2013)

	total N monitored at station	total N MAPESI 2007	total N PINETI-2 2009
Forellenbach (coniferous forest)	13-15	37	19
Neuglobsow (coniferous forest)	11	18	12
Bourtanger Moor (semi-natural)	25 (16-35)	38	20

Table 29.   Comparison of total NOy, NHx and N deposition for 2009 in PINETI-2, EMEP and the 2013 EMEP recalculation.

Variable	Unit	PINETI-2	EMEP	EMEP_rec2013
NOy	eq ha^{-1}	385	351	428
NHx	eq ha^{-1}	672	711	670
total N	eq ha^{-1}	1057	1062	1098
NOy	mg N m^{-2}	539	491	599
NHx	mg N m^{-2}	941	996	938
total N	mg N m^{-2}	1480	1487	1537

Figure 32.   Spatial distribution of the total NOy and total NHx deposition over Germany for 2009 from EMEP for 2009 (panels) and the recalculated results from EMEP for 2009 in 2013 (lower panels). For comparison the results of this study is shown in the upper graphs.
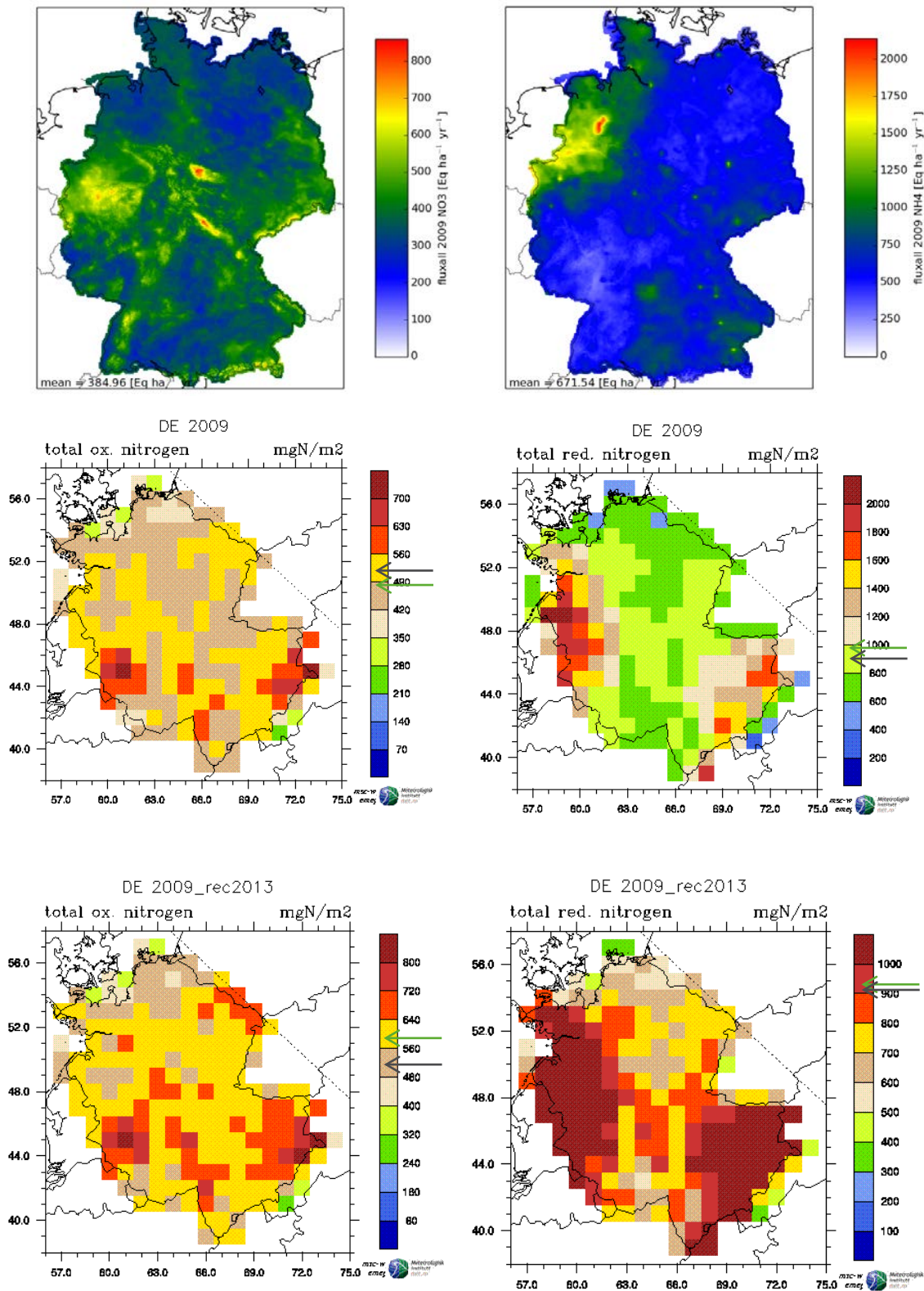
8.2.4 Comparison to the Dutch background deposition maps

In Figure 33, a comparison between reported total N deposition in the Netherlands and the results from the MAPESI project (Builtjes et al., 2011) for 2007 (left figure) and the PINETI-2 project for 2009 (right figure) is made. Note that the red coloured hotspots in the Netherlands are caused by the high resolution 1 x 1 km² emission inventory and consequent plume modelling that are used for the Netherlands, while for Germany we rely on coarser emission information and model resolution. Although the reported years are different, the figures show that the total N deposition in MAPESI for the year 2007 was systematically larger in Germany than on the other side of the border in the Netherlands. The background deposition in the PINETI-2 results for 2009 appear to match much better with the total N deposition in the Netherlands. Hence, consistency has improved within PINETI-2.

Figure 33.　　　Comparison between the total N deposition in the Netherlands for 2012 and the total N deposition in Germany in 2007 (MAPESI project) and 2009 (PINETI-2 project).
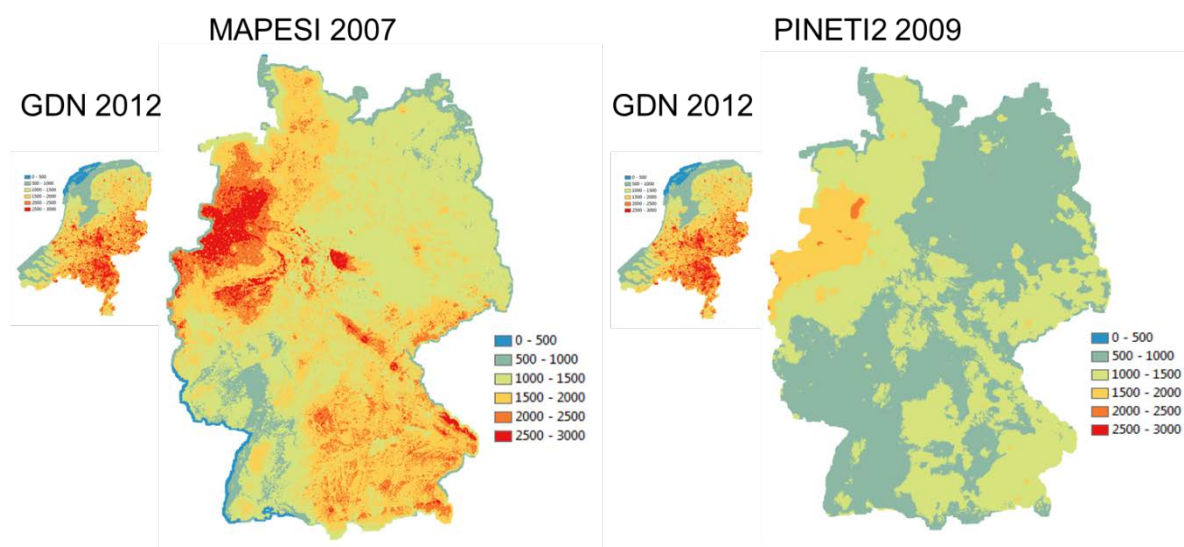
8.2.5 Comparison to canopy budget models

A further source of total N deposition estimates is provided from canopy budget (KRB) models based on through fall measurements. It is commonly accepted that the canopy budget models should underestimate the actual total deposition slightly. Hence, an overestimation of PINETI-2 estimates in comparison to the KRB data was anticipated.

To make the comparison a few datasets were collected. These are the following:

- 50 ICP Forest Level 2 sites in Germany provided by Thünen Institute for 2009.
- 6 stations for Saxony
- 17 stations for Bavaria
- 19 stations for Baden-Württemberg

The data provided by individual states are partly overlapping with the ICP Forest Level 2 sites. Note that the canopy budget model data provided by the states are not implemented in the same way. Moreover, the data from the individual states contained several years of data. Before, comparing all data the different datasets allowed to make a few observations:

- The data reported by the states themselves are on average slightly lower (~10%) than those reported by the ICP Forest-monitoring.

- Comparing the 2009 data to the 5-year means for Bavaria and Baden-Württemberg showed that the 5 year average is within a few percent of 2009 average over all stations. For individual stations differences can reach +/- 30%.

- The evaluation of 4 different approaches for the canopy budget model available for Bavaria showed much closer correspondence for the 5 year mean than for individual years.

Based on these observations we build a combined comparison in which we use the 2009 data provided by ICP Forest complemented by the 5 year mean values for additional stations Bavaria and Baden-Württemberg and 2009 data for two sites in Saxony. In Figure 34 the comparison between this compilation and the PINETI-2 data is shown.

In general, the PINETI-2 total deposition shows estimates for most stations in the range between 1000 and 1500 eq ha^{-1} yr^{-1}, whereas the KRB data lie within a range of 500 to 2500 eq ha^{-1} yr^{-1}. Hence, considering all stations a positive relation between PINETI-2 estimates and KRB data seems absent. However, the comparison shows a mixed picture and a number of features are striking. For instance, all KRB data for Bavarian stations are overestimated by PINETI-2, whereas for Baden-Württemberg all but one stations are underestimated. Moreover, the comparison for stations in Niedersachsen, Sachsen-Anhalt and Brandenburg is favorable with values close to the 1:1 line for most stations. Also for Bavaria and Sachsen the PINETI-2 estimates rise with increasing KRB estimate. However, for Baden-Württemberg and Thüringen these relation is almost absent. In short, the anticipated underestimation is not found and the comparison seems to be state dependent. It appears that the comparison is much better for relative flat areas in comparison to high land.

Figure 34.   Comparison of PINETI-2 2009 total deposition (eq ha^{-1} yr^{-1}) to deposition estimates derived from canopy budget models. The data for individual federal states are indicated.
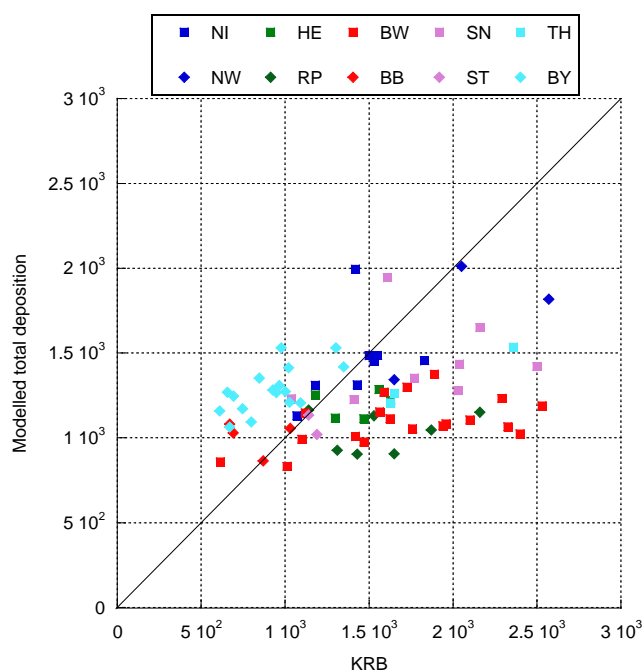
Figure 35.   Comparison of PINETI-2 total deposition (eq ha⁻¹ yr⁻¹) to deposition estimates derived from canopy budget models for each station available
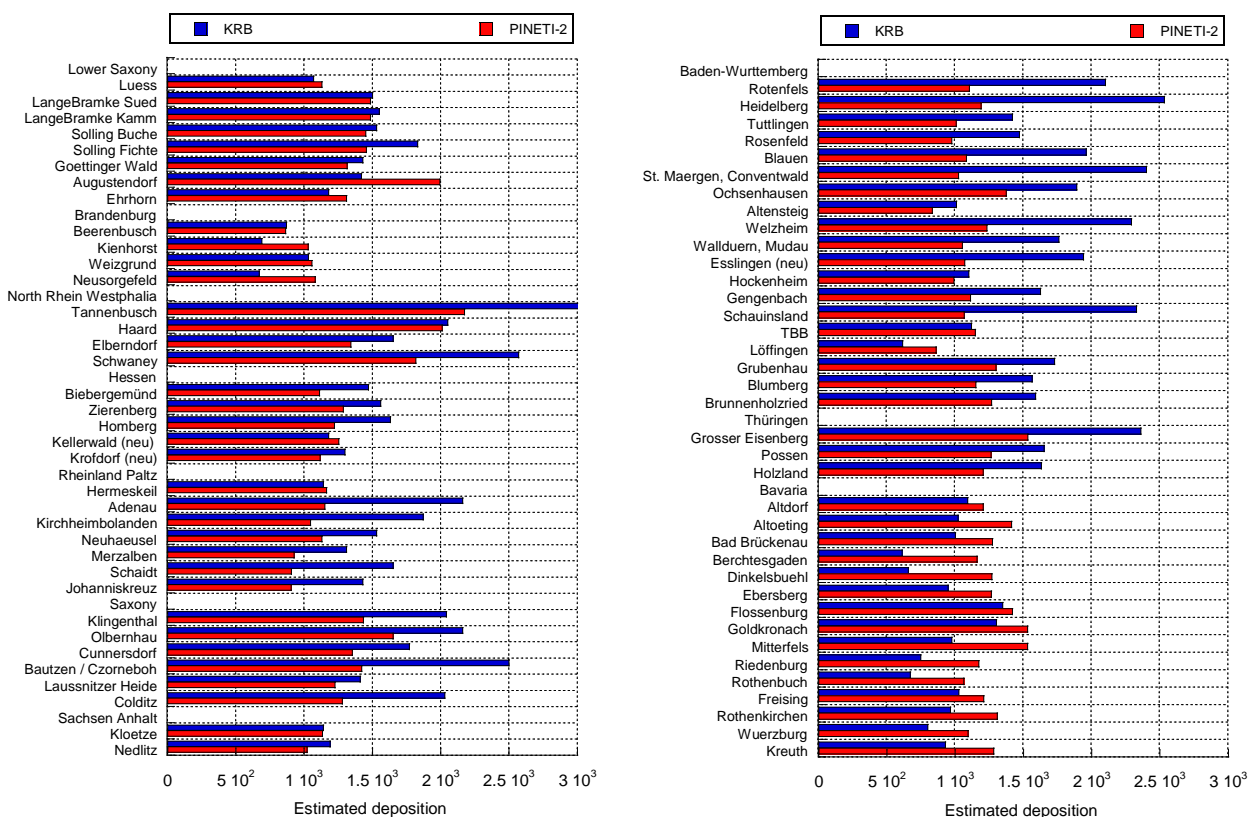
The differences observed between the KRB data and the PINETI-2 estimates are much larger than the differences due to the different methodologies or choice of year. Hence, the origin of the discrepancy must be sought in more fundamental reasons. Given the differences between states a careful analysis of the differences needs to be performed in cooperation with the network operators.

A first step was made through a visit of three stations in Baden-Württemberg, i.e. Schauinsland, Blauen and Löffingen. Schauinsland is located in a small forest with pastures around with grazing animals within 100 m. Blauen is located on a very steep slope of the Rhine Valley on the edge of the black forest. Löffingen is located within a large, relatively flat forest area in the east part of the black forest with no local sources around. From these stations the PINETI-2 data overestimate the KRB data from Löffingen, whereas the other two stations are largely underestimated. Based on the field experience and the discussions surrounding it, we postulate that the KRB data are not in contradiction with the PINETI-2 estimates. However, we feel that the background deposition estimates of PINETI-2 are not representative for locations that are prone to high amounts of occult deposition.

To support this hypothesis we have classified the KRB stations for which we have the station height at our disposal. Table 30 shows the average total N deposition for four height classes. The average values for the KRB data show an increasing tendency with increasing station height. In contrast, the PINETI-2 assessment shows little variation over the data selection. Note that considerable variability is present in the data as evidenced by the station in Löffingen which is located at 800 m with one of the lowest KRB estimates in the country. Despite the variability the classification supports our hypothesis.

Table 30.   Comparison of PINETI-2 total deposition (eq ha^{-1} yr^{-1}) to deposition estimates derived from canopy budget models after categorizing the stations as function of altitude range. The means over N stations are provided as well as the ratio of the fluxes.

Altitude range	N stations	KRB (eq ha^{-1} yr^{-1})	PINETI-2 (eq ha^{-1} yr^{-1})	Ratio KRB/PINETI-2
0-250	14	1250	1217	1.03
250-500	15	1667	1267	1.32
500-750	20	1709	1205	1.42
> 750	10	1861	1158	1.61

A more detailed evaluation of the KRB data is possible for the station of Schauinsland using measured air concentrations and average in combination with dry deposition velocities (Table 31). Measured air concentrations were taken for the UBA station at Schauinsland, located near to the through fall measurement site. The average KRB estimate is 34.9 kg ha^{-1} a^{-1} where the measured wet deposition is 10.7 kg ha^{-1} a^{-1}. To estimate the dry deposition flux from the observed concentrations we use the average dry deposition velocity from the PINETI-2 project. Adding the fluxes of the individual components yields a dry deposition estimate which is four times lower than 24 kg N ha^{-1} a^{-1} allocated to other deposition pathways than wet deposition by the KRB model. Besides the dry deposition values of PINETI-2 we use the values from the VDI 3782-5 as well as a doubling of the latter. The doubled VDI dry deposition velocities shows values which are only observed during mid-day at a beautiful summer day. Hence, they represent absolute maximum values for a given time in the year and are anticipated to be much larger than an annual mean. Even with these values the dry deposition estimate is still lower than the KRB indicates. Hence, even with extreme assumptions on the dry deposition velocity the derived flux by the KRB is not explained by background concentrations. Possible explanations are significant additional inputs through local sources or occult deposition or a large exposure (through e.g. edge effects (Draaijers et al., 1994)).

Table 31.   Dry deposition estimate based on observed annual mean concentrations and different estimates of dry deposition velocities (for explanation see text).

	C (ug m^{-3})	V_d PINETI-2 (cm s^{-1})	V_d VDI (cm s^{-1})	V_d VDI*2 (cm s^{-1})	F_{dry} PINETI-2 (kg ha^{-1} a^{-1})	F_{dry} VDI (kg ha^{-1} a^{-1})	F_{dry} VDI*2 (kg ha^{-1} a^{-1})
NO$_2$	1	0.14	0.3	0.6	0.4	0.9	1.9
NH$_3$	0.8	1.4	2	4	3.5	5.0	10.1
HNO$_3$	0.3	1.5	2.5	5	1.4	2.4	4.7
NH$_4$	0.4	0.2	1	2	0.3	1.3	2.5
NO$_3$	0.3	0.2	1	2	0.2	0.9	1.9
Sum					5.8	10.5	21.1

Next to wet and dry deposition fluxes, the occult deposition contributes significantly to ecosystem acidification and eutrophication (Katata et al., 2011; Klemm and Wrzesinsky, 2007; Grunow, 1954; Baumgartner, 1958,1959). Due to their exposed position forests on mountain slopes or the mountain ridge are especially affected by occult input through advected fogs or clouds. Due to typically higher concentrations of solutes in fog water compared to those in rain water (e.g. Zimmermann et al., 2003; Aleksic et al., 2009) the occult deposition flux may even in these regions be in the same range as the wet deposition flux (e.g. Herckes et al., 2002; Lange et al., 2003; Beudert and Breit, 2012). However,

the occult input does not simply increase with increasing absolute altitude but depends on terrain morphology at the given local area. Increasing relative height, island-mountain type of morphology and position at a windward side of a larger massif favour the occult input (Błaś et al., 2002). This dependency on local terrain morphology may lead to high spatial gradients in the occult input. The latter was already illustrated by Baumgartner in the late 1950s (Baumgartner, 1958). Figure 36 shows the distribution of rain amount and total water deposition amount consisting of rain, dew and fog from May to October 1955 moving from the western slope of the Großer Falkenstein mountain over the summit to the eastern slope of the mountain. While the variation of rain amount is comparatively low along the measuring track, the total water deposition shows an extremely high variation resulting from the fog contribution with an increase in amount of almost 200% within a horizontal distance of below 1 km and a vertical distance of below 100 m. This example shows that the local variability within a 7x7 km² area as assessed by PINETI-2 for occult deposition can be very high and that the design of the sampling strategy (exposed versus background sites) may yield very different total deposition estimates.

Figure 36   Distribution of rain amount and total precipitation amount consisting of rain, dew and fog (y-axis) from May to October 1955 moving from the western slope of the Großer Falkenstein over the summit to the eastern slope of the mountain (x-axis). On the x-axis the horizontal distance from the summit is given in km. The numbers next to the graph give the height a.s.l. of the involved measurement sites. Source: Baumgartner (1958).
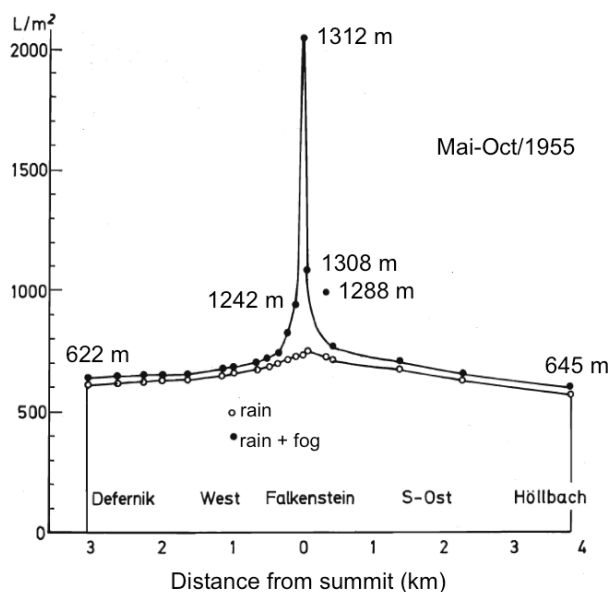
The comparison shown here highlights the necessity to analyze the observed differences between canopy budget model results and the PINETI-2 estimates. As local conditions are relevant this exercise should be performed in cooperation with the network operators. Special attention should be provided to station representativeness with respect to elevation and land use, importance of occult deposition, the role of organic nitrogen and the assumptions concerning sodium deposition in continental conditions. These analyses should confirm or falsify our postulation that the canopy budget results are not in contradiction with the PINETI-2 estimates as the background deposition estimates of this study are not representative for locations that are prone to high amounts of occult deposition.

9 Assessment of the deposition in 2010 and 2011

9.1 Total deposition estimates

After the validation of the new deposition maps for 2009 the system was applied to the two subsequent years. Figure 37 and Figure 38 show the 1 x 1 km² total deposition fields for ammonium, nitrate, total nitrogen, sulphate, sodium, magnesium, potassium and calcium over Germany as derived for 2010 and 2011, respectively. The total deposition has been obtained by summing the fluxes for dry, wet and occult deposition, which are reported in Table 32 for all components. The total N deposition amounts to 1052 eq ha^{-1} a^{-1} and 962 eq ha^{-1} a^{-1} on average across the country for 2010 and 2011, respectively, while for 2009, 1057 eq ha^{-1} a^{-1} was calculated. The spatial patterns look similar for the three years, with maxima in the agricultural regions in the North West and south east of the country. Local maxima are found in mountainous areas because of the higher amounts of rain in these regions.

Spatial patterns for all species do not vary significantly over the period 2009-2011. For most species, deposition in 2010 is within 2% to that of 2009, while for 2011 in general lower deposition values are calculated. An exception to this are Na$^+$ and Mg^{2+}, base cat-ions mainly originating from sea salt. These show an increase of 4-7% in 2010 compared to 2009, while in 2011 they are 10-15% higher than in 2009. For all base cat-ions, the contribution of wet deposition to total deposition is almost constant over the years at 75-80%. For nitrogen and sulphur, the ratio between wet and total deposition is about the same in 2009 and 2010, but this share drops sharply (by on average 4-6 %-points) for 2011 because this was a relatively dry year compared to 2009 and 2010. The annual mean precipitation across Germany in 2011 (= 722 mm) was by 12% lower than the mean of the previous 30 years (Böhme et al., 2012). In 2010, the annual mean precipitation across Germany was 847 mm. Figure 39 shows annual precipitation maps for 2010 and 2011 for the German territory. While a small part in the north north-eastern part of the country received slightly higher precipitation amounts in 2011 compared to 2010, the rest of the country, especially mid, western and south-western Germany, received considerably lower precipitation amounts. These patterns can also be recognised in the total deposition distributions of e.g. total N. In 2011 the total N input over parts of north and north-eastern Germany was increased compared to 2010, while in mid, western and south-western Germany including mountainous areas like the Harz and the Black Forest the total N deposition was considerably lower compared to 2010.

9.2 Using 2009 as a representative year for deposition

For reasons of consistency it can be useful to base regulations and e.g. permit decisions on a 'representative deposition year' rather than updating the deposition information underlying policy decisions every year. It was shown above that specific years may be associated with abnormal meteorological conditions. The meteorology of 2011 was characterized by very dry conditions over large parts of the country (see Figure 39). Hence, using 2011 as a central year is unfortunate to base decisions on.

Unfortunately, there is currently no long time series with deposition maps that were derived with the same methodology. Only for the wet deposition we could extend the time series with the years 2007 and 2008 as the mapping methodology was developed and applied in the PINETI-I project (Wichink Kruit et al., 2014). In Figure 40, the average wet NH$_x$ deposition over Germany is plotted for each year in the period 2007-2011. The 5-year average is also displayed, showing that the wet NH$_x$ deposition for Germany as a whole in 2009 is very close to the five year average. Of course, the total deposition mapped for 2009 is not so close to the five year average for every location in Germany as year-to-year differences as region to region variability can be significant compared to the country-wide variability. All in all, 2009 seems to be the best choice for a representative year for the period 2007-2011.

Table 32.   Average calculated wet, dry, occult and total deposition (eq ha^{-1} yr^{-1}) of base cat-ions, sulfate and nitrogen for Germany for 2010 and 2011.

Species	2010				2011			
	Wet	Dry	Occult	Total	Wet	Dry	Occult	Total
Ca	72	19	1	91	63	16	1	80
Ca_nss	65	17	1	84	57	14	1	72
K	25	5	0	31	22	4	0	26
K_nss	22	5	0	27	18	4	0	22
Mg	44	13	0	57	48	13	1	61
Mg_nss	11	3	0	15	12	3	0	15
Na	144	40	1	185	163	39	2	204
NH$_4$	339	310	8	658	288	330	7	625
NO$_3$	256	132	6	395	197	134	5	336
SO$_4$	184	119	3	306	149	114	3	266
SO$_4$_nss	167	114	3	284	130	110	3	242
N	596	443	14	1052	485	464	13	962

Figure 37.　　Overview of total deposition (eq ha^{-1} yr^{-1}) for ammonium, nitrate, total Nr, sulfate, sodium, magnesium, potassium and calcium for 2010
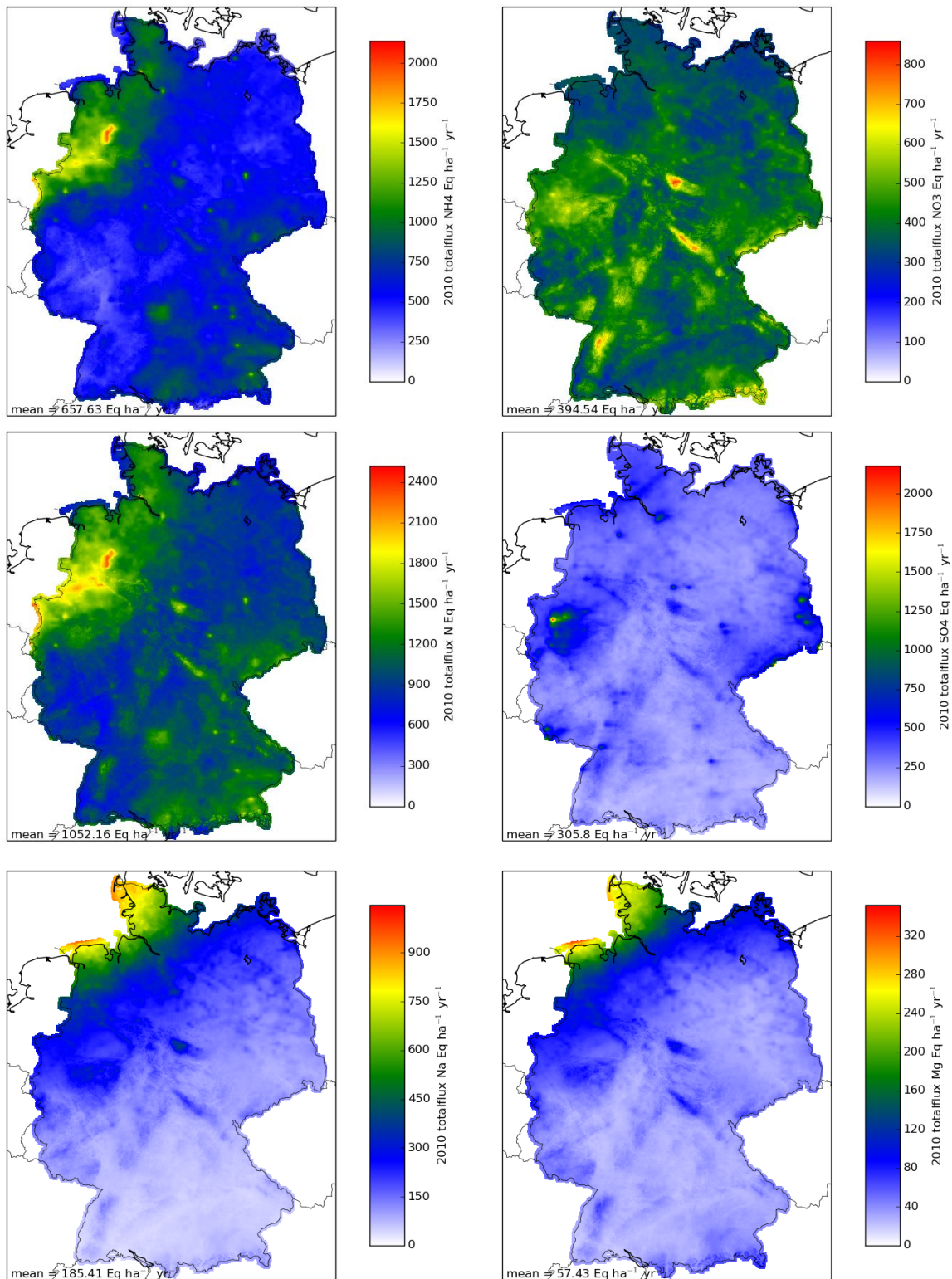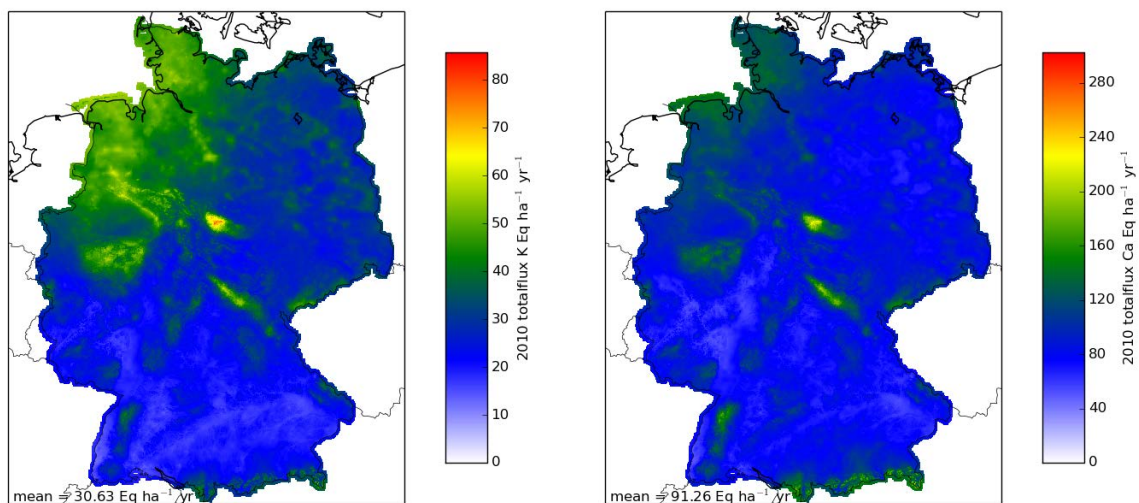
Figure 38. Overview of total deposition (eq ha⁻¹ yr⁻¹) for ammonium, nitrate, total Nr, sulfate, sodium, magnesium, potassium and calcium for 2011
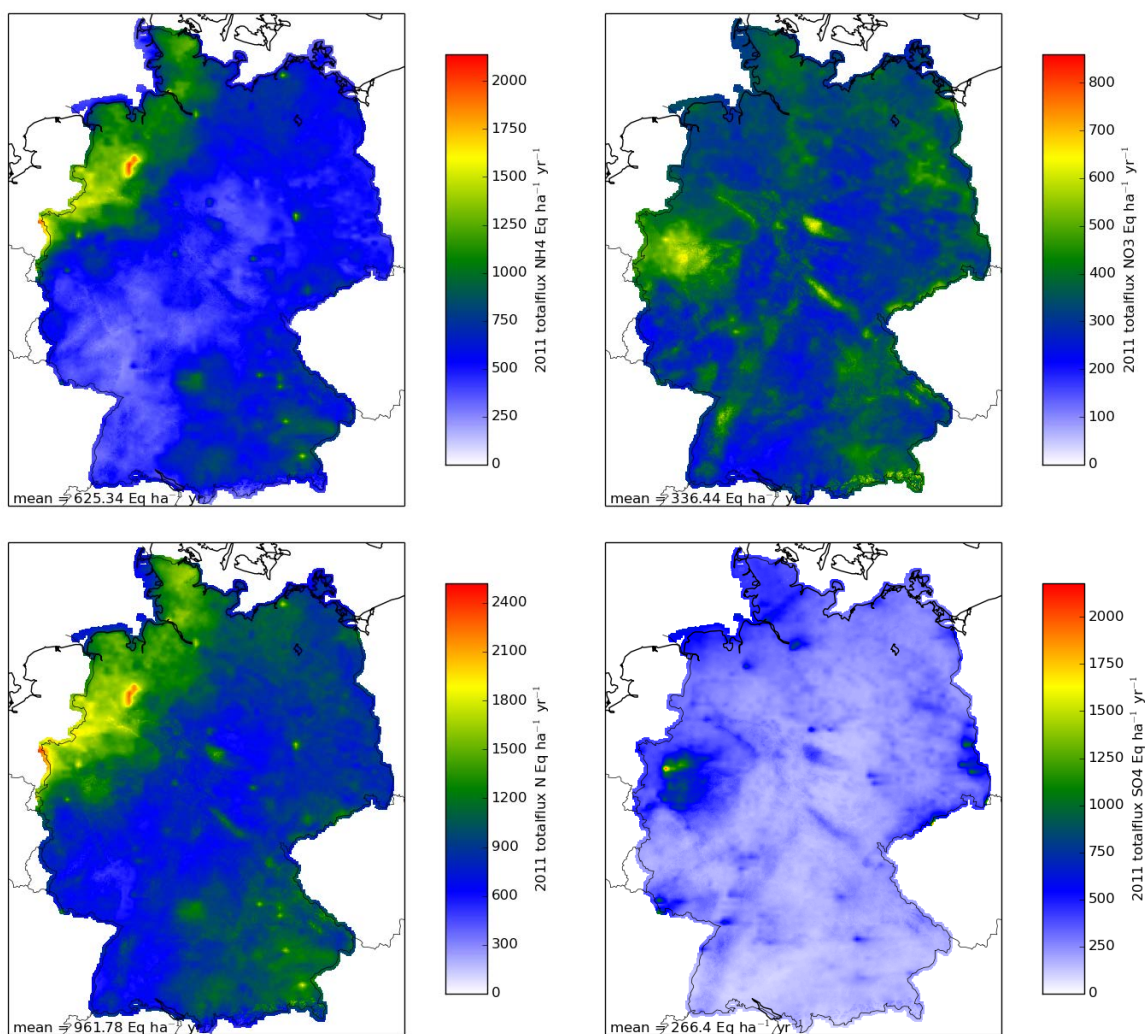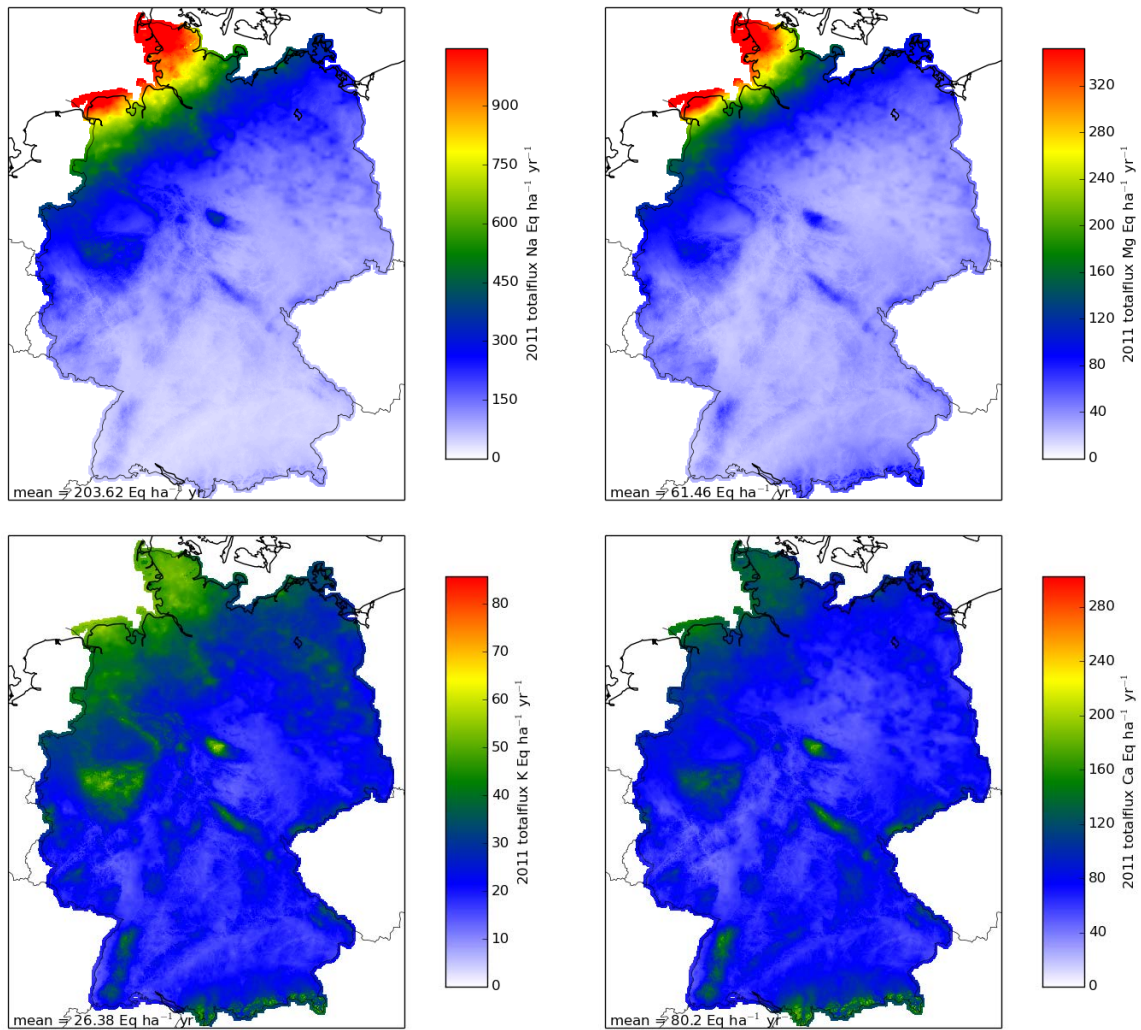
Figure 39.   Annual precipitation (mm) for 2010 (left panel) and 2011 (right panel)
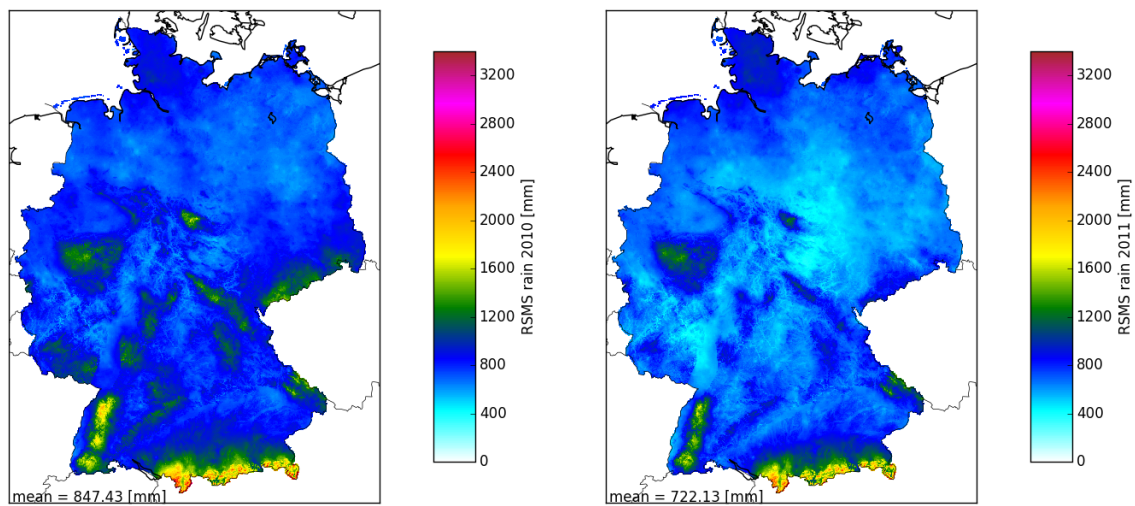
Figure 40.   Wet NH$_x$ deposition for the period 2007-2011, as well as the 5-yr average.
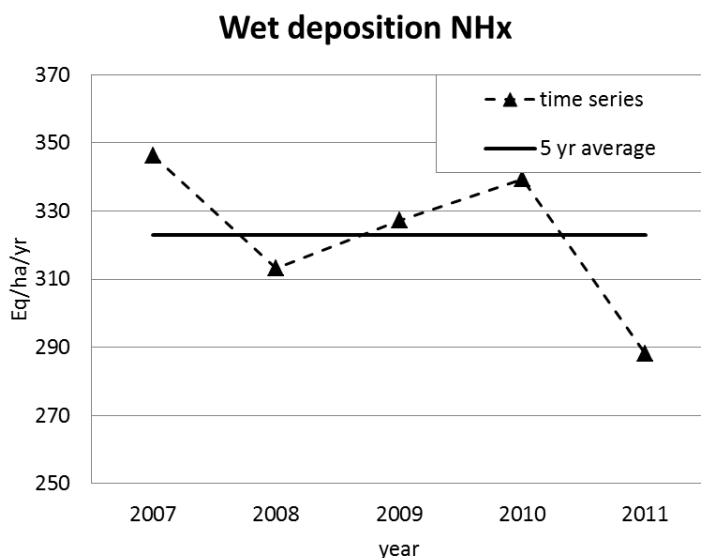
10   Conclusion and recommendations

In this study we have presented a new quantitative estimates of the deposition of atmospheric nitrogen and sulfur compounds as well as base cat-ions to ecosystems across Germany. On average the nitrogen deposition in Germany was 1057 eq ha^{-1} yr^{-1} in 2009. Separate maps are available for the major land use classes. The results of this study are systematically lower than provided in earlier studies, i.e. MAPESI (Builtjes et al., 2011). The main reasons are an improved wet deposition estimation and the consolidation of improved process descriptions in the LOTOS-EUROS model, which has led to a better agreement with observations. The methodologies applied in this study reflect the current state-of-the-art. The PINETI-2 deposition estimates show a better agreement with results obtained by integrated monitoring and deposition mapping by EMEP than MAPESI results. A challenge that remains is that the underestimation of canopy budget model estimates is more pronounced in PINETI-2 than in MAPESI. It appears that the underestimation is especially present at elevations locations with potentially high impacts of occult deposition.

10.1   Recommendations

In this report the estimates of the deposition for 2009, 2010 and 2011 are presented. Comparison to earlier studies shows that the estimate for the total deposition on German territory is considerably lower than estimated before in MAPESI and earlier projects. The reason can be found in the large update in methodological approached for the three deposition pathways within the PINETI and PINETI-2 projects. Such impacts of methodological changes can also be observed between results of earlier studies. The impact of methodological changes within the sequence of deposition assessments clearly overrules the impact of emission reductions and meteorological variability. Hence, it is recommended to reassess the time series of total deposition based on consistent input information and assessment methodology from 2000 onwards.

Due to variability in meteorological conditions from year to year the deposition estimates at a given location in the country can vary considerably between years. For example, in a dry year the wet deposition in an area could be 30% less than in the previous and wetter year. This effect is clearly visible for 2011, which has considerably lower wet deposition over large parts of the country than in previous years. To monitor the impact of environmental policies one would like to remove the meteorological variability from the time series. Given the use of the deposition distributions in environmental impact assessments the mapping of the deposition under (more) average meteorological conditions could

generate a better level playing field. Unfortunately, the generation of an average meteorological dataset for a country as a whole is not possible. Therefore, it could be assessed if averaging deposition fluxes over several years (3-5) would yield more representative distributions. The latter seems possible as the meteorological variability has a larger impact than the at most few percent emission change assumed between individual years. Hence, we recommend to assess the use of multi-year averages based on the reanalysis recommended above.

A more detailed model evaluation should be carried out concerning the following aspects:

- Expand the evaluation of the ammonia distributions started in this study.

- Analyze the observed differences between canopy budget model results and the PINETI-2 estimates in cooperation with network operators and experts. Special attention should be provided to station representativeness with respect to elevation and land use, importance of occult deposition, the role of organic nitrogen and the assumptions concerning sodium deposition in continental conditions. These analyses should confirm or falsify our postulation that the canopy budget results are not in contradiction with the PINETI-2 estimates as the background deposition estimates of this study are not representative for locations that are prone to high amounts of occult deposition

- Investigate and review the role of organic nitrogen in the nitrogen deposition.

- There is a general lack of dry deposition measurements. Time series of dry deposition fluxes to different ecosystems in different pollution regimes are needed to verify deposition parameterizations. Especially with respect to ammonia and particles novel techniques may allow to build a better basis for model evaluation and improvement.

Concerning the emission information used in the modelling we recommend the following:

- Update the spatial emission distribution which currently reflects the 2005 situation.

- Investigate why the NOx concentrations and trends in Europe decline slower than anticipated based on emission inventories (Banzhaf et al., 2014). Specific attention is needed to explain this mismatch and the corrective action needs to be taken when the causes are known.

- Investigate the use of improved spatial allocation maps for manure application on arable land.

- Investigate the use of improved temporal emission variability. Skjoth et al (2011) and Mues et al. (2013) showed that meteorological dependent emission descriptions have a positive impact on the model performance in comparison to observations. Agricultural emissions are dependent on synoptic variability in e.g. ambient temperature. However, this dependency is currently neglected as all activities have the same temporal allocation. Updates in temporal emission variability may affect nitrogen budgets regionally.

To be able to perform scenario studies aimed at emission mitigation and climate change impacts the CTM LOTOS-EUROS should be further improved and become as close as possible in agreement with representative observations. In the ideal situation the model should incorporate all important deposition processes and components. Hence, further developments could aim at:

- Incorporate a plume in grid approach to enhance the resolution of the assessment. Anticipating on detailed emission information concerning the agricultural sector the short distance dispersion and deposition could be described using a plume modelling approach. To correctly incorporate the non-linear chemistry and long range transport the plume modelling should be integrated into the eulerian grid model. Currently, such approaches are tested for the LOTOS-EUROS model.

- Improve the modelling capacity for estimating base cat-ion deposition. To leave the fully empirical approach for base cat-ions the capacity to model the distributions of potassium and calcium should be enhanced. The modelled distributions for sodium and magnesium already show a performance that is sufficient to use them in a similar way as the nitrogen components in the mapping approach.

- Including a process description for the occult deposition. Based on the abovementioned results a new process description for occult deposition should be developed and tested.

- Investigating the use of high resolution meteorological modelling data. Given the wish for increased resolution and improved process descriptions higher quality meteorological data need to be secured. Currently, meteorological modelling at a resolution of a few kilometer is becoming available. It should be explored if this high resolution modelling offers benefits for the current assessments.

The listed model improvements require considerable effort and time, but are anticipated to improve the quality of future assessments.

11 Quellenverzeichnis

Acker, K., Moller, D., Marquardt, W., Bruggemann, E., Wieprecht, W., Auel, R., Kalaß, D., 1998. Atmospheric research program for studying changing emission patterns after German unification. Atmos Environ 1998; Vol 32, No. 20, pp. 3435 –3443.

Aleksic, N., Roy, K., Sistla, G., Dukett, J., Houck, N., Casson, P., 2009. Analysis of cloud and precipitation chemistry at Whiteface Mountain, NY. Atmospheric Environment, Volume: 43 , Issue: 17.

Banzhaf, S., Schaap, M., Kerschbaumer, A., Reimer, E., Stern, R., van der Swaluw, E. and Builtjes, P. (2012): Implementation and evaluation of pH-dependent cloud chemistry and wet deposition in the chemical transport model REM-Calgrid. Atmospheric Environment 49, 378-390.

Banzhaf, S., Schaap, M., Kranenburg, R., Manders, A. M. M., Segers, A. J., Visschedijk, A. H. J., Denier van der Gon, H. A. C., Kuenen, J. J. P., van Meijgaard, E., van Ulft, L. H., Cofala, J. and Builtjes, P. J. H. (2014): Dynamic model evaluation for secondary inorganic aerosol and its precursors over Europe between 1990 and 2009. Geosci. Model Dev. Discuss., 7, 4645-4703, doi:10.5194/gmdd-7-4645-2014.

Baumgartner, A., 1958. Nebel und Niederschlag als Standortfaktor am Großen Falkenstein (Bayrischer Wald) Forstwiss. Centralblatt 13, 257–272.

Baumgartner, A., 1959. Das Wasserangebot aus Regen und Nebel sowie die Schneeerteilung in den Wäldern am Großen Falkenstein (Bayrischer Wald). Wald und Wasser 3, 45-54.

Beltman, J. B., Hendriks, C., Tum, M., & Schaap, M. (2013). The impact of large scale biomass production on ozone air pollution in europe. Atmospheric Environment, 71, 352-363.

Beudert, B. und Breit, W., 2012. Horizontaler Niederschlag, nasse und feuchte Deposition im Inneren Bayerischen Wald. Integrated Monitoring Programm an der Messstelle Forellenbach im Nationalpark Bayerischer Wald. Umweltbundesamt Förderkennzeichen 351 01 012/04.

Beudert, B. and W. Breit (2014). Kronenraumbilanzen zur Abschätzung der Stickstoffgesamtdeposition in Waldökosysteme des Nationalparks Bayerischer Wald. Integrated Monitoring Programm an der Messstelle Forellenbach im Nationalpark Bayerischer Wald, Projektnummer 24314, Im Auftrag des Umweltbundesamtes

Błaś, M., Sobik, M., Quiel, F., Netzel, P. (2002): Temporal and spatial variations of fog in the Western Sudety Mts., Poland, Atmospheric Research, Volume 64, Issues 1–4, Pages 19-28, ISSN 0169-8095, http://dx.doi.org/10.1016/S0169-8095(02)00076-5

Bleeker, A., Draaijers, G .P. J., Klap, J. M. and Van Jaarsveld, J. A., 2000. Deposition of Acidifying Components and Base Cations in the Period 1987-1995 in Germany. Study on Behalf and for the Account of Umweltbundesamt, Berlin (FE. Nr. 108 03 081). National Institute of Public Health and the Environment (RIVM). Bilthoven. Report No. 722108027.

Bobbink, R., Hornung, M., Roelofs, J.G.M., 1998. The effects of air-borne nitrogen pollutants on species diversity in natural and semi-natural European vegetation. Journal of Ecology 86, 717-738.

Böhme, M., Böttcher, F., Lefebvre, C., Löpmeier, F.-J., Müller-Westermeier, G., Pietzsch, S., Riecke, W., Schmitt, H.-H., 2012: Die Witterung in Deutschland 2011, Klimastatusbericht 2011, Deutscher Wetterdienst (DWD), Offenbach, Germany.

Bormann, B.T., R.F. Tarrant, M.H. McClellan and T. Savage, 1989. Chemistry of rainwater and cloud water at remote sites in Alaska and Oregon. Journal of Environmental Quality, 18, 149-152.

Brantner, B., H. Fierlinger and H. Puxbaum (1994), Cloud water chemistry in the subcooled droplet regime at Mount Sonnblick. Water, Air and Soil Pollution, 74, 363-384.

Builtjes, P.J.H., Hendriks, E., Koenen, M., Schaap, M., Banzhaf, S., Kerschbaumer, A., Gauger, T., Nagel, H.-D., Scheuschner, T., Schlutow, A., 2011. Erfassung, Prognose und Bewertung von Stoffeintraegen und ihren Wirkungen in Deutschland (in German). MAPESI-Project: Modeling of Air Pollutants and Ecosystem Impact. UBA Bericht zu BMU/UBA FE-Nr. 3707 64 200; Texte 38/2011; ISSN 1862-4804; Umweltbundesamt, Dessau-Roßlau, 2011.

Burkard, R., Butzberger, P., Eugster, W., 2003. Vertical fogwater flux measurements above an elevated forest canopy at the Lageren research site, Switzerland. Atmospheric Environment 37, 2979-2990.

CLRTAP, 2004. Manual on Methodologies and Criteria for Modelling and Mapping Critical Loads and Levels and Air Pollution Effects, Risks and Trends. (www.icpmapping.org)

CLRTAP, 2011. Mapping Manual. Chapter 3. Update June 2011. (www.icpmapping.org)

Collet, J., B. Oberholzer and J. Staehelin, 1993. Cloud chemistry at Mt. Rigi, Switzerland: dependence on drop size and relationship to precipitation chemistry. Atmospheric Environment, 27a, 33-42.

Crossley, A., D.B. Wilson and R. Milne, 1992. Pollution in the upland environment. Environmental Pollution, 75, 81-87

Curier, R. L., Timmermans, R., Calabretta-Jongen, S., Eskes, H., Segers, A., Swart, D., et al. (2012). Improving ozone forecasts over europe by synergistic use of the LOTOS-EUROS chemical transport model and in-situ measurements. Atmospheric Environment, 60, 217-226.

Curier, R.L., Kranenburg, R., Segers, A.J.S., Timmermans, R.M.A., Schaap, M. (2014), Synergistic use of OMI NO2 tropospheric columns and LOTOS-EUROS to evaluate the NOx emission trends across Europe, Remote Sensing of Environment, 149, pp. 58-69.

Dasch, J.M., 1988. Hydrological and chemical inputs to fir trees from rain and clouds during a 1-month study at Clingmans Peak, NC. Atmospheric Environment Vol. 22, No. 10, 2255–2262.

Doms, G. ; Förstner, J. ; Heise, E. ; Herzog, H.-J. ; Mironov, D. ; Raschendorfer, M. ; Reinhardt, T. ; Ritter, B. ; Schrodin, R. ; Schulz, J.-P. ; Vogel, G.: A Description of the Nonhydrostatic Regional COSMO-Model. Part II: Physical Parameterization. Printed at Deutscher Wetterdienst, P.O. Box 100465, 63004 Offenbach, Germany, 2011

Draaijers, G. P. J., Van Leeuwen, E.P., de Jong, P.G.H., Erisman, J.W., 1996. Deposition of base-cations in Europe and its role in acid neutralization and forest nutrition. RIVM Report 722108017, Bilthoven, the Netherlands. 79 pp.

Draaijers, G. P. J., R.Van Ek, and W. Bleuten, 1994. Atmospheric deposition in complex forest landscapes, Boundary Layer Meteorol., 69, 343–366, doi:10.1007/BF00718124.

EMEP, 1996: EMEP manual for sampling and chemical analysis, EMEP/CCC-Report 1/95, Norwegian Institute for Air Research, Kjeller, Norway.

EMEP, 2012: Model description at www.emep.int

Hurkuck, M., Brümmer, C., Mohr, K., Grünhage, L., Flessa, H., Kutsch, W.L. (2014): Determination of atmospheric nitrogen deposition to a semi-natural peat bog site in an intensively managed agricultural landscape, Atmospheric Environment, 97, pp. 296-309

Erisman, J. W., & Schaap, M. (2004). The need for ammonia abatement with respect to secondary PM reductions in europe. Environmental Pollution, 129(1), 159-163.

Erisman, J.W., Bleeker, A., Galloway, J., Sutton, M.S. Reduced nitrogen in ecology and the environment (2007) Environmental Pollution, 150 (1), pp. 140-149.

Fountoukis, C. and Nenes, A.: ISORROPIA II (2007): a computationally efficient thermodynamic equilibrium model for K+,Ca2+,Mg2+,NH4+,Na+,SO42 ,NO3-,Cl-, H2O aerosols. Atmos. Chem. and Phys., 7, 4639-4659.

Fowler, D., I.D. Leith, J. Binnie, A. Crossley, D.W.F. Inglis, T.W. Choulartan, J.W.S. Longhurst and D.E. Colan, 1995: Orographic enhancement of wet deposition in the United Kingdom: continuous monitoring. Water, Air and Soil Pollution, 85, 2107-2112.

Fowler D., Pilegaard K., Sutton M.A., et al., 2009. Atmospheric Composition Change: Ecosystems - Atmosphere interactions. Atmospheric Environment 43, 5193-5267.

Galloway, J.N., Aber, J.D., Erisman, J.W., Seitzinger, S.P., Howarth, R.W., Cowling, E.B., Cosby, B.J. The nitrogen cascade (2003) BioScience, 53 (4), pp. 341-356

Gauger Th, Köble R, Anshelm F (2000) Kritische Luftschadstoff-Konzentrationen und Eintragsraten sowie ihre Überschreitung für Wald- und Agrarökosysteme sowie naturnahe waldfreie Ökosysteme. Teil 1: Deposition Loads. Teil 2: Critical Levels. Forschungsvorhaben im Auftrag des BMU/UBA, FENr. 297 85 079. Institut für Navigation, Universität Stuttgart. [http://www.nav.uni-stuttgart.de/navigation/forschung/critical_loads/INS_UBA29785079_1.pdf]

Gauger Th, Haenel HD, Rösemann C, Dämmgen U, Bleeker A, Erisman JW, Vermeulen AT, Schaap M, Timmermanns RMA, Builtjes PJH, Duyzer JH (2008) National Implementation of the UNECE Convention on Long-range Transboundary Air Pollution (Effects) / Nationale Umsetzung UNECELuftreinhaltekonvention (Wirkungen): Part 1: Deposition Loads: Methods, modelling and mapping results, trends. BMU/UBA FE-Nr. 204 63 252. UBA-Texte 38/08 (1). ISSN 1862-4804 . Teil 2: Wirkungen und Risiokoabschätzungen: Critical Loads, Biodiversität, Dynamische Modellierung, Critical Levels Überschreitungen, Materialkorrosion. BMU/UBA 204 63 252.

UBA-Texte 38/08 (2). ISSN 1862-4804. [http://www.umweltdaten.de/publikationen/fpdf-l/3646.pdf & http://www.umweltda-ten.de/publikationen/fpdf-l/3647.pdf]

Grubbs, F., 1969. Procedures for Detecting Outlying Observations in Samples. Technometrics 11, 1-21.

Grunow, J., 1954. Bedeutung und Erfassung des Nebelniederschlags. IAHS Info 36, 402-415.

Hendriks, C., Kranenburg, R., Kuenen, J., et al. (2013). The origin of ambient particulate matter concentrations in the Netherlands. Atmospheric Environment, 69, 289-303.

Herckes, P., Mirabel, P. and Wortham, H. 2002. Cloud water deposition at a high-elevation site in the Vosges Mountains (France). Sci. Total Environ. 296, 59–75.

Im, U., Bianconi, R., Solazzo, E., Kioutsioukis, I., Badia, A., Balzarini, A., Baró, R., Bellasio, R., Brunner, D., Chemel, C., Curci, G., Denier van der Gon, H., Flemming, J., Forkel, R., Giordano, L., Jiménez-Guerrero, P., Hirtl, M., Hodzic, A., Honzak, L., Jorba, O., Knote, C., Makar, P.A., Manders-Groot, A., Neal, L., Pérez, J.L., Pirovano, G., Pouliot, G., San Jose, R., Savage, N., Schroder, W., Sokhi, R.S., Sy-rakov, D., Torian, A., Tuccella, P., Wang, K., Werhahn, J., Wolke, R., Zabkar, R., Zhang, Y., Zhang, J., Hogrefe, C., Galmarini, S., 2015. Evaluation of operational online-coupled regional air quality models over Europe and North America in the context of AQMEII phase 2. Part II: Particulate matter, Atmospheric Environment, 115, pp. 421-441

Inglis, D.W.F., T.W. Choularton, A.J. Wicks, D. Fowler, I.D. Leith, B. Werkman and J. Binnie, 1995. Orographic enhancement of wet deposition in the United Kingdom: case studies and modelling. Water, Air and Soil Pollution, 85, 2119-2124.

Jörß, W., Kugler, U., Theloke, J., 2010. " Emissionen im PAREST Referenzszenario 2005-2020", Parest-Bericht Mai 2010.

Katata, G., H. Nagai, T. Wrzesinsky, O. Klemm, W. Eugster, and R. Burkard, 2008. Development of a land surface model including cloud water deposition on vegetation, J. Appl. Meteorol. Climatol., 47, 2129–2146, doi:10.1175/2008JAMC1758.1.

Katata, G., Kajino, M., Hiraki, T., Aikawa, M., Kobayashi, T., Nagai, H., 2011. A method for simple and accurate estimation of fog deposition in a mountain forest using a meteorological model. Journal of Geophysical Research , Vol. 116, No. D20, doi:10.1029/2010JD015552.

Klemm, O. and Wrzesinsky, T., 2007. Fog deposition fluxes of water and ions to a mountainous site in Central Europe. Tellus B (59), 705–714.

Kuenen, J.J.P., Visschedijk, A.J.H., Jozwicka, M., Denier Van Der Gon, H.A.C. (2014): TNO-MACC-II emission inventory; A multi-year (2003-2009) consistent high-resolution European emission inventory for air quality modelling, Atmospheric Chemistry and Physics, 14 (20), pp. 10963-10976.

Lange, C. A., Matschullat, J., Zimmermann, F., Stertig, G. and Wienhaus, O., 2003. Fog chemistry and chemical composition of fog water—a relevant contribution to atmospheric deposition in the eastern Erzgebirge, Germany. Atmos. Environ. 37, 3731–3739.

Manders, A. M. M., Schaap, M., & Hoogerbrugge, R. (2009). Testing the capability of the chemistry transport model LOTOS-EUROS to forecast PM10 levels in the netherlands. Atmospheric Environment, 43(26), 4050-4059.

Manders, A. M. M., Schaap, M., Querol, X., Albert, M. F. M. A., Vercauteren, J., Kuhlbusch, T. A. J., et al. (2010). Sea salt concentra-tions across the european continent. Atmospheric Environment, 44(20), 2434-2442

Miller, E.K., J.A. Panek, A.J. Friedland, J. Kadlecek and V.A. Mohnen, 1993. Atmospheric deposition to a high-elevation forest at Whiteface Mountain, New York, USA. Tellus, 45b, 209-227.

Mohr et al. (2013), Emsland: Erfassung der Stickstoffbelastungen aus der Tierhaltung zur Erarbeitung innovativer Lösungsansätze für eine zukunftsfähige Landwirtschaft bei gleichzeitigem Schutz der sensiblen Moorlandschaft (ERNST),

Mues, A., Kuenen, J., Hendriks, C., Manders, A., Segers, A., Scholz, Y., Hueglin, C., Builtjes, P., Schaap, M. (2014), Sensitivity of air pollution simulations with LOTOS-EUROS to the temporal distribution of anthropogenic emissions, Atmospheric Chemistry and Physics, 14 (2), pp. 939-955

Posch M., Slootweg J., Hettelingh J.-P., (eds.) (2012): Modelling and Mapping of Atmospherically –induced Ecosystem Impacts in Europe, CCE Status Report 2012, Coordination Centre for Effects, RIVM, Bilthoven

Pouliot, G., Pierce, T., Denier van der Gon, H., Schaap, M., Moran, M., & Nopmongcol, U. (2012). Comparing emission inventories and model-ready emission datasets between europe and north america for the AQMEII project. Atmospheric Environment, 53, 4-14.

Reynolds, B., D. Fowler and S. Thomas, 1996. Chemistry of cloud water at an upland site in mid-Wales. The Science of the Total Environment, 188, 115-125.

Schaap, M., van Loon, M., ten Brink, H. M., Dentener, F. J., & Builtjes, P. J. H. (2004). Secondary inorganic aerosol simulations for europe with special attention to nitrate. Atmospheric Chemistry and Physics, 4(3), 857-874.

Schaap, M., Timmermans, R. M. A., Roemer, M., Boersen, G. A. C., Builtjes, P. J. H., Sauter, F. J., et al. (2008). The LOTOS-EUROS model: Description, validation and latest developments. International Journal of Environment and Pollution, 32(2), 270-290.

Schaap, M., Otjes, R. P., & Weijers, E. P. (2011). Illustrating the benefit of using hourly monitoring data on secondary inorganic aerosol and its precursors for model evaluation. Atmospheric Chemistry and Physics, 11(21), 11041-11053.

Schaap, M., Kranenburg, R., Curier, L., Jozwicka, M., Dammers, E., Timmermans, R. (2013), Assessing the sensitivity of the OMI-NO2 product to emission changes across Europe, Remote Sensing, 5 (9), pp. 4187-4208.

Schaap, M., Wichink Kruit, R.J., Kranenburg, R., Banzhaf, S., Manders, A.M.M. (2016), Sensitivity of modelled land use specific deposition fluxes to improved process descriptions in LOTOS-EUROS, MS in preparation to be submitted to atmospheric environment.

Schaap, M., C. Cuvelier, C. Hendriks, B. Bessagnet, J.M. Baldasano, A. Colette, P. Thunis, D. Karam, H. Fagerli, A. Graff, R. Kranenburg, A. Nyiri, M.T. Pay, L. Rouïl, M. Schulz, D. Simpson, R. Stern, E. Terrenoire, P. Wind (2015), Performance of European chemistry transport models as function of horizontal resolution, Atmospheric Environment, 112, 90-105

Schemenauer, R. S., Banic, C. M. and Urquizo, N. 1995. High-elevation fog and precipitation chemistry in Southern Quebec, Canada. Atmos. Environ. 29, 2235–2252.

Schrader, F, and Brümmer, C. (2014): Genfer Luftreinhaltekonvention der UNECE: Literaturstudie zu Messungen der Ammoniak-Depositionsgeschwindigkeit, UBA report 67/2014, Dessau, http://www.umweltbundesamt.de/sites/default/files/medien/378/publikationen/texte_67_2014_literaturstudie_zu_messungen_der_ammoniak-depositionsgeschwindigkeit.pdf

Simpson, D.; Benedictow, A.; Berge, H.; Bergström, R.; Emberson, L.D.; Fagerli, H.; Flechard, C.R.; Hayman, G.D.; Gauss, M.; Jonson, J.E.; Jenkin, M.E.; Nyíri, A.; Richter, C.; Semeena, V.S.; Tsyro, S.; Tuovinen, J.-P.; Valdebenito, Á.; Wind, P., 2012: The EMEP MSC-W chemical transport model - technical description. Atmospheric Chemistry and Physics, 12 (16). 7825-7865.

Skjøth, C.A., Geels, C., Berge, H. et al.. 2011. Spatial and temporal variations in ammonia emissions: a freely accessible model code for Europe. Atmospheric Chemistry and Physics, 11 (11), 5221-5236

Skybova M., 2006. Chemical composition of fog/cloud and rain water in the Beskydy mountains-Czech Republic. Fresenius Environmental Bulletin, 15: 448–451.

Schulte-Bisping, H. and F. Beese (2016). "N-fluxes and N-turnover in a mixed beech–pine forest under low N-inputs." European Journal of Forest Research: 1-13

Thalmann, E., Burkard, R., Wrzesinsky, T., Eugster, W. and Klemm, O. 2002. Ion fluxes from fog and rain to an agricultural and a forest ecosystem in Europe. Atmos. Res. 64, 147–158.

UBA, 2004: Qualitätssicherungs-Handbuch des UBA-Messnetzes (in German), UBA Texte 28/04, (Federal Environmental Agency), Dr. Klaus Nienerowski, Umweltbundesamt, Berlin, Germany.

UBA, 2014: http://www.umweltbundesamt.de/sites/default/files/medien/376/dokumente/de_2014_nfr-tabellen.zip

Van Damme, M., R. J. Wichink Kruit, M. Schaap, L. Clarisse, C. Clerbaux, P.-F., Coheur, E. Dammers, A. J. Dolman, J. W. Erisman (2014), Evaluating 4 years of atmospheric ammonia (NH3) over Europe using IASI satellite observations and LOTOS-EUROS model results, J. Geophys. Res. Atmos., 119, doi:10.1002/2014JD021911.

Van Zanten, M.C., Sauter, F.J., Wichink Kruit, R.J., Van Jaarsveld, J.A., Van Pul, W.A.J. (2010): Description of the DEPAC module: Dry deposition modelling with DEPAC GCN2010, RIVM Report 680180001/2010.

Vautard, R., Schaap, M., Bergström, R., Bessagnet, B., Brandt, J., Builtjes, P.J.H., Christensen, J.H., Cuvelier, C., Foltescu, V., Graff, A., Kerschbaumer, A., Krol, M., Roberts, P., Rouïl, L., Stern, R., Tarrason, L., Thunis, P., Vignati, E., Wind, P., 2009. Skill and uncertainty of a regional air quality model ensemble. Atmospheric Environment 43, 4822-4832.

Vong, R.J., B.M. Baker, F.J. Brechtel, R.T. Collier, J.C. Harris, A.S. Kowalski, N.C. McDonals and L.M. McInnes, 1997. Ionic and trace element composition of cloud water collected on the olimpic peninsula of Washington State. Atmospheric Environment, 31, 1991-2001.

Wichink Kruit, R., Schaap, M., Segers, A., Banzhaf, S., Schauschner, T., Builtjes, P., Heslinga, D., 2014: PINETI (Pollutant INput and EcosysTem Impact) report. Modelling and mapping of atmospheric nitrogen and sulphur deposition and critical loads for ecosystem specific assessment of threats to biodiversity in Germany Hrsg: Umweltbundesamt, UBA-Texte

Wichink Kruit, R.J., Schaap, M., Sauter, F.J., Van Zanten, M.C., Van Pul, W.A.J. (2012), Modeling the distribution of ammonia across Europe including bi-directional surface-atmosphere exchange, Biogeosciences, 9 (12), 5261-5277

WMO-GAW report 160, 2004. Manual for the GAW precipitation chemistry programme. Guidelines, Data Quality Objectives and Standard Operating Procedures. WMO TD No. 1251.

Zapletal, M., Kuňák, D., Chroust, P., 2007. Chemical characterization of rain and fog water in the Cervenohorske sedlo (Hruby Jesenik Mountains, Czech Republic). Water, Air & Soil Pollution, Vol. 186, No.1, 85–96.

Zhang, L., Gong, S., Padro, J., Barrie, L. (2001): A size-segregated particle dry deposition scheme for an atmospheric aerosol module, Atmospheric Environment, 35 (3), pp. 549-560

Zier, M., 1992. Über die Variabilität der Spurenstoffkonzentration im Nebelwasser im Verlaufe einzelner Nebelereignisse auf dem Kamm des Erzgebirges. Meteorologische Zeitschrift 1, 221– 228.

Zimmermann F, Lux H, Maenhaut W, Matschullat J, Plessow K, Reuter F, Wienhaus O, 2003: A Review of air pollution and atmospheric deposition dynamics in Southern Saxony, Central Europe. Atmospheric Environment 37, 671-691